



Searches for exclusive Higgs and Z boson decays into a vector quarkonium state and a photon using 139 fb⁻¹ of ATLAS $\sqrt{s} = 13$ TeV proton–proton collision data

The ATLAS Collaboration

Searches for the exclusive decays of Higgs and Z bosons into a vector quarkonium state and a photon are performed in the $\mu^+\mu^-\gamma$ final state with a proton–proton collision data sample corresponding to an integrated luminosity of 139 fb⁻¹ collected at $\sqrt{s} = 13$ TeV with the ATLAS detector at the CERN Large Hadron Collider. The observed data are compatible with the expected backgrounds. The 95% confidence-level upper limits on the branching fractions of the Higgs boson decays into $J/\psi\gamma$, $\psi(2S)\gamma$, and $\Upsilon(1S, 2S, 3S)\gamma$ are found to be 2.0×10^{-4} , 10.5×10^{-4} , and $(2.5, 4.2, 3.4) \times 10^{-4}$, respectively, assuming Standard Model production of the Higgs boson. The corresponding 95% CL upper limits on the branching fractions of the Z boson decays are 1.2×10^{-6} , 2.4×10^{-6} , and $(1.1, 1.3, 2.4) \times 10^{-6}$. An observed 95% CL interval of $(-133, 175)$ is obtained for the κ_c/κ_γ ratio of Higgs boson coupling modifiers, and a 95% CL interval of $(-37, 40)$ is obtained for κ_b/κ_γ .

1 Introduction

The Higgs boson, H , was first observed by the ATLAS [1] and CMS [2] collaborations in 2012 [3, 4] with a mass of approximately 125 GeV. Detailed measurements of its properties [5, 6] have confirmed its role in the spontaneous breaking of electroweak symmetry and the mass generation of the massive vector bosons [7, 8]. In the Standard Model (SM), the mass generation for fermions is implemented through Yukawa interactions. The ATLAS and CMS collaborations have reported observations of Higgs boson decays into a pair of τ -leptons [9, 10], a pair of bottom quarks [11, 12], and associated production of Higgs bosons with top-quark pairs [13, 14]. These measurements represent a complete observation of Higgs boson couplings to third-generation charged fermions, and are in agreement with SM expectations. Recently, evidence has been reported for the Higgs boson coupling to muons in the second generation through the decay $H \rightarrow \mu^+ \mu^-$ [15, 16]. Direct searches for $H \rightarrow c\bar{c}$ have been performed by both the ATLAS and CMS collaborations [17–20], as have searches for $H \rightarrow e^+ e^-$ decays [21, 22], but no further experimental evidence currently exists for the Higgs boson couplings to the first and second generations of fermions. Searches for potential beyond-the-SM (BSM) couplings of the Higgs boson have also been performed by the ATLAS and CMS collaborations, including searches for flavour-changing neutral currents via the t -quark decays $t \rightarrow cH$ and $t \rightarrow uH$ [23–26], and the lepton-flavour-violating decays $H \rightarrow e\mu$, $H \rightarrow e\tau$ and $H \rightarrow \mu\tau$ [21, 27, 28]. No evidence for these couplings has been found.

A direct method for accessing the couplings of the first- and second-generation quarks is the study of inclusive $H \rightarrow q\bar{q}$ decays. While these channels have large branching fractions, their experimental sensitivity is substantially obscured by large multi-jet backgrounds. Searches for the exclusive, radiative decays of the Higgs boson into a vector meson state and a photon offer an alternative way to probe the quark Yukawa couplings [29–31]. Although their branching fractions are comparatively small, these radiative decays have a distinct experimental signature, which helps suppress the large multi-jet backgrounds that affect the $H \rightarrow q\bar{q}$ searches. Figure 1 shows Feynman diagrams depicting the $H \rightarrow Q\gamma$ process, where Q is a vector quarkonium state. There are two primary contributions to the decay amplitude: the direct amplitude \mathcal{A}_{dir} occurs via the quark Yukawa coupling; the indirect amplitude \mathcal{A}_{ind} occurs at the one-loop level in the SM through the $H \rightarrow \gamma\gamma^*$ decay, where the virtual photon subsequently fragments into a vector quarkonium state. The two processes interfere destructively, and despite being loop-induced, the indirect amplitude is typically the more dominant contribution in decays of the Higgs boson into a vector meson state and a photon.

Higgs boson decays in the charmonium sector, $H \rightarrow J/\psi\gamma$ and $H \rightarrow \psi(2S)\gamma$, offer an opportunity to access both the magnitude and the sign of the charm-quark Yukawa coupling [29, 30]; the corresponding decays in the bottomonium sector, $H \rightarrow \Upsilon(1S, 2S, 3S)\gamma$, can provide information about the real and imaginary parts of the bottom-quark coupling to the Higgs boson [31]. Studies of these decays complement searches for the inclusive $H \rightarrow c\bar{c}$ and $H \rightarrow b\bar{b}$ decays. The results of recent independent calculations of the branching fractions expected for these decays in the SM are presented in Table 1, and are of the order of 10^{-6} for $H \rightarrow J/\psi\gamma$ and of order 10^{-9} to 10^{-8} for $H \rightarrow \Upsilon(1S, 2S, 3S)\gamma$ [31–36]. The branching fraction for $H \rightarrow \psi(2S)\gamma$ is expected to be $(1.03 \pm 0.06) \times 10^{-6}$. This was obtained via a private communication from the authors of Ref. [34], who used an estimate of the value of the order- v^2 non-relativistic QCD long-distance matrix element, where v is the velocity of the heavy quarks in the Q rest frame. It is noted that the branching fractions for decays in the bottomonium sector are small compared to those in the charmonium sector: in this case there is an almost perfect cancellation between the direct and indirect decay amplitudes, caused by the mass of the b -quark being large compared to the masses of quarks in the first and second generations.

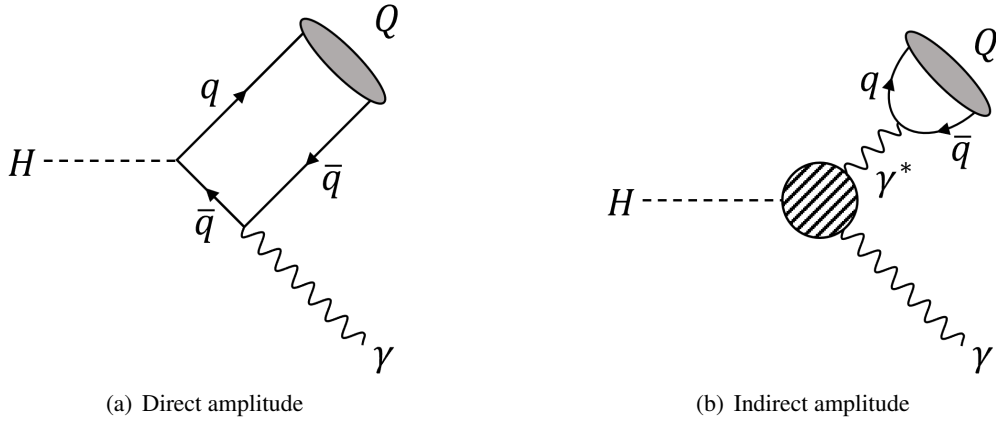


Figure 1: Feynman diagrams depicting the (a) direct amplitude and (b) indirect amplitude contributing to the $H \rightarrow Q \gamma$ process, where Q is a vector quarkonium state. The hatched circle in (b) denotes a set of one-loop diagrams.

Table 1: Recent calculations of the $H \rightarrow Q \gamma$ branching fractions expected in the Standard Model.

Vector quarkonium state	SM branching fraction, $\mathcal{B}(H \rightarrow Q \gamma)$		
	Ref. [31] (2015)	Refs. [33, 34] (2017)	Ref. [36] (2019)
J/ψ	$2.95^{+0.17}_{-0.17} \times 10^{-6}$	$2.99^{+0.16}_{-0.15} \times 10^{-6}$	$3.01^{+0.15}_{-0.15} \times 10^{-6}$
$\Upsilon(1S)$	$4.61^{+1.76}_{-1.23} \times 10^{-9}$	$5.22^{+2.02}_{-1.70} \times 10^{-9}$	$9.97^{+4.04}_{-3.03} \times 10^{-9}$
$\Upsilon(2S)$	$2.34^{+0.76}_{-1.00} \times 10^{-9}$	$1.42^{+0.72}_{-0.57} \times 10^{-9}$	$2.62^{+1.39}_{-0.91} \times 10^{-9}$
$\Upsilon(3S)$	$2.13^{+0.76}_{-1.13} \times 10^{-9}$	$0.91^{+0.48}_{-0.38} \times 10^{-9}$	$1.87^{+1.05}_{-0.69} \times 10^{-9}$

Deviations of the quark Yukawa couplings from SM expectations can lead to significant enhancements in the branching fractions of these radiative decays, particularly in the bottomonium sector. Such deviations can arise in BSM theories [37]. For instance, the quark masses may not originate entirely from the Higgs mechanism, but could also be induced by other, subdominant, sources of electroweak symmetry breaking [38]. Some further examples are the Froggatt–Nielsen mechanism [39], the Randall–Sundrum family of models [40], the minimal flavour violation framework [41], the Higgs-dependent Yukawa couplings model [42], and the possibility of the Higgs boson being a composite pseudo-Goldstone boson [43].

The Z boson production cross section at the LHC [44] is approximately 1000 times larger than the Higgs boson production cross section [37, 45], which allows rare Z boson decays to be probed to much smaller branching fractions than Higgs boson decays to the same final state. Similarly to the Higgs boson decays in Figure 1, radiative decays of the Z boson into a vector quarkonium state and a photon receive analogous contributions from direct and indirect amplitudes. In $Z \rightarrow Q \gamma$ decays, the power corrections in terms of the ratio of the QCD energy scale to the vector-boson mass are small. As discussed in Ref. [46], this allows the light-cone distribution amplitudes (LCDAs) of the mesons to be probed in a theoretically clean region where power corrections are in control, which is not possible in other applications of the QCD factorisation approach. These decays have not yet been measured, but recent independent calculations of the SM branching fractions for $Z \rightarrow J/\psi \gamma$ and $Z \rightarrow \Upsilon(1S, 2S, 3S) \gamma$ are presented in Table 2 and are expected to be of order 10^{-8} to 10^{-7} [46–48]. No value has been calculated for $Z \rightarrow \psi(2S) \gamma$.

Table 2: Overview of calculations of the Standard Model $Z \rightarrow Q \gamma$ branching fractions.

Vector quarkonium state	SM branching fraction, $\mathcal{B}(Z \rightarrow Q \gamma)$		
	Ref. [46] (2015)	Ref. [47] (2015)	Ref. [48] (2018)
J/ψ	$8.02^{+0.46}_{-0.44} \times 10^{-8}$	$9.96^{+1.86}_{-1.86} \times 10^{-8}$	$8.96^{+1.51}_{-1.38} \times 10^{-8}$
$\Upsilon(1S)$	$5.39^{+0.17}_{-0.15} \times 10^{-8}$	$4.93^{+0.51}_{-0.51} \times 10^{-8}$	$4.80^{+0.26}_{-0.25} \times 10^{-8}$
$\Upsilon(2S)$	-	-	$2.44^{+0.14}_{-0.13} \times 10^{-8}$
$\Upsilon(3S)$	-	-	$1.88^{+0.11}_{-0.10} \times 10^{-8}$

Decays of the Higgs and Z bosons into J/ψ or $\Upsilon(1S, 2S, 3S)$ and a photon were searched for by the ATLAS Collaboration, initially with up to 20.3 fb^{-1} of data collected at $\sqrt{s} = 8 \text{ TeV}$ [49] and subsequently with up to 36.1 fb^{-1} of data collected at $\sqrt{s} = 13 \text{ TeV}$ [50]; the latter search also introduced the study of the $\psi(2S)$ decay channels. The obtained 95% confidence level (CL) upper limits on the branching fractions were 3.5×10^{-4} and 2.0×10^{-3} for $H \rightarrow J/\psi \gamma$ and $H \rightarrow \psi(2S) \gamma$, respectively, and $(4.9, 5.9, 5.7) \times 10^{-4}$ for $H \rightarrow \Upsilon(1S, 2S, 3S) \gamma$. The corresponding 95% CL upper limits for the analogous Z boson decays were 2.3×10^{-6} , 4.5×10^{-6} and $(2.8, 1.7, 4.8) \times 10^{-6}$. The $H \rightarrow J/\psi \gamma$ and $Z \rightarrow J/\psi \gamma$ decays have also been searched for by the CMS Collaboration [51, 52], yielding similar upper limits of 7.6×10^{-4} and 1.4×10^{-6} from 35.9 fb^{-1} of data collected at $\sqrt{s} = 13 \text{ TeV}$. In addition, the ATLAS Collaboration has searched for the rare Higgs and Z boson decays to light vector mesons $H(Z) \rightarrow \phi \gamma$ and $H(Z) \rightarrow \rho \gamma$ [53, 54], while the CMS Collaboration has also searched for Higgs boson decays into a Z boson and a ρ or ϕ meson [55], and Higgs and Z boson decays into pairs of J/ψ or $\Upsilon(1S, 2S, 3S)$ mesons [56].

This paper describes searches for Higgs and Z boson decays into the exclusive final states $J/\psi \gamma$, $\psi(2S) \gamma$, and $\Upsilon(1S, 2S, 3S) \gamma$, and then into $\mu^+ \mu^- \gamma$, using 139 fb^{-1} of ATLAS proton–proton (pp) collision data collected between 2015 and 2018 at $\sqrt{s} = 13 \text{ TeV}$. Hereafter, where no distinction is relevant, the J/ψ and $\psi(2S)$ states are collectively denoted by $\psi(nS)$, and the $\Upsilon(1S, 2S, 3S)$ states are denoted by $\Upsilon(nS)$. The results are interpreted in the kappa framework [37, 57] in terms of the ratios κ_c/κ_γ and κ_b/κ_γ , where κ_c , κ_b and κ_γ are the modifiers of the coupling between the Higgs boson and the charm quark, bottom quark, and the effective coupling between the Higgs boson and the photon, respectively.

2 ATLAS detector and data sample

ATLAS [1] is a multipurpose particle detector with an approximately forward–backward symmetric cylindrical geometry and near 4π coverage in solid angle.¹ It consists of an inner tracking detector, electromagnetic and hadronic calorimeters, and a muon spectrometer.

The inner tracking detector (ID) covers the pseudorapidity range $|\eta| < 2.5$ and is surrounded by a thin superconducting solenoid providing a 2 T magnetic field. At small radii, a high-granularity silicon pixel detector covers the vertex region and typically provides four measurements per track. The first hit is usually

¹ ATLAS uses a right-handed coordinate system with its origin at the nominal interaction point (IP) in the centre of the detector and the z -axis along the beam pipe. The x -axis points from the IP to the centre of the LHC ring, and the y -axis points upward. Cylindrical coordinates (r, ϕ) are used in the transverse plane, ϕ being the azimuthal angle around the z -axis. The pseudorapidity is defined in terms of the polar angle θ as $\eta = -\ln \tan(\theta/2)$.

in the insertable B-layer, an additional layer installed in 2015 before 13 TeV data taking began [58, 59]. It is followed by a silicon microstrip tracker, which provides up to eight measurement points per track. The silicon detectors are complemented by a gas-filled straw-tube transition radiation tracker, which enables radially extended track reconstruction up to $|\eta| = 2.0$ with typically 35 measurements per track.

Electromagnetic (EM) calorimetry within $|\eta| < 3.2$ is provided by barrel and endcap high-granularity lead/liquid-argon (LAr) EM calorimeters with an additional thin LAr presampler covering $|\eta| < 1.8$ to correct for energy loss in upstream material; for $|\eta| < 2.5$ the EM calorimeter is divided into three layers in depth. A steel/scintillator-tile calorimeter provides hadronic calorimetry for $|\eta| < 1.7$. LAr technology with copper as absorber is used for the hadronic calorimeters in the endcap region, $1.5 < |\eta| < 3.2$. The solid-angle coverage is completed with forward copper/LAr and tungsten/LAr calorimeter modules in $3.1 < |\eta| < 4.9$ optimised for EM and hadronic measurements, respectively.

The muon spectrometer (MS) surrounds the calorimeters and features trigger and high-precision tracking chambers measuring the deflection of muons in a magnetic field provided by three air-core superconducting toroidal magnets. The field integral of the toroids ranges between 2.0 and 6.0 Tm across most of the detector. The precision chamber system covers the region $|\eta| < 2.7$ with three layers of monitored drift tubes, complemented by cathode strip chambers in the forward regions. The muon trigger system covers the range $|\eta| < 2.4$, featuring resistive plate chambers in the barrel and thin gap chambers in the endcap regions.

A two-level trigger and data acquisition system is used to record events for offline analysis [60]. The first-level trigger is implemented in hardware and uses a subset of detector information. This is followed by a software-based high-level trigger which outputs events for permanent storage at an average rate of 1 kHz, reduced from the maximum first-level rate of 100 kHz. An extensive software suite [61] is used in the reconstruction and analysis of real and simulated data, in detector operations, and in the trigger and data acquisition systems of the experiment.

Data samples considered in this analysis were collected during stable beam conditions with all relevant detector systems functional [62] and were recorded by a combination of triggers requiring a photon and either one or two muons in the event. Due to the increasing instantaneous luminosity, the transverse momentum thresholds and identification requirements were modified during the data-taking periods. Available throughout the data collection period was a trigger requiring a photon fulfilling the ‘medium’ identification criteria [63] and transverse momentum p_T^γ greater than 25 GeV, and at least one muon identified at the first-level trigger with p_T^μ greater than 24 GeV. In the 2015 and 2016 data collection periods, this was complemented with a trigger requiring a photon fulfilling the ‘loose’ identification criteria [63] and $p_T^\gamma > 35$ GeV, and at least one muon identified at the high-level trigger with $p_T^\mu > 18$ GeV. During the 2017 and 2018 data collection, a trigger requiring an isolated photon fulfilling the ‘tight’ identification criteria [63] and $p_T^\gamma > 35$ GeV and at least one muon identified at the high-level trigger with $p_T^\mu > 18$ GeV, and a trigger requiring a ‘loose’ photon with $p_T^\gamma > 35$ GeV, a muon identified at the first-level trigger with $p_T^\mu > 15$ GeV and an additional muon identified at the high-level trigger with $p_T^\mu > 2$ GeV were used. For candidate signal events that fulfil the analysis selection, described in Section 3, the trigger efficiency exceeds 97% in all cases. The uncertainty in the trigger efficiency is estimated to be 0.8% [64, 65]. After applying trigger and data-quality requirements, the integrated luminosity of the data sample used in this search corresponds to $139.0 \pm 2.4 \text{ fb}^{-1}$, obtained using the LUCID-2 detector [66] for the primary luminosity measurements and with the uncertainty in the integrated luminosity derived using the method described in Refs. [67, 68]. The average number of pp interactions per bunch crossing ranged from about 13 in 2015 to about 39 in 2018.

3 Event selection

In addition to the trigger and data-quality requirements, selection criteria based on geometric acceptance, event kinematics, isolation, and vertex quality are imposed to select candidate $H(Z) \rightarrow Q\gamma \rightarrow \mu^+\mu^-\gamma$ events. Reconstructed muon candidates must be either ‘segment-tagged’, where an ID track matches at least one track segment in the MS, or ‘combined’, where an ID track matches a full track in the MS [69]. Muons must also have an absolute value of pseudorapidity $|\eta^\mu| < 2.5$ and a transverse momentum $p_T^\mu > 3$ GeV. Pairs of oppositely charged muons are fitted to a common vertex with the track parameter uncertainties taken into account [70]. Pairs satisfying a loose χ^2 requirement for this fit are combined to reconstruct candidate $Q \rightarrow \mu^+\mu^-$ decays. The higher- p_T muon in each pair, called the leading muon, is required to have $p_T^\mu > 18$ GeV. Dimuons with a mass $m_{\mu^+\mu^-}$ between 2.4 GeV and 4.3 GeV are selected as $\psi(nS) \rightarrow \mu^+\mu^-$ candidates, and those with a mass $8.0 \text{ GeV} < m_{\mu^+\mu^-} < 12.0$ GeV are selected as $Y(nS) \rightarrow \mu^+\mu^-$ candidates. To improve the sensitivity of the $Y(nS)\gamma$ analysis in resolving the individual $Y(nS)$ states, events are classified into two exclusive categories based upon muon pseudorapidity to account for differences in resolution across the ATLAS detector. Events where both muons satisfy $|\eta^\mu| < 1.05$ are placed in the higher-resolution barrel (B) category, otherwise they are placed in the endcap (EC) category.

Candidate $Q \rightarrow \mu^+\mu^-$ decays are subjected to further isolation and vertex-quality requirements. The sum of the p_T of ID tracks within a cone of variable size $\Delta R = \sqrt{(\Delta\phi)^2 + (\Delta\eta)^2} = \min\{10 \text{ GeV}/(p_T^\mu [\text{GeV}]), 0.3\}$ around the leading muon is required to be less than 6% of the Q candidate’s transverse momentum, $p_T^{\mu^+\mu^-}$ [71]. This sum excludes the ID track associated with the leading muon itself, as well as the ID track associated with the subleading muon if it falls inside the ΔR cone. To mitigate the effects of multiple pp interactions in the same or neighbouring bunch crossings, only ID tracks that originate from the primary vertex are considered, which is defined as the reconstructed vertex with the highest Σp_T^2 of all associated tracks used in the formation of the vertex. To reject contributions from events involving b -hadron decays which result in displaced vertices, the vector leading from the primary vertex to the dimuon vertex is projected onto the direction of the Q candidate’s transverse momentum, and the signed projection L_{xy} is required to be smaller than three times its uncertainty, $\sigma_{L_{xy}}$, such that $|L_{xy}/\sigma_{L_{xy}}| < 3$.

Photons are reconstructed from clusters of energy in the electromagnetic calorimeter. Clusters that match ID tracks consistent with the hypothesis of a photon conversion into e^+e^- are classified as converted photon candidates, whilst clusters that have no matching ID tracks are classified as unconverted candidates [63]. Reconstructed photon candidates are required to satisfy the ‘tight’ photon identification criteria [63], have absolute pseudorapidity $|\eta^\gamma| < 2.37$, excluding the calorimeter barrel/endcap transition region $1.37 < |\eta^\gamma| < 1.52$, and have transverse momentum $p_T^\gamma > 35$ GeV. Further track- and calorimeter-isolation requirements are imposed to suppress contamination from jets: the sum of the p_T of all ID tracks originating from the primary vertex and within $\Delta R = 0.2$ of the photon direction, excluding any associated with the reconstructed photon, is required to be less than 5% of p_T^γ ; the sum of the p_T of the calorimeter energy clusters within $\Delta R = 0.4$ of the photon direction, excluding the energy cluster of the reconstructed photon, is required to be less than $(2.45 \text{ GeV} + 0.022 \times p_T^\gamma [\text{GeV}])$. The calorimeter isolation variable is corrected to account for contributions associated with other pp interactions in the same bunch crossing [63].

Combinations of a $Q \rightarrow \mu^+\mu^-$ candidate and a photon that satisfy $\Delta\phi(Q, \gamma) > \pi/2$ are retained for further analysis: this requirement suppresses contributions from events where the quarkonium and photon candidates have a small angular separation. If multiple combinations are possible, a situation that arises in fewer than 2% of events that pass the trigger requirements, the combination of the highest- p_T photon and the Q candidate with an invariant mass closest to that of the J/ψ meson is retained. To

maintain a common event selection for the Higgs and Z boson analyses, while ensuring near-optimal sensitivity for both, a variable $p_T^{\mu^+\mu^-}$ threshold that depends on the invariant mass of the $Q\gamma$ system, $m_{\mu^+\mu^-\gamma}$, is applied. For the $\psi(nS) \rightarrow \mu^+\mu^-$ ($\Upsilon(nS) \rightarrow \mu^+\mu^-$) candidates, the $p_T^{\mu^+\mu^-}$ threshold is 40 GeV (34 GeV) for $m_{\mu^+\mu^-\gamma} \leq 91$ GeV, and 54.4 GeV (52.7 GeV) for $m_{\mu^+\mu^-\gamma} \geq 140$ GeV. In the region $91 \text{ GeV} < m_{\mu^+\mu^-\gamma} < 140$ GeV, the $p_T^{\mu^+\mu^-}$ threshold varies linearly between its fixed values outside this region. The $p_T^{\mu^+\mu^-}$ thresholds are chosen to optimise the significance of potential signals at the Higgs and Z boson masses.

4 Signal modelling

The expected $H(Z) \rightarrow Q\gamma$ signals were modelled using Monte Carlo (MC) simulated events to extract analytical approximations of the final observables. Several Higgs boson production modes were considered in the simulation of the $H \rightarrow Q\gamma$ events. In order of decreasing production cross section, these are gluon–gluon fusion (ggH), vector-boson fusion (VBF), and associated production of a H boson with a Z boson (ZH), a W^\pm boson (WH) or a $t\bar{t}$ top-quark pair ($t\bar{t}H$). Explicit simulation of the $t\bar{t}H$ Higgs boson production mechanism is an addition with respect to the analysis strategy of the 36.1 fb^{-1} study [50]. The contribution of Higgs bosons produced in association with a $b\bar{b}$ bottom-quark pair ($b\bar{b}H$) was not directly simulated, but was included by scaling up the production cross section used to normalise the ggH sample. This assumes that the efficiency for $b\bar{b}H$ events is equal to that for ggH ; their inclusion increases the signal yield by less than 1%. For the $Z \rightarrow Q\gamma$ signal events, Z boson production was modelled inclusively.

The POWHEG BOX v2 MC event generator [72–76] was used to model the ggH and VBF Higgs boson production mechanisms, calculated up to next-to-leading order (NLO) in α_s . POWHEG BOX was interfaced with PYTHIA 8.212 [77, 78], which used the CTEQ6L1 parton distribution functions [79] and a set of tuned parameters called the AZNLO tune [80] to model the parton shower, hadronisation, and underlying event. The PYTHIA 8.212 event generator was used to model the ZH and WH production mechanisms, with NNPDF2.3LO parton distribution functions [81] and the A14 tune [82] for hadronisation and the underlying event. The MADGRAPH5_AMC@NLO 2.2.2 [83] event generator, interfaced with PYTHIA 8.212 for the parton shower, was used to model the $t\bar{t}H$ production mechanism, using the same parton distribution functions and event tune as the ZH and WH samples. Inclusive Z boson production was modelled with the same event generators, parton distribution functions, and event tune as the ggH and VBF Higgs boson production mechanisms. The subsequent decays of the Higgs and Z bosons into $J/\psi \gamma$, $\psi(2S) \gamma$ and $\Upsilon(1S, 2S, 3S) \gamma$ were simulated as a cascade of two-body decays, where the explicit simulation of $\psi(2S) \gamma$ decays is an addition to the analysis strategy compared to the 36.1 fb^{-1} study [50], which modelled these events by using $J/\psi \gamma$ samples. Interference effects between $J/\psi \gamma$ produced in Z boson decays and non-resonant QCD gluon-mediated processes [84] are expected to be small and were neglected. The generated events were passed through the detailed GEANT4 simulation of the ATLAS detector [85, 86] and processed with the same software as used to reconstruct the data. Conditions in the ATLAS detector, such as the average number of pp interactions per bunch crossing, changed throughout Run 2. Separate samples were produced with 2015–2016 conditions, 2017 conditions, and 2018 conditions, where each sample is normalised according to the integrated luminosity of the corresponding run period. The effect of multiple interactions in the same or neighbouring bunch crossings (pile-up) was modelled by overlaying each simulated hard-scattering event with inelastic pp events generated with PYTHIA 8.186 using the NNPDF2.3LO parton distribution functions and the A3 tune [87].

The production rates for the SM Higgs boson with $m_H = 125$ GeV, obtained from the CERN Yellow Reports [37, 45], are assumed throughout this analysis. The ggH sample is normalised such that it reproduces the total cross section predicted by a next-to-next-to-next-to-leading-order (N³LO) QCD calculation with NLO electroweak corrections applied [88–91]. The VBF sample is normalised to an approximate next-to-next-to-leading-order (NNLO) QCD cross section with NLO electroweak corrections applied [92–94]. The samples for the associated production of a W or Z boson with a Higgs boson are normalised to cross sections calculated at NNLO in QCD with NLO electroweak corrections [95, 96] including the NLO QCD corrections [97] for $gg \rightarrow ZH$. The production of $t\bar{t}H$ is normalised to cross sections calculated at NLO in QCD with NLO electroweak corrections [37]. The production cross section used to scale the ggH sample to account for the $b\bar{b}H$ mechanism was calculated at a mix of NNLO and NLO accuracy in QCD, with no electroweak corrections [37]. The production rate for the Z boson is normalised to the total cross section obtained from a measurement by the ATLAS Collaboration using 81 pb^{-1} of $\sqrt{s} = 13$ TeV data [44]. The branching fractions for the decays $Q \rightarrow \mu^+\mu^-$ used in signal normalisation are taken from the Review of Particle Physics [98], as are the inclusive branching fractions for t -quark decays to hadrons or leptons in the normalisation of the $t\bar{t}H$ samples. The effects of meson polarisation on the dimuon kinematic distributions are accounted for via a reweighting of the simulated events, which are initially simulated without polarisation. The quarkonium states in the decay of the Higgs boson are expected to be transversely polarised; the quarkonium states in the decay of the Z boson are expected to be longitudinally polarised, due to a vanishing contribution from the transversely polarised meson [47]. Accounting for meson polarisation results in a 2%–3% decrease in Higgs boson signal efficiency and a 9%–10% increase in Z boson signal efficiency.

Figure 2 shows the generator-level photon and muon p_T distributions from the simulated $H(Z) \rightarrow Q\gamma$ signal events. For the $J/\psi \gamma \rightarrow \mu^+\mu^- \gamma$ and $\psi(2S) \gamma \rightarrow \mu^+\mu^- \gamma$ final states, the total signal efficiency is 19% for the Higgs boson decays and 10% for the Z boson decays. These values take into account the trigger, reconstruction, identification, and isolation efficiencies, as well as the kinematic acceptance. The corresponding values for the $\Upsilon(1S, 2S, 3S) \gamma \rightarrow \mu^+\mu^- \gamma$ final states are 21% and 13%. The difference in efficiency between the Higgs and Z boson decays arises primarily from the softer photon and muon p_T distributions associated with $Z \rightarrow Q\gamma$ production, as seen by comparing Figures 2(a) and 2(d) for the $J/\psi \gamma$ case, Figures 2(b) and 2(e) for the $\psi(2S) \gamma$ case, and Figures 2(c) and 2(f) for the $\Upsilon(nS) \gamma$ case.

The $m_{\mu^+\mu^- \gamma}$ resolution is 1.6%–1.8% for both the Higgs and Z boson decays. For each of the final states, a two-dimensional probability density function (PDF) is used to model the signal in $m_{\mu^+\mu^- \gamma}$ and $m_{\mu^+\mu^-}$. The Higgs boson signals are modelled with the sum of two bivariate Gaussian distributions, which describe the approximately 60% correlations between the two mass variables in each decay channel as well as the effects of detector resolution. For Z boson decays, since the Z boson natural width is comparable to the detector resolution, the correlation between $m_{\mu^+\mu^- \gamma}$ and $m_{\mu^+\mu^-}$ is small, of order 10%, and is neglected, and the two mass distributions are treated as uncorrelated. The $m_{\mu^+\mu^- \gamma}$ distributions of the Z boson signals are modelled with the sum of two Voigtian PDFs corrected with a mass-dependent efficiency factor, which accounts for the changing selection efficiency along the Z lineshape that arises from the kinematic requirements described in Section 3. The Voigtian shape is a convolution of a Breit–Wigner distribution, which describes the natural width of the Z boson, and a Gaussian distribution, which describes detector resolution effects. The $m_{\mu^+\mu^-}$ distributions of the Z boson decays are modelled with a sum of two Gaussian PDFs, where the peak value and resolution parameters of the PDFs are fixed to the values obtained in a fit to the simulated event samples.

Systematic uncertainties in the signal yield and inferred branching fraction of the H and Z boson decays are considered. Uncertainties in the Higgs boson production cross sections total 5.8% [37, 45]. The uncertainty

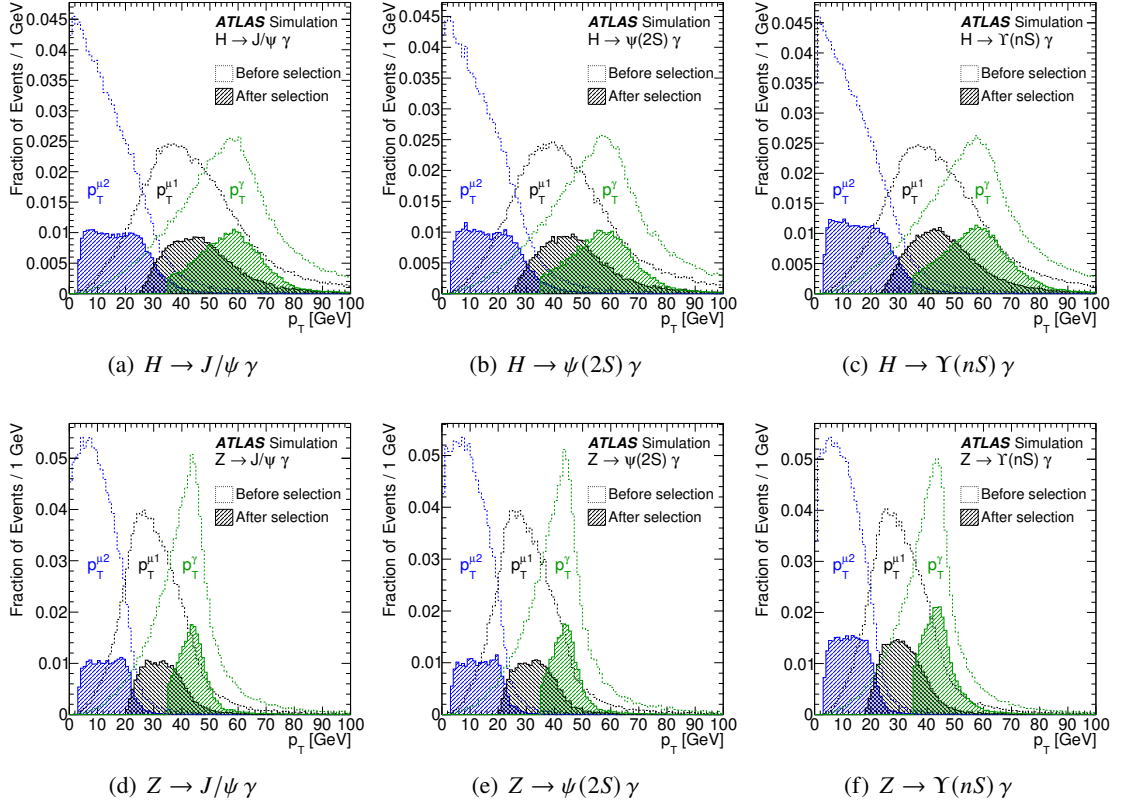


Figure 2: Generator-level transverse momentum (p_T) distributions of the photon and muons for (a) $H \rightarrow J/\psi \gamma$, (b) $H \rightarrow \psi(2S) \gamma$, (c) $H \rightarrow Y(nS) \gamma$, (d) $Z \rightarrow J/\psi \gamma$, (e) $Z \rightarrow \psi(2S) \gamma$ and (f) $Z \rightarrow Y(nS) \gamma$ simulated events, respectively. The dashed-line distributions with a clear fill show the events at generator level which fall within the analysis geometric acceptance (both muons are required to have $|\eta^\mu| < 2.5$, while the photon is required to have $|\eta^\gamma| < 2.37$, excluding the region $1.37 < |\eta^\gamma| < 1.52$), and are each normalised to unity. The solid-line distributions with a hatched fill show the fraction of these events which pass the full analysis event selection described in Section 3. The relative difference between the two sets of distributions corresponds to the effects of reconstruction, trigger, and event selection efficiencies. The leading muon candidate is denoted by $p_T^{\mu 1}$ (black), the subleading candidate by $p_T^{\mu 2}$ (blue), and the photon candidate is denoted by p_T^γ (green).

in the measured Z boson production cross section is 2.9% [44], where the luminosity component of the uncertainty in the Z boson production cross-section measurement is treated as completely uncorrelated with the integrated luminosity uncertainty of data set used in this search. The uncertainty in the integrated luminosity is estimated to be 1.7% [67, 68], using primary luminosity measurements from the LUCID-2 detector [66]. The uncertainty in the acceptance of the Higgs boson signal due to the choice of MC generator parameter values, parton distribution functions, set of tuned parameters for the underlying event, and parton showering, is estimated by studying how different choices affect the acceptance at generator level. The total uncertainty in the Higgs boson signal acceptance is estimated to be 1.8%. For the Z boson, the respective signal acceptance uncertainty is determined to be 1.0% by comparing the Z boson kinematic distributions in simulated events with measurements in data [99]. Trigger efficiencies for photons are determined from samples enriched with $Z \rightarrow e^+e^-$ events in data [100]. The photon trigger efficiency is estimated to contribute a systematic uncertainty of 0.8% to the expected signal yields [64, 65]. Photon identification efficiencies are determined using the enriched $Z \rightarrow e^+e^-$ event samples, as well as inclusive

photon events and $Z \rightarrow \ell^+ \ell^- \gamma$ events [101, 102]. The photon identification efficiency uncertainties, for both the converted and unconverted photons, are 1.7%–1.9% for the Higgs and Z boson signals. The effect of the muon reconstruction and identification efficiency uncertainty is 2.2%–2.4% [103]. The photon energy scale uncertainty, determined from $Z \rightarrow e^+ e^-$ events and validated using $Z \rightarrow \ell^+ \ell^- \gamma$ events [104, 105], is propagated through the simulated samples as a function of η^γ and p_T^γ . The uncertainty associated with the photon energy scale and resolution in the simulation has a 0.1%–0.2% effect on the Higgs and Z boson signal yields. Similarly, the systematic uncertainty associated with the scale of the muon momentum measurement has a 0.1%–0.5% effect on the signal yields [103]. To assess any effect on the expected signal yield from imperfect modelling of pile-up, the average number of pile-up interactions is varied in the simulation; the corresponding uncertainty is 0.7%–1.1%. These systematic uncertainties in the expected signal yields are summarised in Table 3. The effect of the energy and momentum scale and resolution uncertainties on the Higgs and Z boson signal shapes is negligible.

Table 3: Summary of the systematic uncertainties in the expected signal yields. In the case of the H decays, the ‘signal acceptance’ uncertainty was estimated through parton distribution function variations, scale variations and variations of the underlying-event tune. For the Z decays, the ‘signal acceptance’ uncertainty was estimated by comparing simulation to data.

Source of systematic uncertainty	Signal yield uncertainty			
	$H \rightarrow \psi(nS) \gamma$	$H \rightarrow \Upsilon(nS) \gamma$	$Z \rightarrow \psi(nS) \gamma$	$Z \rightarrow \Upsilon(nS) \gamma$
Total cross section	5.8%	5.8%	2.9%	2.9%
Integrated luminosity	1.7%	1.7%	1.7%	1.7%
Signal acceptance	1.8%	1.8%	1.0%	1.0%
Muon reconstruction	2.3%	2.2%	2.4%	2.4%
Photon identification	1.7%	1.7%	1.9%	1.9%
Pile-up uncertainty	0.8%	0.7%	1.1%	1.1%
Trigger efficiency	0.7%	0.7%	0.8%	0.8%
Photon energy scale	0.1%	0.1%	0.2%	0.2%
Muon momentum scale	0.1%	0.1%	0.5%	0.2%
Muon momentum resolution (ID)	<0.01%	0.01%	0.06%	0.02%
Muon momentum resolution (MS)	0.02%	0.01%	0.04%	0.01%

5 Background modelling

The background is considered to be composed of two distinct contributions which are modelled separately in this analysis. The first is an exclusive contribution originating from $\mu^+ \mu^- \gamma$ events produced via the Drell–Yan process, where a highly energetic photon typically arises from final-state radiation. The second, which is the dominant background, is an inclusive contribution mostly from multi-jet and γ +jet events involving dimuon or Q production. The exclusive background is modelled with simulation, similarly to the signal model in Section 4, whilst the inclusive background is modelled with a data-driven technique, discussed in detail in Ref. [106]. The background is modelled independently for the $\psi(nS)$ dimuon mass region, and the B and EC categories of the $\Upsilon(nS)$ dimuon mass region.

5.1 Exclusive background

The Drell–Yan production of dimuons with a highly energetic photon, typically from final-state radiation, $q\bar{q} \rightarrow \gamma^*/Z^* \rightarrow \mu^+\mu^-\gamma$, constitutes a significant background contribution, exhibiting a characteristic resonant structure in the $m_{\mu^+\mu^-\gamma}$ distribution. The shapes of this background in $m_{\mu^+\mu^-\gamma}$ and $m_{\mu^+\mu^-}$ are modelled using events simulated with `SHERPA 2.2.10` [107] at leading order with the NNPDF3.0 parton distribution function set in the $\psi(nS)$ and $\Upsilon(nS)$ $m_{\mu^+\mu^-}$ regions. The normalisation of this background is determined from a fit to the data in the signal region following the selection described in Section 3. The resonant shape in $m_{\mu^+\mu^-\gamma}$ is modelled analytically as the sum of a Voigtian function and a threshold function defined as $f(x) = \sqrt{x-x_0} e^{-A(x-x_0)}$, where A and x_0 are constants, $f(x) = 0$ for $x < x_0$, and x is the three-body mass $m_{\mu^+\mu^-\gamma}$. The Voigtian function describes the on-shell Z production, which dominates in the $\Upsilon(nS)$ channels, whereas the threshold function describes the off-shell γ^*/Z^* production, which dominates in the $\psi(nS)$ channels. Different forms of the threshold function were considered, but the function above was found to provide the best description of the background shape. The shape in $m_{\mu^+\mu^-}$ is non-resonant and is modelled with a first-order Chebyshev polynomial. The parameters of the shape functions used to model each mass distribution are obtained from a fit to the simulated samples in each category once the signal region selection described in Section 3 is imposed. The statistical uncertainty associated with the parameters of the $m_{\mu^+\mu^-\gamma}$ shape function is accounted for via nuisance parameters in the maximum-likelihood fit to data in Section 7, based on the fit to the simulated samples, and is found to have a negligible effect on the final result.

5.2 Inclusive background

The dominant background arises from inclusive multi-jet or γ +jet events that involve the production of Q states, which subsequently decay into $\mu^+\mu^-$, or the production of non-resonant dimuon pairs such as from the Drell–Yan process or from random combinations of muons; the photon candidate may be genuine or, typically, a misidentified jet. The contribution from dimuon events in the inclusive background is separate from the exclusive $q\bar{q} \rightarrow \mu^+\mu^-\gamma$ background discussed in Section 5.1, as the latter involves a genuine photon candidate originating from the same hard-scattering process. The complicated mixture of background contributions, which involve QCD processes and misidentification of physics objects, and the highly selective phase-space region of interest makes it challenging to model this inclusive background accurately with simulation. Furthermore, the features of the background shape, which exhibits a broad kinematic peak at the location of a possible $Z \rightarrow Q\gamma$ signal, combined with the relatively low number of events in the signal region make background modelling through direct fits of parametric models to the data unsuitable. For this reason, a generative approach is pursued, where the $m_{\mu^+\mu^-\gamma}$ shape of the inclusive background is obtained with a non-parametric data-driven model, described in Ref. [106] and used in several previous analyses [49, 50, 53, 54], using templates to describe the kinematic distributions. The background normalisation is extracted directly from a fit to the data, and shape variations are incorporated in the background model in the final discriminating variable; these shape variations are also profiled in the fit.

The background model generation uses a sample of approximately 1.8×10^4 $\psi(nS)$ γ and 8.9×10^3 $\Upsilon(nS)$ γ candidate events. These events pass all the kinematic selection requirements described in Section 3, except that the Q and γ candidates are not required to satisfy the nominal isolation requirements, and a looser minimum $p_T^{\mu^+\mu^-}$ requirement of 30 GeV is imposed; these events define the background-dominated generation region (GR). The exclusive background contribution is subtracted from the data to prepare for

the construction of the inclusive background model. The exclusive background mass shape is obtained from a fit to the simulated events that meet the GR selection criteria. The background model is derived iteratively; in each iteration the exclusive $q\bar{q} \rightarrow \mu^+\mu^-\gamma$ contribution and the background model are fitted to the data in the GR to derive the exclusive background normalisation. PDFs are constructed to describe the distributions of the relevant kinematic and isolation variables and their most important correlations. The PDFs of these kinematic and isolation variables are sampled to generate an ensemble of pseudocandidate events, each with complete Q and γ candidate four-vectors and their associated isolation values. The important correlations among the kinematic and isolation variables of the background events, in particular between the Q and γ candidate transverse momenta p_T^Q and p_T^γ , are retained in the generation of the pseudocandidate events through the following sequential sampling scheme, shown diagrammatically in Figure 3:

1. The Q -candidate pseudorapidity η_Q , mass m_Q , and azimuthal angle ϕ_Q , are drawn independently from one-dimensional PDFs, and values for p_T^Q and p_T^γ are drawn simultaneously from a two-dimensional PDF.
2. The pseudorapidity difference between the Q and γ candidates, $\Delta\eta(Q, \gamma)$, and the γ -candidate calorimeter isolation are drawn simultaneously from a three-dimensional PDF, based on the value previously drawn for p_T^Q .
3. The Q -candidate track isolation and the azimuthal angular separation between the Q and γ candidates, $\Delta\phi(Q, \gamma)$, are drawn separately from two three-dimensional PDFs, given the selected values of the γ -candidate calorimeter isolation and p_T^Q .
4. The γ -candidate track isolation is drawn from a three-dimensional PDF using the previously sampled values of the Q -candidate track isolation and γ -candidate calorimeter isolation variables, and the values for η_γ and ϕ_γ are calculated from the values drawn for η_Q , ϕ_Q , $\Delta\eta(Q, \gamma)$, and $\Delta\phi(Q, \gamma)$.

The nominal selection requirements are imposed and the surviving pseudocandidates are used to construct templates for the $m_{\mu^+\mu^-\gamma}$ distributions, which are then smoothed using a Gaussian kernel density estimation method [108]. Potential contamination of the GR sample from signal events is expected to be negligible. Signal injection tests were performed where a significant amount of signal, much larger than the signal branching fraction excluded in the presented analysis, was added to the GR to investigate the effect of such a potential signal contamination on the model; it was found that the presence of the signal is largely inconsequential to the shape of the background model and does not lead to any peaking structures in the background templates. The ability to predict data using the background model is studied in several validation regions (VRs), defined by selections looser than the nominal signal requirements and tighter than the generation region requirements. The requirements imposed in each of the selection regions used in the analysis are summarised in Table 4. The application of the $p_T^{\mu^+\mu^-}$ requirement (VR1), the muon isolation requirements (VR2), and the photon isolation requirement (VR3) are each checked with this method, and in all regions the background model is found to describe the data well. This is shown in the comparison of the background model with data in each VR in Figure 4, which includes the exclusive background contribution. The exclusive background shape in each selection region is obtained from a fit to the simulated events, and the normalisation is extrapolated from the fit to data in the GR.

The shape of the background model in three-body mass, $m_{\mu^+\mu^-\gamma}$, is allowed to vary around the nominal shape, and the parameters controlling these systematic variations are treated as nuisance parameters in the maximum-likelihood fit described in Section 6. Three such shape variations are implemented to allow the background template to adjust to the observed data. The first variation is produced via a scale variation of

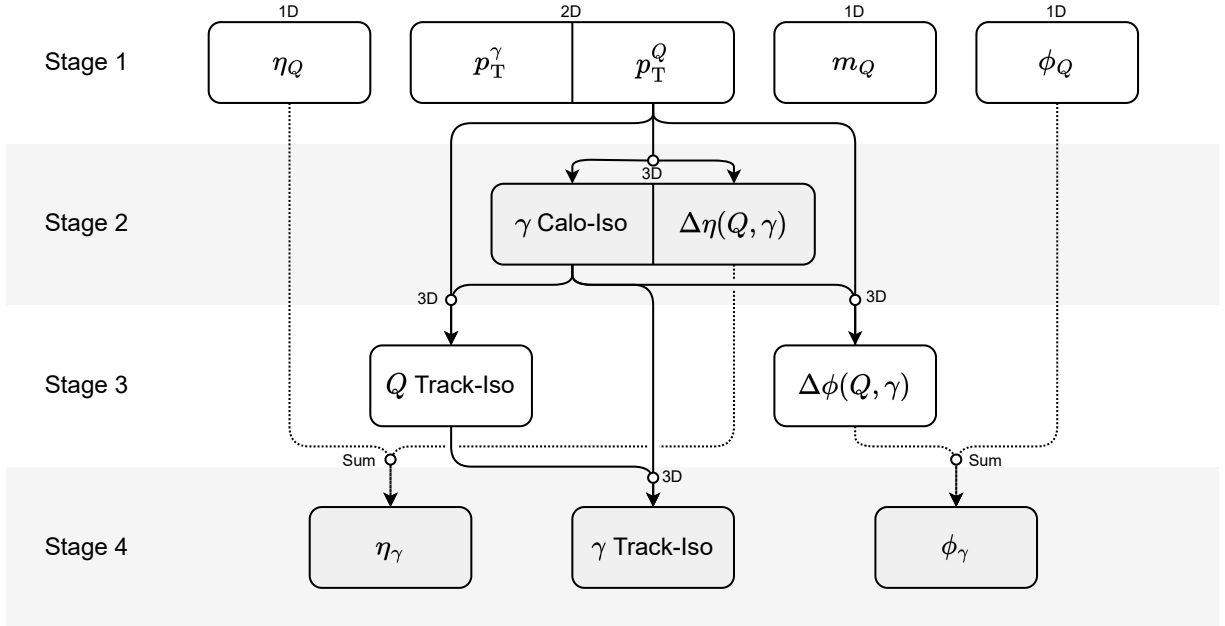


Figure 3: The data-driven sequential sampling method used to generate pseudocandidate events for the inclusive background model. The labels ‘1D’ and ‘2D’ refer to the dimensionality of the PDFs used in the model generation of the variables underneath. Vertices labelled ‘3D’ signify that the output variable (or variables), identified by the arrow leading out of the vertex, is sampled from a three-dimensional PDF described in bins of the input variable (or variables), identified by the lines leading into the vertex. If two variables share a border, they are sampled simultaneously from a joint PDF. Vertices labelled ‘Sum’ signify that the output variable is calculated directly from the sum of the input variables.

Table 4: Summary of the selection regions used in the analysis. The term ‘Full’ indicates the corresponding requirement applied in the SR, and discussed in Section 3. The relaxed photon isolation requires the sum of the p_T of all ID tracks originating from the primary vertex and within $\Delta R = 0.2$ of the photon direction, excluding any associated with the reconstructed photon, to be less than 20% of p_T^γ and the sum of the p_T of the calorimeter energy clusters within $\Delta R = 0.4$ of the photon direction, excluding the energy of the reconstructed photon, to be less than $(2.45 \text{ GeV} + 0.4 \times p_T^\gamma [\text{GeV}])$. The relaxed Q isolation requires the sum of the p_T of the ID tracks within $\Delta R = \min\{10 \text{ GeV}/(p_T^\mu [\text{GeV}]), 0.3\}$ of the leading muon to be less than 40% of p_T^Q .

Region	$p_T^{\mu\mu}$	Photon Isolation	Q Isolation
Generation Region (GR)	$> 30 \text{ GeV}$	Relaxed	Relaxed
Validation Region 1 (VR1)	Full	Relaxed	Relaxed
Validation Region 2 (VR2)	$> 30 \text{ GeV}$	Relaxed	Full
Validation Region 3 (VR3)	$> 30 \text{ GeV}$	Full	Relaxed
Signal Region (SR)	Full	Full	Full

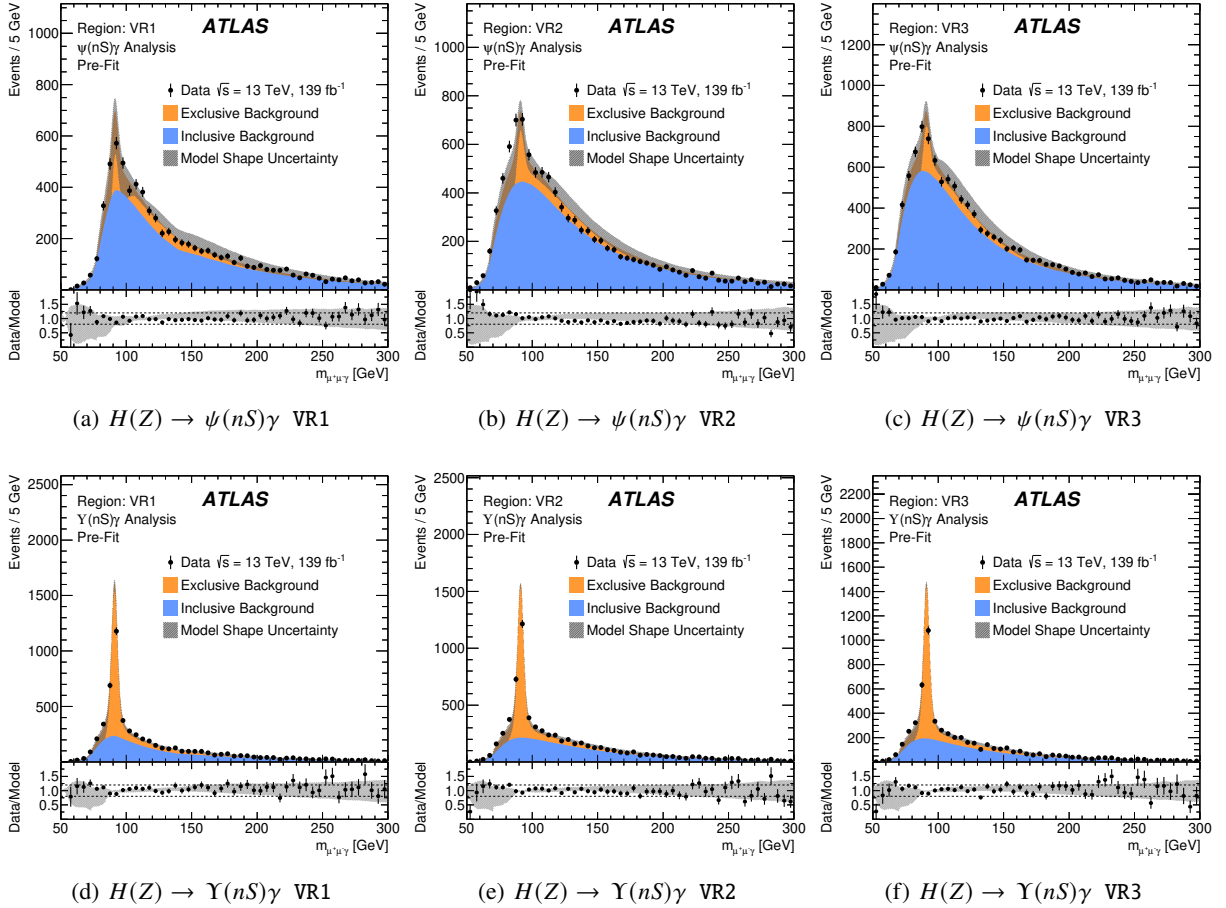


Figure 4: The distribution of $m_{\mu^+\mu^-\gamma}$ in data compared to the prediction of the background model for ((a), (b) and (c)) $H(Z) \rightarrow \psi(nS)\gamma$ and ((d), (e) and (f)) $H(Z) \rightarrow \Upsilon(nS)\gamma$ in the VR1, VR2 and VR3 validation regions. The total background is normalised to the observed number of events within the region shown, where the ratio of the exclusive and inclusive background components is extrapolated from the generation region. The uncertainty band corresponds to the uncertainty envelope derived from variations in the inclusive background modelling procedure. The dashed lines in the ratio plot in each figure indicate 1.2 and 0.8 on the y-axis. It should be noted that these plots are pre-fit, where the shapes of the inclusive and exclusive background components are fixed to the nominal template. In the maximum-likelihood fit to data in the signal region, the normalisation of each background is free, and their shapes are allowed to morph according to the defined shape variations.

the p_T^γ distribution in the model, which allows the peak of the three-body mass distribution to shift to lower or higher masses; the second variation is produced via a linear distortion of the shape of the $\Delta\phi(Q, \gamma)$ distribution, which allows the width of the three-body mass distribution to increase or decrease; the third variation is produced via a global tilt of the three-body mass distribution around a pivot point, which allows the background to adapt to slopes with respect to the data. The first two variations are straightforward alterations to the underlying kinematics of the pseudocandidates, which cause corresponding changes in the three-body mass. Their nuisance parameters are loosely constrained by a Gaussian term in the likelihood, which arbitrarily assigns the $\pm 1\sigma$ variations to a relatively large change in the shape, and these are subsequently constrained by the data. The third variation is applied directly to the final three-body mass template and left unconstrained in the final fit.

The $m_{\mu^+\mu^-}$ distribution for $\psi(nS)\gamma$ candidates that meet the background model generation criteria is shown in Figure 5(a) and exhibits clear peaks at the J/ψ and $\psi(2S)$ masses. In Figures 5(b) and 5(c), the corresponding distributions for the selected $\Upsilon(nS)\gamma$ candidates are shown respectively for the B and EC categories, where the individual $\Upsilon(1S), \Upsilon(2S)$, and $\Upsilon(3S)$ peaks can be observed. During the $m_{\mu^+\mu^-}\gamma$ background model generation, a value for $m_{\mu^+\mu^-}$ is drawn from the distributions shown in Figure 5. No significant correlations between $m_{\mu^+\mu^-}$ and $m_{\mu^+\mu^-}\gamma$ are observed. Thus, the $m_{\mu^+\mu^-}$ distribution itself is modelled independently of $m_{\mu^+\mu^-}\gamma$ using analytical PDFs. The $\psi(nS)$ and $\Upsilon(nS)$ peaks are modelled with Gaussian PDFs, while the inclusive background is modelled with a first-order Chebyshev polynomial function; these functions were found to be sufficient to describe the data, given its statistical uncertainty. The parameters of these PDFs are obtained by means of a one-dimensional fit to events selected in the background model generation region, as shown in Figure 5, and are used to model the $m_{\mu^+\mu^-}$ distribution in the maximum-likelihood fit in Section 6. It is noted that the slope of the inclusive background is allowed to adapt to the observed data in the fit to the signal region, and that the relative normalisations of the different contributions to $m_{\mu^+\mu^-}$ are left free.

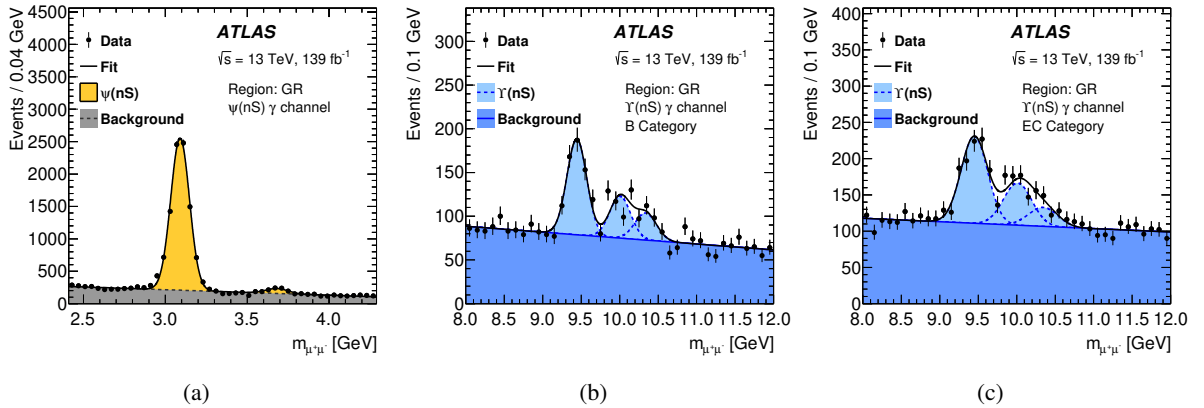


Figure 5: Distribution of $\mu^+\mu^-$ invariant mass for (a) $\psi(nS)\gamma$, (b) $\Upsilon(nS)\gamma$ barrel category (B) and (c) $\Upsilon(nS)\gamma$ endcap category (EC). Candidates satisfy the requirements of the background generation region (GR) defined in Section 5.2. The error bars on the data points denote their statistical uncertainty.

6 Statistical methods

The data selected by the signal region criteria are compared with background and signal predictions using a two-dimensional (2D) unbinned maximum-likelihood fit in $m_{\mu^+\mu^-\gamma}$ and $m_{\mu^+\mu^-}$, for events with $m_{\mu^+\mu^-\gamma} < 300$ GeV. This allows the $H(Z) \rightarrow Q\gamma$ signals to be distinguished from each other, as well as from the exclusive and inclusive background contributions. The likelihood function \mathcal{L} for each of the $\psi(nS)$ and $Y(nS)$ analyses is constructed using the signal and background models described in Sections 4 and 5. The parameters of interest $\vec{\mu} = \{\mu_i\}$ are the signal strengths, which correspond to the signal rate normalised to the SM expectation, for each of the Higgs and Z boson signals counted by the index i . The likelihood for the $\psi(nS)$ analysis when n events are observed in the signal region is defined as:²

$$\begin{aligned} \mathcal{L}(\vec{\mu}, \vec{b}, \alpha, \theta, \theta') = & \mathcal{P}(n | \sum_{i=1}^4 \mu_i \cdot s_i(\vec{\alpha}) + \sum_{j=1}^4 b_j) \times \prod_r \mathcal{G}(\alpha_r | 0, 1) \\ & \times \prod_{k=1}^n \left(\sum_{i=1}^4 \mathcal{F}_i^s \cdot \mathcal{S}_i(m_{\mu^+\mu^-\gamma}^k, m_{\mu^+\mu^-}^k | \mu_i) + \sum_{j=1}^4 \mathcal{F}_j^b \cdot \mathcal{R}_j(m_{\mu^+\mu^-\gamma}^k | \vec{\theta}) \mathcal{M}_j(m_{\mu^+\mu^-}^k | \theta') \right) \\ & \times \prod_l \mathcal{G}(\theta_l | 0, 1) \end{aligned}$$

In the above equation, \mathcal{P} is the Poisson distribution for n observed events given the total signal and background. The symbol $s_i(\vec{\alpha})$ denotes the expected SM signal yield for signal i as modified by the nuisance parameters $\vec{\alpha}$, which correspond to the signal normalisation systematic uncertainties discussed in Section 4. These nuisance parameters are counted by index r and are constrained with standard Gaussian PDF terms, \mathcal{G} . The normalisation parameters associated with each independent background contribution are denoted by $\vec{b} = \{b_j\}$. These are not constrained and are determined directly from the fit to the data. In the case of the $\psi(nS)$ analysis, the background components are exclusive $q\bar{q} \rightarrow \mu^+\mu^-\gamma$ production, inclusive J/ψ decays, inclusive $\psi(2S)$ decays, and inclusive non-resonant dimuon production.³ The symbols \mathcal{F}_i^s and \mathcal{F}_j^b denote the signal i and background j as fractions of the total signal and background, respectively. The shape of signal i in $(m_{\mu^+\mu^-\gamma}, m_{\mu^+\mu^-})$ is given by the PDF \mathcal{S}_i . Correspondingly, the shape of the background component j is given by the product of PDFs $\mathcal{R}_j(m_{\mu^+\mu^-\gamma})$ and $\mathcal{M}_j(m_{\mu^+\mu^-})$, since no correlations between $m_{\mu^+\mu^-}$ and $m_{\mu^+\mu^-\gamma}$ are observed in background shape. The nuisance parameters $\vec{\theta}$ parameterise the systematic variations of the background shapes discussed in Section 5. They are counted by index l and are constrained with standard Gaussian terms. The only exception is the nuisance parameter related to the ‘global tilt’ systematic shape variation of the inclusive background, which is not constrained. The nuisance parameter θ' corresponds to the slope in $m_{\mu^+\mu^-}$ of the non-resonant component of the inclusive background, which is free in the fit.

Upper limits are set on the branching fractions for the Higgs and Z boson decays into $Q\gamma$ using the CL_s modified frequentist formalism [109] with the profile-likelihood-ratio test statistic and the asymptotic approximations derived in Ref. [110]. When setting limits for one of the signals, the other potential signal contributions are treated as nuisance parameters and are profiled in the fit. Only the decays $Q \rightarrow \mu^+\mu^-$ are considered in the limit setting, feed-down from $Q' \rightarrow Q + X$ transitions are not included.

² The likelihood for the $Y(nS)$ analysis is defined similarly, but with the events divided further into two exclusive categories.

³ In the case of the $Y(nS)$ analysis, the background components are exclusive $q\bar{q} \rightarrow \mu^+\mu^-\gamma$ production, inclusive $Y(1S)$, $Y(2S)$, and $Y(3S)$ decays, and inclusive non-resonant dimuon production, and are fit separately in the B and EC categories.

The ability of the fit to identify potential signal contributions was verified through signal injection tests. Signals corresponding to a branching fraction of 5×10^{-4} and 5×10^{-7} for the Higgs and Z boson decays, respectively, were injected into an Asimov dataset [110] constructed from a background-only fit in the signal region. The full fit accurately recovered the injected signals.

7 Results

In total, 3394 events are observed in the $\psi(nS) \gamma$ signal region and 3577 events are observed in the $\Upsilon(nS) \gamma$ signal region. The results of the background-only fits for the $\psi(nS) \gamma$ and $\Upsilon(nS) \gamma$ analyses are shown in Figures 6 and 7 respectively, where the signal distributions shown correspond to the extracted 95% confidence-level (CL) branching fraction upper limits. The expected and observed numbers of background events within the $m_{\mu^+\mu^- \gamma}$ ranges relevant to the Higgs and Z boson signals are given in Table 5, where the expected backgrounds are obtained from these background-only fits. The exclusive contribution to the total background in these regions of relevance ranges from approximately 10% for the $H \rightarrow J/\psi \gamma$ and 22% for $H \rightarrow \psi(2S) \gamma$ to 21% and 41% for the corresponding Z boson decay searches. For the $\Upsilon(nS) \gamma$ analysis the exclusive contribution ranges from 24% to 29% for the ranges of relevance for the Higgs boson searches, while for the ranges of relevance for the Z boson searches it is between 75% and 79%. Table 5 also shows the expected number of signal events for reference branching fractions near the sensitivity of the analysis: 10^{-3} for $H \rightarrow Q \gamma$ and 10^{-6} for $Z \rightarrow Q \gamma$.

Table 5: Numbers of observed and expected background events for the $m_{\mu^+\mu^- \gamma}$ ranges of interest. Each expected background and the corresponding uncertainty of its mean is obtained from a background-only fit to the data; the uncertainty does not take into account statistical fluctuations in each mass range. Expected Z and Higgs boson signal contributions, with their corresponding total systematic uncertainty, are shown for reference branching fractions of 10^{-6} and 10^{-3} , respectively. The ranges in $m_{\mu^+\mu^-}$ are centred around each quarkonium resonance, with a width driven by the resolution of the detector; in particular, the ranges for the $\Upsilon(nS)$ resonances are based on the resolution in the endcaps. It is noted that the discrepancy between the observed and expected backgrounds for $m_{\mu^+\mu^-} = 9.0\text{--}9.8$ GeV in the endcaps was found to have a small impact on the observed limit for $Z \rightarrow \Upsilon(1S) \gamma$.

Category	$m_{\mu^+\mu^-}$ range [GeV]	Observed (expected) background				Z signal for $\mathcal{B} = 10^{-6}$	H signal for $\mathcal{B} = 10^{-3}$
		$m_{\mu^+\mu^- \gamma}$ range [GeV]					
		86–96		122–128			
Inclusive	2.9–3.3	198	(185.6 ± 5.9)	61	(59.1 ± 1.6)	49.3 ± 2.4	87.8 ± 6.1
Inclusive	3.5–3.9	83	(82.5 ± 4.0)	21	(22.9 ± 0.9)	6.5 ± 0.3	11.8 ± 0.8
Barrel	9.0–9.8	125	(125.3 ± 4.7)	12	(11.6 ± 0.6)	11.4 ± 0.6	20.2 ± 1.4
Barrel	9.6–10.4	118	(121.9 ± 4.6)	14	(10.7 ± 0.6)	8.8 ± 0.4	15.3 ± 1.1
Barrel	9.9–10.7	102	(119.9 ± 4.5)	11	(10.2 ± 0.6)	10.1 ± 0.5	17.4 ± 1.2
Endcap	9.0–9.8	133	(162.9 ± 5.7)	16	(13.6 ± 0.7)	15.5 ± 0.8	20.5 ± 1.4
Endcap	9.6–10.4	150	(157.1 ± 5.6)	11	(11.7 ± 0.5)	11.7 ± 0.6	15.8 ± 1.1
Endcap	9.9–10.7	171	(156.7 ± 5.8)	7	(11.4 ± 0.6)	13.5 ± 0.7	17.6 ± 1.2

From the fit to the observed data, the largest observed local excess is 1.9σ in the search for $Z \rightarrow J/\psi \gamma$, followed by a 0.8σ excess in the search for $H \rightarrow \psi(2S) \gamma$. The expected and observed 95% CL upper limits on the branching fractions for Higgs and Z boson decays into a quarkonium state and a photon are presented in Table 6, along with the observed upper limits in terms of Higgs and Z boson production cross section times branching fraction to a quarkonium state and a photon. The expected sensitivity improves by a factor of approximately two relative to the previous ATLAS result presented in Ref. [50]; this is in

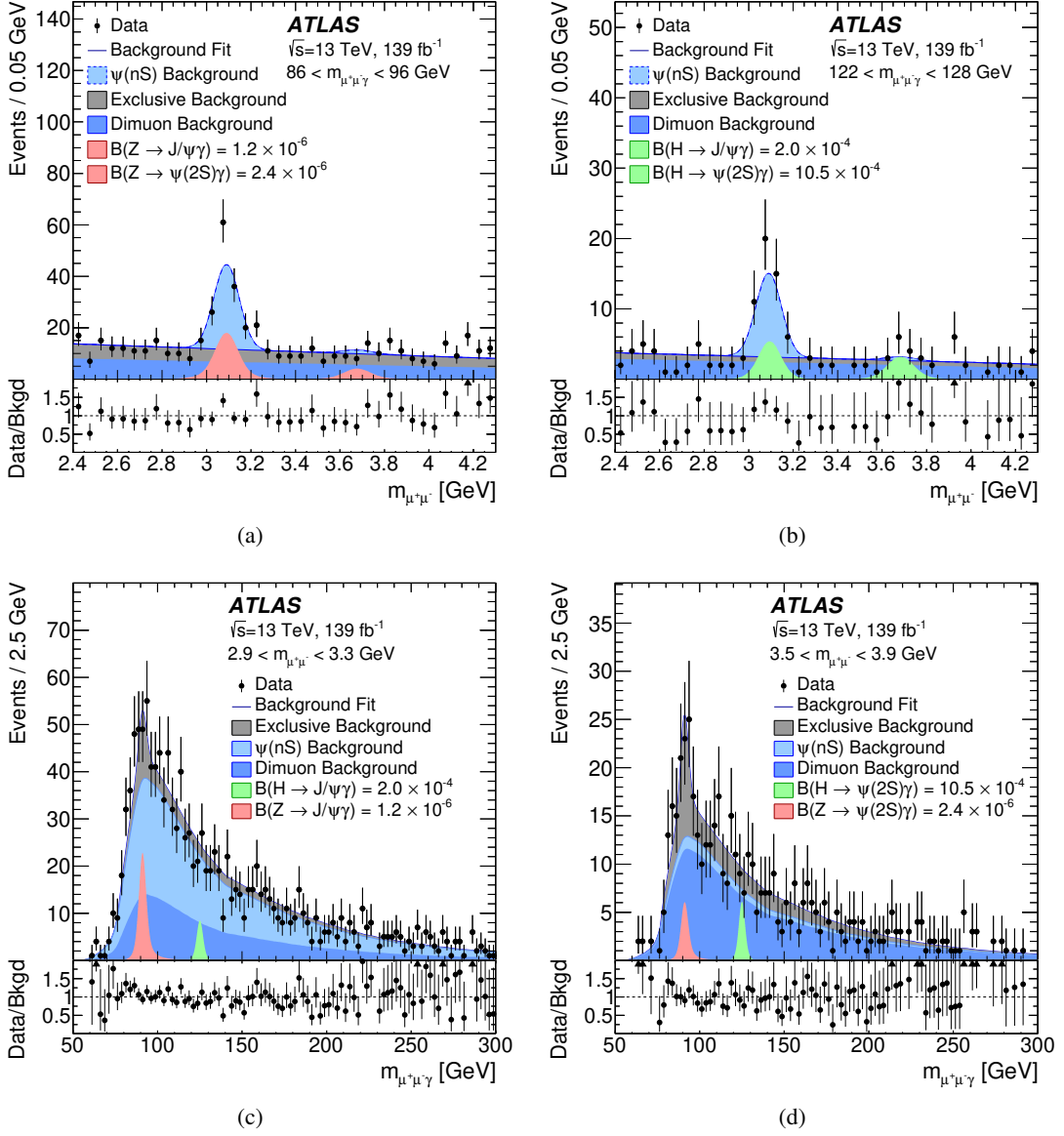


Figure 6: Projection of the $\psi(nS)$ channel fit in $m_{\mu^+\mu^-}$ for the (a) Z boson and (b) Higgs boson $m_{\mu^+\mu^-}\gamma$ regions, and in $m_{\mu^+\mu^-}\gamma$ for the (c) J/ψ and (d) $\psi(2S)$ $m_{\mu^+\mu^-}$ regions. The dimuon/ $Q(nS)$ backgrounds in the legend refer to the inclusive background contribution which is non-resonant/resonant in $m_{\mu^+\mu^-}$. The branching fraction of each of the signals is set to the observed 95% CL upper limit.

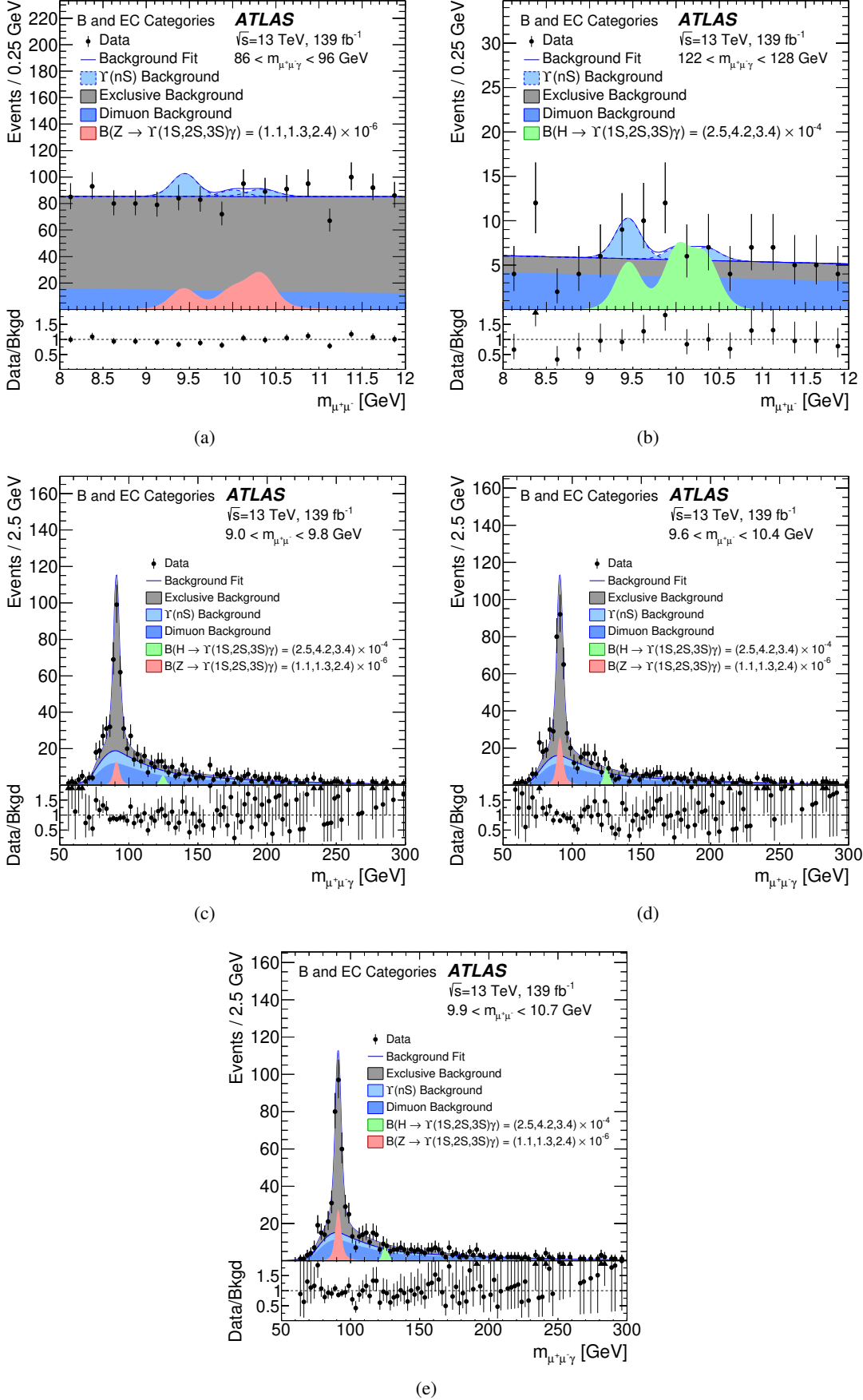


Figure 7: Projection of the $Y(nS)$ channel fit in $m_{\mu^+\mu^-}$ for the (a) Z boson and (b) Higgs boson $m_{\mu^+\mu^-}$ regions, and in $m_{\mu^+\mu^-}$ for the $Y(1S, 2S, 3S)$ $m_{\mu^+\mu^-}$ regions in (c), (d) and (e), respectively. The dimuon/ $Q(nS)$ backgrounds in the legend refer to the inclusive background contribution which is non-resonant/resonant in $m_{\mu^+\mu^-}$. The branching fraction of each of the signals is set to the observed 95% CL upper limit.

line with what is expected from the increase in integrated luminosity for this search, as this analysis is limited primarily by statistical uncertainties. The systematic uncertainties in the signal normalisation and background shape described respectively in Sections 4 and 5 result in a 0.8% increase of the expected 95% CL upper limit on the branching fraction of the $H \rightarrow J/\psi \gamma$ decay. For the $Z \rightarrow J/\psi \gamma$ decay the effect is larger, 4.2%, mostly due to the systematic uncertainty in the background shape. The increase is 0.1% for $H \rightarrow \psi(2S) \gamma$, and 0.6% for $Z \rightarrow \psi(2S) \gamma$. Similar behaviour is observed in the $\Upsilon(nS) \gamma$ analysis, with systematic uncertainties resulting in a 0.1%–0.8% deterioration in the sensitivity to the $H \rightarrow \Upsilon(1S, 2S, 3S) \gamma$ decays and a 0.3%–0.5% deterioration in the sensitivity to the $Z \rightarrow \Upsilon(1S, 2S, 3S) \gamma$ decays.

For the interpretation of these searches in terms of constraints on the charm- and bottom-quark Yukawa couplings the approach presented in Refs. [31, 38] is employed: The ratio of signal strength (μ) measurements for the $H \rightarrow J/\psi \gamma$ and $H \rightarrow \gamma\gamma$ channels corresponds to the ratio of measurements of their production cross section times branching fraction $\sigma \times \mathcal{B}$, normalised to their respective SM expectations. This is, to a good approximation, equal to the ratio of the respective partial decay widths Γ normalised to their SM expectation Γ^{SM} , since the dependence on the production mechanism and Higgs total width cancels out. The ratio κ_c/κ_γ of the coupling modifiers, each of which is the ratio of the coupling to its SM value, for the charm-quark Yukawa coupling and the effective coupling of Higgs boson to photons can be estimated as:

$$\frac{\mu_{H \rightarrow J/\psi \gamma}}{\mu_{H \rightarrow \gamma\gamma}} = \frac{\sigma_H \mathcal{B}_{H \rightarrow J/\psi \gamma} / \sigma_H^{\text{SM}} \mathcal{B}_{H \rightarrow J/\psi \gamma}^{\text{SM}}}{\sigma_H \mathcal{B}_{H \rightarrow \gamma\gamma} / \sigma_H^{\text{SM}} \mathcal{B}_{H \rightarrow \gamma\gamma}^{\text{SM}}} \approx \frac{\Gamma_{H \rightarrow J/\psi \gamma} / \Gamma_{H \rightarrow J/\psi \gamma}^{\text{SM}}}{\Gamma_{H \rightarrow \gamma\gamma} / \Gamma_{H \rightarrow \gamma\gamma}^{\text{SM}}} = \frac{|\mathcal{A}_{\text{ind}} + \mathcal{A}_{\text{dir}} \kappa_c / \kappa_\gamma|^2}{\Gamma_{H \rightarrow J/\psi \gamma}^{\text{SM}}}$$

The indirect and direct amplitudes \mathcal{A} for $H \rightarrow J/\psi \gamma$ and $H \rightarrow \Upsilon(nS) \gamma$ interfere destructively and are obtained from Ref. [36].⁴ The signal strength for $H \rightarrow \gamma\gamma$ is obtained from Ref. [111]. An observed 95% CL interval of $(-133, 175)$ is obtained for κ_c/κ_γ , with the expected interval being $(-120, 161)$. The interval is dominated by the statistical uncertainty of the $H \rightarrow J/\psi \gamma$ search. The correlated components in the uncertainties of the two measurements were removed, but this had negligible impact. The theoretical uncertainties of the amplitudes result in a widening of the obtained interval by approximately 8%, mainly through the uncertainty in the real part of the direct amplitude. Furthermore, the magnitude of the direct amplitude, which is sensitive to the charm-quark coupling to the Higgs boson, is significantly smaller in the most recent theory calculations [34, 36] than in earlier ones [29], leading to much weaker constraints. Very large values of κ_c lead to tensions with other ATLAS [112] and CMS [113] measurements of Higgs boson couplings [114]. A similar relation can be written for the ratio κ_b/κ_γ , where κ_b is the coupling modifier for the bottom-quark Yukawa coupling. Combining the three $\Upsilon(nS) \gamma$ decays, and accounting for the -21% correlation between $\mu_{H \rightarrow \Upsilon(2S) \gamma}$ and $\mu_{H \rightarrow \Upsilon(3S) \gamma}$, a 95% CL interval of $(-37, 40)$ is obtained for κ_b/κ_γ . The corresponding expected 95% CL interval is $(-37, 39)$. The $\Upsilon(1S) \gamma$ decay contributes most of the sensitivity to κ_b/κ_γ thanks to its indirect amplitude being the largest amongst the $\Upsilon(nS) \gamma$ decays. Similarly to the κ_c/κ_γ case, the statistical uncertainty of the search for exclusive Higgs boson decays into $\Upsilon(nS) \gamma$ dominates the interval. The theoretical uncertainties of the amplitudes enlarge the interval by 12%.

⁴ The corresponding direct and indirect amplitude values for $H \rightarrow \psi(2S) \gamma$ could not be obtained from the literature.

Table 6: Expected, with the corresponding $\pm 1\sigma$ intervals, and observed 95% CL branching fraction upper limits for the Higgs and Z boson decays into a quarkonium state and a photon. Standard Model production of the Higgs boson is assumed. The corresponding upper limits on the production cross section times branching fraction $\sigma \times \mathcal{B}$ are also shown.

Decay channel	95% CL upper limits					
	Branching fraction				$\sigma \times \mathcal{B}$	
	Higgs boson [10^{-4}]		Z boson [10^{-6}]		Higgs boson [fb]	Z boson [fb]
	Expected	Observed	Expected	Observed	Observed	Observed
$J/\psi \gamma$	$1.8^{+0.8}_{-0.5}$	2.0	$0.7^{+0.3}_{-0.2}$	1.2	11	69
$\psi(2S) \gamma$	$8.1^{+3.6}_{-2.3}$	10.5	$3.0^{+1.3}_{-0.8}$	2.4	58	142
$\Upsilon(1S) \gamma$	$2.7^{+1.2}_{-0.8}$	2.5	$1.6^{+0.6}_{-0.4}$	1.1	14	62
$\Upsilon(2S) \gamma$	$3.4^{+1.5}_{-1.0}$	4.2	$2.1^{+0.8}_{-0.6}$	1.3	24	74
$\Upsilon(3S) \gamma$	$3.0^{+1.3}_{-0.8}$	3.4	$1.9^{+0.8}_{-0.5}$	2.4	19	143

8 Summary

Searches for the exclusive decays of Higgs and Z bosons into a vector quarkonium state and a photon have been performed with a $\sqrt{s} = 13$ TeV pp collision data sample collected with the ATLAS detector at the LHC and corresponding to an integrated luminosity of 139 fb^{-1} . The observed data are compatible with the background expectations. The 95% CL upper limits obtained for the $J/\psi \gamma$ final state are $\mathcal{B}(H \rightarrow J/\psi \gamma) < 2.0 \times 10^{-4}$ and $\mathcal{B}(Z \rightarrow J/\psi \gamma) < 1.2 \times 10^{-6}$. The corresponding upper limits for the $\psi(2S) \gamma$ final state are $\mathcal{B}(H \rightarrow \psi(2S) \gamma) < 10.5 \times 10^{-4}$ and $\mathcal{B}(Z \rightarrow \psi(2S) \gamma) < 2.4 \times 10^{-6}$. The 95% CL upper limits $\mathcal{B}(H \rightarrow \Upsilon(nS) \gamma) < (2.5, 4.2, 3.4) \times 10^{-4}$ and $\mathcal{B}(Z \rightarrow \Upsilon(nS) \gamma) < (1.1, 1.3, 2.4) \times 10^{-6}$ are set for the $\Upsilon(1S, 2S, 3S) \gamma$ final states. These upper limits represent an improvement by a factor of approximately two relative to the previous results from the ATLAS Collaboration using 36.1 fb^{-1} of $\sqrt{s} = 13$ TeV pp collision data. Further, constraints are set on the ratio κ_c/κ_γ and κ_b/κ_γ of the Higgs boson coupling modifiers. An observed 95% CL interval of $(-133, 175)$ is obtained for κ_c/κ_γ , and a 95% CL interval of $(-37, 40)$ is obtained for κ_b/κ_γ .

Acknowledgements

We thank CERN for the very successful operation of the LHC, as well as the support staff from our institutions without whom ATLAS could not be operated efficiently.

We acknowledge the support of ANPCyT, Argentina; YerPhI, Armenia; ARC, Australia; BMWFW and FWF, Austria; ANAS, Azerbaijan; CNPq and FAPESP, Brazil; NSERC, NRC and CFI, Canada; CERN; ANID, Chile; CAS, MOST and NSFC, China; Minciencias, Colombia; MEYS CR, Czech Republic; DNRF and DNSRC, Denmark; IN2P3-CNRS and CEA-DRF/IRFU, France; SRNSFG, Georgia; BMBF, HGF and MPG, Germany; GSRI, Greece; RGC and Hong Kong SAR, China; ISF and Benozziyo Center, Israel; INFN, Italy; MEXT and JSPS, Japan; CNRST, Morocco; NWO, Netherlands; RCN, Norway; MEiN, Poland; FCT, Portugal; MNE/IFA, Romania; MESTD, Serbia; MSSR, Slovakia; ARRS and MIZŠ, Slovenia; DSI/NRF, South Africa; MICINN, Spain; SRC and Wallenberg Foundation, Sweden; SERI, SNSF and Cantons of

Bern and Geneva, Switzerland; MOST, Taiwan; TENMAK, Türkiye; STFC, United Kingdom; DOE and NSF, United States of America. In addition, individual groups and members have received support from BCKDF, CANARIE, Compute Canada and CRC, Canada; PRIMUS 21/SCI/017 and UNCE SCI/013, Czech Republic; COST, ERC, ERDF, Horizon 2020 and Marie Skłodowska-Curie Actions, European Union; Investissements d’Avenir Labex, Investissements d’Avenir Idex and ANR, France; DFG and AvH Foundation, Germany; Herakleitos, Thales and Aristeia programmes co-financed by EU-ESF and the Greek NSRF, Greece; BSF-NSF and MINERVA, Israel; Norwegian Financial Mechanism 2014-2021, Norway; NCN and NAWA, Poland; La Caixa Banking Foundation, CERCA Programme Generalitat de Catalunya and PROMETEO and GenT Programmes Generalitat Valenciana, Spain; Göran Gustafssons Stiftelse, Sweden; The Royal Society and Leverhulme Trust, United Kingdom.

The crucial computing support from all WLCG partners is acknowledged gratefully, in particular from CERN, the ATLAS Tier-1 facilities at TRIUMF (Canada), NDGF (Denmark, Norway, Sweden), CC-IN2P3 (France), KIT/GridKA (Germany), INFN-CNAF (Italy), NL-T1 (Netherlands), PIC (Spain), ASGC (Taiwan), RAL (UK) and BNL (USA), the Tier-2 facilities worldwide and large non-WLCG resource providers. Major contributors of computing resources are listed in Ref. [115].

References

- [1] ATLAS Collaboration, *The ATLAS Experiment at the CERN Large Hadron Collider*, [JINST **3** \(2008\) S08003](#).
- [2] CMS Collaboration, *The CMS experiment at the CERN LHC*, [JINST **3** \(2008\) S08004](#).
- [3] ATLAS Collaboration, *Observation of a new particle in the search for the Standard Model Higgs boson with the ATLAS detector at the LHC*, [Phys. Lett. B **716** \(2012\) 1](#), arXiv: [1207.7214 \[hep-ex\]](#).
- [4] CMS Collaboration, *Observation of a new boson at a mass of 125 GeV with the CMS experiment at the LHC*, [Phys. Lett. B **716** \(2012\) 30](#), arXiv: [1207.7235 \[hep-ex\]](#).
- [5] ATLAS Collaboration, *A detailed map of Higgs boson interactions by the ATLAS experiment ten years after the discovery*, [Nature **607** \(2022\) 52](#), arXiv: [2207.00092 \[hep-ex\]](#).
- [6] CMS Collaboration, *A portrait of the Higgs boson by the CMS experiment ten years after the discovery*, [Nature **607** \(2022\) 60](#), arXiv: [2207.00043 \[hep-ex\]](#).
- [7] F. Englert and R. Brout, *Broken symmetry and the mass of gauge vector mesons*, [Phys. Rev. Lett. **13** \(1964\) 321](#).
- [8] P. W. Higgs, *Broken symmetries, massless particles and gauge fields*, [Phys. Lett. **12** \(1964\) 132](#).
- [9] ATLAS Collaboration, *Measurements of Higgs boson production cross-sections in the $H \rightarrow \tau^+ \tau^-$ decay channel in pp collisions at $\sqrt{s} = 13$ TeV with the ATLAS detector*, [JHEP **08** \(2022\) 175](#), arXiv: [2201.08269 \[hep-ex\]](#).
- [10] CMS Collaboration, *Measurements of Higgs boson production in the decay channel with a pair of τ leptons in proton–proton collisions at $\sqrt{s} = 13$ TeV*, (2022), arXiv: [2204.12957 \[hep-ex\]](#).

- [11] ATLAS Collaboration, *Observation of $H \rightarrow b\bar{b}$ decays and VH production with the ATLAS detector*, *Phys. Lett. B* **786** (2018) 59, arXiv: [1808.08238 \[hep-ex\]](#).
- [12] CMS Collaboration, *Observation of Higgs Boson Decay to Bottom Quarks*, *Phys. Rev. Lett.* **121** (2018) 121801, arXiv: [1808.08242 \[hep-ex\]](#).
- [13] ATLAS Collaboration, *Observation of Higgs boson production in association with a top quark pair at the LHC with the ATLAS detector*, *Phys. Lett. B* **784** (2018) 173, arXiv: [1806.00425 \[hep-ex\]](#).
- [14] CMS Collaboration, *Observation of $t\bar{t}H$ Production*, *Phys. Rev. Lett.* **120** (2018) 231801, arXiv: [1804.02610 \[hep-ex\]](#).
- [15] CMS Collaboration, *Evidence for Higgs boson decay to a pair of muons*, *JHEP* **01** (2021) 148, arXiv: [2009.04363 \[hep-ex\]](#).
- [16] ATLAS Collaboration, *A search for the dimuon decay of the Standard Model Higgs boson with the ATLAS detector*, *Phys. Lett. B* **812** (2021) 135980, arXiv: [2007.07830 \[hep-ex\]](#).
- [17] ATLAS Collaboration, *Search for the Decay of the Higgs Boson to Charm Quarks with the ATLAS Experiment*, *Phys. Rev. Lett.* **120** (2018) 211802, arXiv: [1802.04329 \[hep-ex\]](#).
- [18] ATLAS Collaboration, *Direct constraint on the Higgs-charm coupling from a search for Higgs boson decays into charm quarks with the ATLAS detector*, (2022), arXiv: [2201.11428 \[hep-ex\]](#).
- [19] CMS Collaboration, *A search for the standard model Higgs boson decaying to charm quarks*, *JHEP* **03** (2020) 131, arXiv: [1912.01662 \[hep-ex\]](#).
- [20] CMS Collaboration, *Search for Higgs boson decay to a charm quark-antiquark pair in proton-proton collisions at $\sqrt{s} = 13$ TeV*, (2022), arXiv: [2205.05550 \[hep-ex\]](#).
- [21] ATLAS Collaboration, *Search for the Higgs boson decays $H \rightarrow ee$ and $H \rightarrow e\mu$ in pp collisions at $\sqrt{s} = 13$ TeV with the ATLAS detector*, *Phys. Lett. B* **801** (2020) 135148, arXiv: [1909.10235 \[hep-ex\]](#).
- [22] CMS Collaboration, *Search for a standard model-like Higgs boson in the $\mu^+\mu^-$ and e^+e^- decay channels at the LHC*, *Phys. Lett. B* **744** (2015) 184, arXiv: [1410.6679 \[hep-ex\]](#).
- [23] ATLAS Collaboration, *Search for top quark decays $t \rightarrow qH$, with $H \rightarrow \gamma\gamma$, in $\sqrt{s} = 13$ TeV pp collisions using the ATLAS detector*, *JHEP* **10** (2017) 129, arXiv: [1707.01404 \[hep-ex\]](#).
- [24] ATLAS Collaboration, *Search for flavor-changing neutral currents in top quark decays $t \rightarrow Hc$ and $t \rightarrow Hu$ in multilepton final states in proton-proton collisions at $\sqrt{s} = 13$ TeV with the ATLAS detector*, *Phys. Rev. D* **98** (2018) 032002, arXiv: [1805.03483 \[hep-ex\]](#).
- [25] CMS Collaboration, *Search for flavor-changing neutral current interactions of the top quark and the Higgs boson decaying to a bottom quark-antiquark pair at $\sqrt{s} = 13$ TeV*, *JHEP* **02** (2021) 169, arXiv: [2112.09734 \[hep-ex\]](#).
- [26] CMS Collaboration, *Search for flavor-changing neutral current interactions of the top quark and Higgs boson in final states with two photons in proton-proton collisions at $\sqrt{s} = 13$ TeV*, (2021), arXiv: [2111.02219 \[hep-ex\]](#).

- [27] ATLAS Collaboration, *Searches for lepton-flavour-violating decays of the Higgs boson in $\sqrt{s} = 13$ TeV pp collisions with the ATLAS detector*, *Phys. Lett. B* **800** (2020) 135069, arXiv: [1907.06131 \[hep-ex\]](#).
- [28] CMS Collaboration, *Search for lepton-flavor violating decays of the Higgs boson in the $\mu\tau$ and $e\tau$ final states in proton-proton collisions at $\sqrt{s} = 13$ TeV*, *Phys. Rev. D* **104** (2021) 032013, arXiv: [2105.03007 \[hep-ex\]](#).
- [29] G. Bodwin, F. Petriello, S. Stoynev and M. Velasco, *Higgs boson decays to quarkonia and the $H\bar{c}c$ coupling*, *Phys. Rev. D* **88** (2013) 053003, arXiv: [1306.5770 \[hep-ph\]](#).
- [30] M. Doroshenko, V. Kartvelishvili, E. Chikovani and S. Esakiya, *Vector quarkonium in decays of heavy Higgs particles*, *Yad. Fiz.* **46** (1987) 864.
- [31] M. König and M. Neubert, *Exclusive radiative Higgs decays as probes of light-quark Yukawa couplings*, *JHEP* **08** (2015) 012, arXiv: [1505.03870 \[hep-ph\]](#).
- [32] G. T. Bodwin, H. S. Chung, J.-H. Ee, J. Lee and F. Petriello, *Relativistic corrections to Higgs-boson decays to quarkonia*, *Phys. Rev. D* **90** (2014) 113010, arXiv: [1407.6695 \[hep-ph\]](#).
- [33] G. T. Bodwin, H. S. Chung, J.-H. Ee and J. Lee, *New approach to the resummation of logarithms in Higgs-boson decays to a vector quarkonium plus a photon*, *Phys. Rev. D* **95** (2017) 054018, arXiv: [1603.06793 \[hep-ph\]](#).
- [34] G. T. Bodwin, H. S. Chung, J.-H. Ee and J. Lee, *Addendum: New approach to the resummation of logarithms in Higgs-boson decays to a vector quarkonium plus a photon [Phys. Rev. D 95, 054018 (2017)]*, *Phys. Rev. D* **96** (2017) 116014, arXiv: [1710.09872 \[hep-ph\]](#).
- [35] C. Zhou, M. Song, G. Li, Y.-J. Zhou and J.-Y. Guo, *Next-to-leading order QCD corrections to Higgs boson decay to quarkonium plus a photon*, *Chin. Phys. C* **40** (2016) 123105, arXiv: [1607.02704 \[hep-ph\]](#).
- [36] N. Brambilla, H. S. Chung, W. K. Lai, V. Shtabovenko and A. Vairo, *Order v^4 corrections to Higgs boson decay into $J/\psi + \gamma$* , *Phys. Rev. D* **100** (2019) 054038, arXiv: [1907.06473 \[hep-ph\]](#).
- [37] D. de Florian et al., *Handbook of LHC Higgs Cross Sections: 4. Deciphering the Nature of the Higgs Sector*, (2016), arXiv: [1610.07922 \[hep-ph\]](#).
- [38] G. Perez, Y. Soreq, E. Stamou and K. Tobioka, *Constraining the charm Yukawa and Higgs-quark coupling universality*, *Phys. Rev. D* **92** (2015) 033016, arXiv: [1503.00290 \[hep-ph\]](#).
- [39] C. D. Froggatt and H. B. Nielsen, *Hierarchy of quark masses, cabibbo angles and CP violation*, *Nucl. Phys. B* **147** (1979) 277.
- [40] L. Randall and R. Sundrum, *Large Mass Hierarchy from a Small Extra Dimension*, *Phys. Rev. Lett.* **83** (1999) 3370, arXiv: [hep-ph/9905221](#).
- [41] G. D'Ambrosio, G. F. Giudice, G. Isidori and A. Strumia, *Minimal flavor violation: an effective field theory approach*, *Nucl. Phys. B* **645** (2002) 155, arXiv: [hep-ph/0207036](#).

- [42] G. F. Giudice and O. Lebedev, *Higgs-dependent Yukawa couplings*, *Phys. Lett. B* **665** (2008) 79, arXiv: [0804.1753 \[hep-ph\]](#).
- [43] M. J. Dugan, H. Georgi and D. B. Kaplan, *Anatomy of a composite Higgs model*, *Nucl. Phys. B* **254** (1985) 299.
- [44] ATLAS Collaboration, *Measurement of W^\pm and Z-boson production cross sections in pp collisions at $\sqrt{s} = 13$ TeV with the ATLAS detector*, *Phys. Lett. B* **759** (2016) 601, arXiv: [1603.09222 \[hep-ex\]](#).
- [45] A. Dainese et al., *Report on the Physics at the HL-LHC, and Perspectives for the HE-LHC*, (2019), URL: <https://cds.cern.ch/record/2703572>.
- [46] Y. Grossman, M. König and M. Neubert, *Exclusive radiative decays of W and Z bosons in QCD factorization*, *JHEP* **04** (2015) 101, arXiv: [1501.06569 \[hep-ph\]](#).
- [47] T.-C. Huang and F. Petriello, *Rare exclusive decays of the Z boson revisited*, *Phys. Rev. D* **92** (2015) 014007, arXiv: [1411.5924 \[hep-ph\]](#).
- [48] G. T. Bodwin, H. S. Chung, J.-H. Ee and J. Lee, *Z-boson decays to a vector quarkonium plus a photon*, *Phys. Rev. D* **97** (2018) 016009, arXiv: [1709.09320 \[hep-ph\]](#).
- [49] ATLAS Collaboration, *Search for Higgs and Z Boson Decays to $J/\psi\gamma$ and $\Upsilon(nS)\gamma$ with the ATLAS Detector*, *Phys. Rev. Lett.* **114** (2015) 121801, arXiv: [1501.03276 \[hep-ex\]](#).
- [50] ATLAS Collaboration, *Searches for exclusive Higgs and Z boson decays into $J/\psi\gamma$, $\psi(2S)\gamma$, and $\Upsilon(nS)\gamma$ at $\sqrt{s} = 13$ TeV with the ATLAS detector*, *Phys. Lett. B* **786** (2018) 134, arXiv: [1807.00802 \[hep-ex\]](#).
- [51] CMS Collaboration, *Search for a Higgs boson decaying into $\gamma^*\gamma \rightarrow \ell\ell\gamma$ with low dilepton mass in pp collisions at $\sqrt{s} = 8$ TeV*, *Phys. Lett. B* **753** (2016) 341, arXiv: [1507.03031 \[hep-ex\]](#).
- [52] CMS Collaboration, *Search for rare decays of Z and Higgs bosons to J/ψ and a photon in proton-proton collisions at $\sqrt{s} = 13$ TeV*, *Eur. Phys. J. C* **79** (2019) 94, arXiv: [1810.10056 \[hep-ex\]](#).
- [53] ATLAS Collaboration, *Search for Higgs and Z Boson Decays to $\phi\gamma$ with the ATLAS Detector*, *Phys. Rev. Lett.* **117** (2016) 111802, arXiv: [1607.03400 \[hep-ex\]](#).
- [54] ATLAS Collaboration, *Search for exclusive Higgs and Z boson decays to $\phi\gamma$ and $\rho\gamma$ with the ATLAS detector*, *JHEP* **07** (2018) 127, arXiv: [1712.02758 \[hep-ex\]](#).
- [55] CMS Collaboration, *Search for decays of the 125 GeV Higgs boson into a Z boson and a ρ or ϕ meson*, *JHEP* **11** (2020) 039, arXiv: [2007.05122 \[hep-ex\]](#).
- [56] CMS Collaboration, *Search for Higgs and Z boson decays to J/ψ or Υ pairs in the four-muon final state in proton-proton collisions at $\sqrt{s} = 13$ TeV*, *Phys. Lett. B* **797** (2019) 134811, arXiv: [1905.10408 \[hep-ex\]](#).
- [57] LHC Higgs Cross Section Working Group, *Handbook of LHC Higgs Cross Sections: 3. Higgs Properties*, CERN-2013-004 (CERN, Geneva, 2013), arXiv: [1307.1347 \[hep-ph\]](#).

- [58] ATLAS Collaboration, *ATLAS Insertable B-Layer: Technical Design Report*, ATLAS-TDR-19; CERN-LHCC-2010-013, 2010, URL: <https://cds.cern.ch/record/1291633>, Addendum: ATLAS-TDR-19-ADD-1; CERN-LHCC-2012-009, 2012, URL: <https://cds.cern.ch/record/1451888>.
- [59] ATLAS IBL Collaboration, *Production and integration of the ATLAS Insertable B-Layer*, *JINST* **13** (2018) T05008, arXiv: [1803.00844](https://arxiv.org/abs/1803.00844) [[physics.ins-det](#)].
- [60] ATLAS Collaboration, *Performance of the ATLAS trigger system in 2015*, *Eur. Phys. J. C* **77** (2017) 317, arXiv: [1611.09661](https://arxiv.org/abs/1611.09661) [[hep-ex](#)].
- [61] ATLAS Collaboration, *The ATLAS Collaboration Software and Firmware*, ATL-SOFT-PUB-2021-001, 2021, URL: <https://cds.cern.ch/record/2767187>.
- [62] ATLAS Collaboration, *ATLAS data quality operations and performance for 2015–2018 data-taking*, *JINST* **15** (2020) P04003, arXiv: [1911.04632](https://arxiv.org/abs/1911.04632) [[physics.ins-det](#)].
- [63] ATLAS Collaboration, *Electron and photon performance measurements with the ATLAS detector using the 2015–2017 LHC proton-proton collision data*, *JINST* **14** (2019) P12006, arXiv: [1908.00005](https://arxiv.org/abs/1908.00005) [[hep-ex](#)].
- [64] ATLAS Collaboration, *Performance of electron and photon triggers in ATLAS during LHC Run 2*, *Eur. Phys. J. C* **80** (2020) 47, arXiv: [1909.00761](https://arxiv.org/abs/1909.00761) [[hep-ex](#)].
- [65] ATLAS Collaboration, *Performance of the ATLAS muon triggers in Run 2*, *JINST* **15** (2020) P09015, arXiv: [2004.13447](https://arxiv.org/abs/2004.13447) [[hep-ex](#)].
- [66] G. Avoni et al., *The new LUCID-2 detector for luminosity measurement and monitoring in ATLAS*, *JINST* **13** (2018) P07017.
- [67] ATLAS Collaboration, *Luminosity determination in pp collisions at $\sqrt{s} = 8$ TeV using the ATLAS detector at the LHC*, *Eur. Phys. J. C* **76** (2016) 653, arXiv: [1608.03953](https://arxiv.org/abs/1608.03953) [[hep-ex](#)].
- [68] ATLAS Collaboration, *Luminosity determination in pp collisions at $\sqrt{s} = 13$ TeV using the ATLAS detector at the LHC*, ATLAS-CONF-2019-021, 2019, URL: <https://cds.cern.ch/record/2677054>.
- [69] ATLAS Collaboration, *Measurement of the muon reconstruction performance of the ATLAS detector using 2011 and 2012 LHC proton–proton collision data*, *Eur. Phys. J. C* **74** (2014) 3130, arXiv: [1407.3935](https://arxiv.org/abs/1407.3935) [[hep-ex](#)].
- [70] V. Kostyukhin, *VKalVrt - package for vertex reconstruction in ATLAS*, ATL-PHYS-2003-031, CERN, 2003, URL: <https://cds.cern.ch/record/685551>.
- [71] ATLAS Collaboration, *Muon reconstruction and identification efficiency in ATLAS using the full Run 2 pp collision data set at $\sqrt{s} = 13$ TeV*, *Eur. Phys. J. C* **81** (2021) 578, arXiv: [2012.00578](https://arxiv.org/abs/2012.00578) [[hep-ex](#)].
- [72] P. Nason, *A new method for combining NLO QCD with shower Monte Carlo algorithms*, *JHEP* **11** (2004) 040, arXiv: [hep-ph/0409146](https://arxiv.org/abs/hep-ph/0409146).
- [73] S. Frixione, P. Nason and C. Oleari, *Matching NLO QCD computations with parton shower simulations: the POWHEG method*, *JHEP* **11** (2007) 070, arXiv: [0709.2092](https://arxiv.org/abs/0709.2092) [[hep-ph](#)].

- [74] S. Alioli, P. Nason, C. Oleari and E. Re, *A general framework for implementing NLO calculations in shower Monte Carlo programs: the POWHEG BOX*, *JHEP* **06** (2010) 043, arXiv: [1002.2581 \[hep-ph\]](#).
- [75] S. Alioli, P. Nason, C. Oleari and E. Re, *NLO Higgs boson production via gluon fusion matched with shower in POWHEG*, *JHEP* **04** (2009) 002, arXiv: [0812.0578 \[hep-ph\]](#).
- [76] P. Nason and C. Oleari, *NLO Higgs boson production via vector-boson fusion matched with shower in POWHEG*, *JHEP* **02** (2010) 037, arXiv: [0911.5299 \[hep-ph\]](#).
- [77] T. Sjöstrand, S. Mrenna and P. Z. Skands, *A brief introduction to PYTHIA 8.1*, *Comput. Phys. Commun.* **178** (2008) 852, arXiv: [0710.3820 \[hep-ph\]](#).
- [78] T. Sjöstrand, S. Mrenna and P. Z. Skands, *PYTHIA 6.4 physics and manual*, *JHEP* **05** (2006) 026, arXiv: [hep-ph/0603175](#).
- [79] J. Pumplin et al., *New Generation of Parton Distributions with Uncertainties from Global QCD Analysis*, *JHEP* **07** (2002) 012, arXiv: [hep-ph/0201195](#).
- [80] ATLAS Collaboration, *Measurement of the Z/γ^* boson transverse momentum distribution in pp collisions at $\sqrt{s} = 7$ TeV with the ATLAS detector*, *JHEP* **09** (2014) 145, arXiv: [1406.3660 \[hep-ex\]](#).
- [81] NNPDF Collaboration, *Parton distributions with LHC data*, *Nucl. Phys. B* **867** (2013) 244, arXiv: [1207.1303 \[hep-ph\]](#).
- [82] ATLAS Collaboration, *ATLAS Pythia8 tunes to 7 TeV data*, (2014), URL: <https://cds.cern.ch/record/1966419>.
- [83] J. Alwall et al., *The automated computation of tree-level and next-to-leading order differential cross sections, and their matching to parton shower simulations*, *JHEP* **07** (2014) 079, arXiv: [1405.0301 \[hep-ph\]](#).
- [84] E. Jones and W. J. Murray, *Mass biases in exclusive radiative hadronic decays of W bosons at the LHC*, *New J. Phys.* **23** (2021) 113035, arXiv: [2009.01073 \[hep-ex\]](#).
- [85] S. Agostinelli et al., *GEANT4: a simulation toolkit*, *Nucl. Instrum. Meth. A* **506** (2003) 250.
- [86] ATLAS Collaboration, *The ATLAS Simulation Infrastructure*, *Eur. Phys. J. C* **70** (2010) 823, arXiv: [1005.4568 \[physics.ins-det\]](#).
- [87] ATLAS Collaboration, *The Pythia 8 A3 tune description of ATLAS minimum bias and inelastic measurements incorporating the Donnachie-Landshoff diffractive model*, (2016), URL: <https://cds.cern.ch/record/2206965>.
- [88] C. Anastasiou, C. Duhr, F. Dulat, F. Herzog and B. Mistlberger, *Higgs Boson Gluon-Fusion Production in QCD at Three Loops*, *Phys. Rev. Lett.* **114** (2015) 212001, arXiv: [1503.06056 \[hep-ph\]](#).
- [89] C. Anastasiou et al., *High precision determination of the gluon fusion Higgs boson cross-section at the LHC*, *JHEP* **05** (2016) 058, arXiv: [1602.00695 \[hep-ph\]](#).

- [90] S. Actis, G. Passarino, C. Sturm and S. Uccirati, *NLO electroweak corrections to Higgs boson production at hadron colliders*, *Phys. Lett. B* **670** (2008) 12, arXiv: [0809.1301 \[hep-ph\]](#).
- [91] C. Anastasiou, R. Boughezal and F. Petriello, *Mixed QCD-electroweak corrections to Higgs boson production in gluon fusion*, *JHEP* **04** (2009) 003, arXiv: [0811.3458 \[hep-ph\]](#).
- [92] M. Ciccolini, A. Denner and S. Dittmaier, *Strong and Electroweak Corrections to the Production of a Higgs Boson + 2 Jets via Weak Interactions at the Large Hadron Collider*, *Phys. Rev. Lett.* **99** (2007) 161803, arXiv: [0707.0381 \[hep-ph\]](#).
- [93] M. Ciccolini, A. Denner and S. Dittmaier, *Electroweak and QCD corrections to Higgs production via vector-boson fusion at the LHC*, *Phys. Rev. D* **77** (2008) 013002, arXiv: [0710.4749 \[hep-ph\]](#).
- [94] P. Bolzoni, F. Maltoni, S.-O. Moch and M. Zaro, *Higgs Boson Production via Vector-Boson Fusion at Next-to-Next-to-Leading Order in QCD*, *Phys. Rev. Lett.* **105** (2010) 011801, arXiv: [1003.4451 \[hep-ph\]](#).
- [95] O. Brein, A. Djouadi and R. Harlander, *NNLO QCD corrections to the Higgs-strahlung processes at hadron colliders*, *Phys. Lett. B* **579** (2004) 149, arXiv: [hep-ph/0307206 \[hep-ph\]](#).
- [96] A. Denner, S. Dittmaier, S. Kallweit and A. Mück, *Electroweak corrections to Higgs-strahlung off W/Z bosons at the Tevatron and the LHC with HAWK*, *JHEP* **03** (2012) 075, arXiv: [1112.5142 \[hep-ph\]](#).
- [97] L. Altenkamp, S. Dittmaier, R. V. Harlander, H. Rzehak and T. J. E. Zirke, *Gluon-induced Higgs-strahlung at next-to-leading order QCD*, *JHEP* **02** (2013) 078, arXiv: [1211.5015 \[hep-ph\]](#).
- [98] P. Zyla et al. (Particle Data Group), *Review of Particle Physics*, *PTEP* **2020** (2020) 083C01, and 2021 update.
- [99] ATLAS Collaboration, *Measurement of the transverse momentum distribution of Drell–Yan lepton pairs in proton–proton collisions at $\sqrt{s} = 13$ TeV with the ATLAS detector*, *Eur. Phys. J. C* **80** (2020) 616, arXiv: [1912.02844 \[hep-ex\]](#).
- [100] ATLAS Collaboration, *Performance of the Electron and Photon Trigger in p-p Collisions at $\sqrt{s} = 7$ TeV with the ATLAS Detector at the LHC*, ATLAS-CONF-2011-114 (2011), URL: <http://cds.cern.ch/record/1375551>.
- [101] ATLAS Collaboration, *Measurement of the photon identification efficiencies with the ATLAS detector using LHC Run-1 data*, *Eur. Phys. J. C* **76** (2016) 666, arXiv: [1606.01813 \[hep-ex\]](#).
- [102] ATLAS Collaboration, *Photon identification in 2015 ATLAS data*, ATL-PHYS-PUB-2016-014, CERN, 2016, URL: <https://cds.cern.ch/record/2203125>.
- [103] ATLAS Collaboration, *Muon reconstruction performance of the ATLAS detector in proton–proton collision data at $\sqrt{s} = 13$ TeV*, *Eur. Phys. J. C* **76** (2016) 292, arXiv: [1603.05598 \[hep-ex\]](#).
- [104] ATLAS Collaboration, *Electron and photon energy calibration with the ATLAS detector using LHC Run 1 data*, *Eur. Phys. J. C* **74** (2014) 3071, arXiv: [1407.5063 \[hep-ex\]](#).

- [105] ATLAS Collaboration, *Electron and photon energy calibration with the ATLAS detector using data collected in 2015 at $\sqrt{s}=13$ TeV*, ATL-PHYS-PUB-2016-015, CERN, 2016, URL: <https://cds.cern.ch/record/2203514>.
- [106] A. Chisholm et al., *Non-Parametric Data-Driven Background Modelling using Conditional Probabilities*, (2021), arXiv: [2112.00650](https://arxiv.org/abs/2112.00650) [[hep-ex](#)].
- [107] T. Gleisberg et al., *Event generation with SHERPA 1.1*, *JHEP* **02** (2009) 007, arXiv: [0811.4622](https://arxiv.org/abs/0811.4622) [[hep-ph](#)].
- [108] K. Cranmer, *Kernel estimation in high-energy physics*, *Comput. Phys. Commun.* **136** (2001) 198, arXiv: [hep-ex/0011057](https://arxiv.org/abs/hep-ex/0011057).
- [109] A. L. Read, *Presentation of search results: the CL_s technique*, *J. Phys. G* **28** (2002) 2693.
- [110] G. Cowan, K. Cranmer, E. Gross and O. Vitells, *Asymptotic formulae for likelihood-based tests of new physics*, *Eur. Phys. J. C* **71** (2011) 1554, arXiv: [1007.1727](https://arxiv.org/abs/1007.1727) [[physics.data-an](#)], Erratum: *Eur. Phys. J. C* **73** (2013) 2501.
- [111] ATLAS Collaboration, *Measurement of the properties of Higgs boson production at $\sqrt{s}=13$ TeV in the $H \rightarrow \gamma\gamma$ channel using 139 fb^{-1} of pp collision data with the ATLAS experiment*, (2020), URL: <https://cds.cern.ch/record/2725727>.
- [112] ATLAS Collaboration, *Combined measurements of Higgs boson production and decay using up to 80 fb^{-1} of proton–proton collision data at $\sqrt{s} = 13$ TeV collected with the ATLAS experiment*, *Phys. Rev. D* **101** (2020) 012002, arXiv: [1909.02845](https://arxiv.org/abs/1909.02845) [[hep-ex](#)].
- [113] CMS Collaboration, *Combined measurements of Higgs boson couplings in proton–proton collisions at $\sqrt{s} = 13$ TeV*, *Eur. Phys. J. C* **79** (2019) 421, arXiv: [1809.10733](https://arxiv.org/abs/1809.10733) [[hep-ex](#)].
- [114] N. M. Coyle, C. E. M. Wagner and V. Wei, *Bounding the charm Yukawa coupling*, *Phys. Rev. D* **100** (2019) 073013, arXiv: [1905.09360](https://arxiv.org/abs/1905.09360) [[hep-ph](#)].
- [115] ATLAS Collaboration, *ATLAS Computing Acknowledgements*, ATL-SOFT-PUB-2021-003, 2021, URL: <https://cds.cern.ch/record/2776662>.

The ATLAS Collaboration

G. Aad ¹⁰¹, B. Abbott ¹¹⁹, D.C. Abbott ¹⁰², K. Abeling ⁵⁵, S.H. Abidi ²⁹, A. Aboulhorma ^{35e}, H. Abramowicz ¹⁵⁰, H. Abreu ¹⁴⁹, Y. Abulaiti ¹¹⁶, A.C. Abusleme Hoffman ^{136a}, B.S. Acharya ^{68a,68b,p}, B. Achkar ⁵⁵, C. Adam Bourdarios ⁴, L. Adamczyk ^{84a}, L. Adamek ¹⁵⁴, S.V. Addepalli ²⁶, J. Adelman ¹¹⁴, A. Adiguzel ^{21c}, S. Adorni ⁵⁶, T. Adye ¹³³, A.A. Affolder ¹³⁵, Y. Afik ³⁶, M.N. Agaras ¹³, J. Agarwala ^{72a,72b}, A. Aggarwal ⁹⁹, C. Agheorghiesei ^{27c}, J.A. Aguilar-Saavedra ^{129f}, A. Ahmad ³⁶, F. Ahmadov ^{38,z}, W.S. Ahmed ¹⁰³, S. Ahuja ⁹⁴, X. Ai ⁴⁸, G. Aielli ^{75a,75b}, I. Aizenberg ¹⁶⁸, M. Akbiyik ⁹⁹, T.P.A. Åkesson ⁹⁷, A.V. Akimov ³⁷, K. Al Khoury ⁴¹, G.L. Alberghi ^{23b}, J. Albert ¹⁶⁴, P. Albicocco ⁵³, M.J. Alconada Verzini ⁸⁹, S. Alderweireldt ⁵², M. Aleksa ³⁶, I.N. Aleksandrov ³⁸, C. Alexa ^{27b}, T. Alexopoulos ¹⁰, A. Alfonsi ¹¹³, F. Alfonsi ^{23b}, M. Alhroob ¹¹⁹, B. Ali ¹³¹, S. Ali ¹⁴⁷, M. Aliev ³⁷, G. Alimonti ^{70a}, W. Alkakhri ⁵⁵, C. Allaire ³⁶, B.M.M. Allbrooke ¹⁴⁵, P.P. Allport ²⁰, A. Aloisio ^{71a,71b}, F. Alonso ⁸⁹, C. Alpigiani ¹³⁷, E. Alunno Camelia ^{75a,75b}, M. Alvarez Estevez ⁹⁸, M.G. Alvigi ^{71a,71b}, Y. Amaral Coutinho ^{81b}, A. Ambler ¹⁰³, C. Amelung ³⁶, C.G. Ames ¹⁰⁸, D. Amidei ¹⁰⁵, S.P. Amor Dos Santos ^{129a}, S. Amoroso ⁴⁸, K.R. Amos ¹⁶², C.S. Amrouche ⁵⁶, V. Ananiev ¹²⁴, C. Anastopoulos ¹³⁸, T. Andeen ¹¹, J.K. Anders ¹⁹, S.Y. Andrean ^{47a,47b}, A. Andreazza ^{70a,70b}, S. Angelidakis ⁹, A. Angerami ^{41,ac}, A.V. Anisenkov ³⁷, A. Annovi ^{73a}, C. Antel ⁵⁶, M.T. Anthony ¹³⁸, E. Antipov ¹²⁰, M. Antonelli ⁵³, D.J.A. Antrim ^{17a}, F. Anulli ^{74a}, M. Aoki ⁸², T. Aoki ¹⁵², J.A. Aparisi Pozo ¹⁶², M.A. Aparo ¹⁴⁵, L. Aperio Bella ⁴⁸, C. Appelt ¹⁸, N. Aranzabal ³⁶, V. Araujo Ferraz ^{81a}, C. Arcangeletti ⁵³, A.T.H. Arce ⁵¹, E. Arena ⁹¹, J-F. Arguin ¹⁰⁷, S. Argyropoulos ⁵⁴, J.-H. Arling ⁴⁸, A.J. Armbruster ³⁶, O. Arnaez ¹⁵⁴, H. Arnold ¹¹³, Z.P. Arrubarrena Tame ¹⁰⁸, G. Artoni ^{74a,74b}, H. Asada ¹¹⁰, K. Asai ¹¹⁷, S. Asai ¹⁵², N.A. Asbah ⁶¹, J. Assahsah ^{35d}, K. Assamagan ²⁹, R. Astalos ^{28a}, R.J. Atkin ^{33a}, M. Atkinson ¹⁶¹, N.B. Atlay ¹⁸, H. Atmani ^{62b}, P.A. Atmasiddha ¹⁰⁵, K. Augsten ¹³¹, S. Auricchio ^{71a,71b}, A.D. Auriol ²⁰, V.A. Austrup ¹⁷⁰, G. Avner ¹⁴⁹, G. Avolio ³⁶, K. Axiotis ⁵⁶, M.K. Ayoub ^{14c}, G. Azuelos ^{107,ag}, D. Babal ^{28a}, H. Bachacou ¹³⁴, K. Bachas ^{151,s}, A. Bachi ³⁴, F. Backman ^{47a,47b}, A. Badea ⁶¹, P. Bagnaia ^{74a,74b}, M. Bahmani ¹⁸, A.J. Bailey ¹⁶², V.R. Bailey ¹⁶¹, J.T. Baines ¹³³, C. Bakalis ¹⁰, O.K. Baker ¹⁷¹, P.J. Bakker ¹¹³, E. Bakos ¹⁵, D. Bakshi Gupta ⁸, S. Balaji ¹⁴⁶, R. Balasubramanian ¹¹³, E.M. Baldin ³⁷, P. Balek ¹³², E. Ballabene ^{70a,70b}, F. Balli ¹³⁴, L.M. Bales ^{63a}, W.K. Balunas ³², J. Balz ⁹⁹, E. Banas ⁸⁵, M. Bandieramonte ¹²⁸, A. Bandyopadhyay ²⁴, S. Bansal ²⁴, L. Barak ¹⁵⁰, E.L. Barberio ¹⁰⁴, D. Barberis ^{57b,57a}, M. Barbero ¹⁰¹, G. Barbour ⁹⁵, K.N. Barends ^{33a}, T. Barillari ¹⁰⁹, M-S. Barisits ³⁶, T. Barklow ¹⁴², R.M. Barnett ^{17a}, P. Baron ¹²¹, D.A. Baron Moreno ¹⁰⁰, A. Baroncelli ^{62a}, G. Barone ²⁹, A.J. Barr ¹²⁵, L. Barranco Navarro ^{47a,47b}, F. Barreiro ⁹⁸, J. Barreiro Guimarães da Costa ^{14a}, U. Barron ¹⁵⁰, M.G. Barros Teixeira ^{129a}, S. Barsov ³⁷, F. Bartels ^{63a}, R. Bartoldus ¹⁴², A.E. Barton ⁹⁰, P. Bartos ^{28a}, A. Basalae ⁴⁸, A. Basan ⁹⁹, M. Baselga ⁴⁹, I. Bashta ^{76a,76b}, A. Bassalat ^{66,b}, M.J. Basso ¹⁵⁴, C.R. Basson ¹⁰⁰, R.L. Bates ⁵⁹, S. Batlamous ^{35e}, J.R. Batley ³², B. Batool ¹⁴⁰, M. Battaglia ¹³⁵, D. Battulga ¹⁸, M. Baucé ^{74a,74b}, P. Bauer ²⁴, A. Bayirli ^{21a}, J.B. Beacham ⁵¹, T. Beau ¹²⁶, P.H. Beauchemin ¹⁵⁷, F. Becherer ⁵⁴, P. Bechtel ²⁴, H.P. Beck ^{19,r}, K. Becker ¹⁶⁶, C. Becot ⁴⁸, A.J. Beddall ^{21d}, V.A. Bednyakov ³⁸, C.P. Bee ¹⁴⁴, L.J. Beemster ¹⁵, T.A. Beermann ³⁶, M. Begalli ^{81d}, M. Begel ²⁹, A. Behera ¹⁴⁴, J.K. Behr ⁴⁸, C. Beirao Da Cruz E Silva ³⁶, J.F. Beirer ^{55,36}, F. Beisiegel ²⁴, M. Belfkir ¹⁵⁸, G. Bella ¹⁵⁰, L. Bellagamba ^{23b}, A. Bellerive ³⁴, P. Bellos ²⁰, K. Beloborodov ³⁷, K. Belotskiy ³⁷, N.L. Belyaev ³⁷, D. Benckekroun ^{35a}, F. Bendebba ^{35a}, Y. Benhammou ¹⁵⁰, D.P. Benjamin ²⁹,

M. Benoit ²⁹, J.R. Bensinger ²⁶, S. Bentvelsen ¹¹³, L. Beresford ³⁶, M. Beretta ⁵³, D. Berge ¹⁸,
E. Bergeaas Kuutmann ¹⁶⁰, N. Berger ⁴, B. Bergmann ¹³¹, J. Beringer ^{17a}, S. Berlendis ⁷,
G. Bernardi ⁵, C. Bernius ¹⁴², F.U. Bernlochner ²⁴, T. Berry ⁹⁴, P. Berta ¹³², A. Berthold ⁵⁰,
I.A. Bertram ⁹⁰, S. Bethke ¹⁰⁹, A. Betti ^{74a,74b}, A.J. Bevan ⁹³, M. Bhamjee ^{33c}, S. Bhatta ¹⁴⁴,
D.S. Bhattacharya ¹⁶⁵, P. Bhattarai ²⁶, V.S. Bhopatkar ¹²⁰, R. Bi ^{29,aj}, R.M. Bianchi ¹²⁸,
O. Biebel ¹⁰⁸, R. Bielski ¹²², M. Biglietti ^{76a}, T.R.V. Billoud ¹³¹, M. Bindi ⁵⁵, A. Bingul ^{21b},
C. Bini ^{74a,74b}, S. Biondi ^{23b,23a}, A. Biondini ⁹¹, C.J. Birch-sykes ¹⁰⁰, G.A. Bird ^{20,133},
M. Birman ¹⁶⁸, T. Bisanz ³⁶, E. Bisceglie ^{43b,43a}, D. Biswas ^{169,1}, A. Bitadze ¹⁰⁰, K. Bjørke ¹²⁴,
I. Bloch ⁴⁸, C. Blocker ²⁶, A. Blue ⁵⁹, U. Blumenschein ⁹³, J. Blumenthal ⁹⁹, G.J. Bobbink ¹¹³,
V.S. Bobrovnikov ³⁷, M. Boehler ⁵⁴, D. Bogavac ³⁶, A.G. Bogdanchikov ³⁷, C. Bohm ^{47a},
V. Boisvert ⁹⁴, P. Bokan ⁴⁸, T. Bold ^{84a}, M. Bomben ⁵, M. Bona ⁹³, M. Boonekamp ¹³⁴,
C.D. Booth ⁹⁴, A.G. Borbély ⁵⁹, H.M. Borecka-Bielska ¹⁰⁷, L.S. Borgna ⁹⁵, G. Borissov ⁹⁰,
D. Bortoletto ¹²⁵, D. Boscherini ^{23b}, M. Bosman ¹³, J.D. Bossio Sola ³⁶, K. Bouaouda ^{35a},
J. Boudreau ¹²⁸, E.V. Bouhova-Thacker ⁹⁰, D. Boumediene ⁴⁰, R. Bouquet ⁵, A. Boveia ¹¹⁸,
J. Boyd ³⁶, D. Boye ²⁹, I.R. Boyko ³⁸, J. Bracinik ²⁰, N. Brahimy ^{62d}, G. Brandt ¹⁷⁰,
O. Brandt ³², F. Braren ⁴⁸, B. Brau ¹⁰², J.E. Brau ¹²², K. Brendlinger ⁴⁸, R. Brenner ¹⁶⁸,
L. Brenner ³⁶, R. Brenner ¹⁶⁰, S. Bressler ¹⁶⁸, B. Brickwedde ⁹⁹, D. Britton ⁵⁹, D. Britzger ¹⁰⁹,
I. Brock ²⁴, G. Brooijmans ⁴¹, W.K. Brooks ^{136f}, E. Brost ²⁹, T.L. Bruckler ¹²⁵,
P.A. Bruckman de Renstrom ⁸⁵, B. Brüers ⁴⁸, D. Bruncko ^{28b,*}, A. Bruni ^{23b}, G. Bruni ^{23b},
M. Bruschi ^{23b}, N. Bruscinò ^{74a,74b}, L. Bryngemark ¹⁴², T. Buanes ¹⁶, Q. Buat ¹³⁷,
P. Buchholz ¹⁴⁰, A.G. Buckley ⁵⁹, I.A. Budagov ^{38,*}, M.K. Bugge ¹²⁴, O. Bulekov ³⁷,
B.A. Bullard ⁶¹, S. Burdin ⁹¹, C.D. Burgard ⁴⁸, A.M. Burger ⁴⁰, B. Burghgrave ⁸, J.T.P. Burr ³²,
C.D. Burton ¹¹, J.C. Burzynski ¹⁴¹, E.L. Busch ⁴¹, V. Büscher ⁹⁹, P.J. Bussey ⁵⁹, J.M. Butler ²⁵,
C.M. Buttar ⁵⁹, J.M. Butterworth ⁹⁵, W. Buttinger ¹³³, C.J. Buxo Vazquez ¹⁰⁶, A.R. Buzykaev ³⁷,
G. Cabras ^{23b}, S. Cabrera Urbán ¹⁶², D. Caforio ⁵⁸, H. Cai ¹²⁸, Y. Cai ^{14a,14d}, V.M.M. Cairo ³⁶,
O. Cakir ^{3a}, N. Calace ³⁶, P. Calafiura ^{17a}, G. Calderini ¹²⁶, P. Calfayan ⁶⁷, G. Callea ⁵⁹,
L.P. Caloba ^{81b}, D. Calvet ⁴⁰, S. Calvet ⁴⁰, T.P. Calvet ¹⁰¹, M. Calvetti ^{73a,73b},
R. Camacho Toro ¹²⁶, S. Camarda ³⁶, D. Camarero Munoz ²⁶, P. Camarri ^{75a,75b},
M.T. Camerlingo ^{76a,76b}, D. Cameron ¹²⁴, C. Camincher ¹⁶⁴, M. Campanelli ⁹⁵, A. Camplani ⁴²,
V. Canale ^{71a,71b}, A. Canesse ¹⁰³, M. Cano Bret ⁷⁹, J. Cantero ¹⁶², Y. Cao ¹⁶¹, F. Capocasa ²⁶,
M. Capua ^{43b,43a}, A. Carbone ^{70a,70b}, R. Cardarelli ^{75a}, J.C.J. Cardenas ⁸, F. Cardillo ¹⁶²,
T. Carli ³⁶, G. Carlino ^{71a}, J.I. Carlotto ¹³, B.T. Carlson ^{128,t}, E.M. Carlson ^{164,155a},
L. Carminati ^{70a,70b}, M. Carnesale ^{74a,74b}, S. Caron ¹¹², E. Carquin ^{136f}, S. Carrá ^{70a,70b},
G. Carratta ^{23b,23a}, F. Carri Argos ^{33g}, J.W.S. Carter ¹⁵⁴, T.M. Carter ⁵², M.P. Casado ^{13,i},
A.F. Casha ¹⁵⁴, E.G. Castiglia ¹⁷¹, F.L. Castillo ^{63a}, L. Castillo Garcia ¹³, V. Castillo Gimenez ¹⁶²,
N.F. Castro ^{129a,129e}, A. Catinaccio ³⁶, J.R. Catmore ¹²⁴, V. Cavaliere ²⁹, N. Cavalli ^{23b,23a},
V. Cavasinni ^{73a,73b}, E. Celebi ^{21a}, F. Celli ¹²⁵, M.S. Centonze ^{69a,69b}, K. Cerny ¹²¹,
A.S. Cerqueira ^{81a}, A. Cerri ¹⁴⁵, L. Cerrito ^{75a,75b}, F. Cerutti ^{17a}, A. Cervelli ^{23b}, S.A. Cetin ^{21d},
Z. Chadi ^{35a}, D. Chakraborty ¹¹⁴, M. Chala ^{129f}, J. Chan ¹⁶⁹, W.Y. Chan ¹⁵², J.D. Chapman ³²,
B. Chargeishvili ^{148b}, D.G. Charlton ²⁰, T.P. Charman ⁹³, M. Chatterjee ¹⁹, S. Chekanov ⁶,
S.V. Chekulaev ^{155a}, G.A. Chelkov ^{38,a}, A. Chen ¹⁰⁵, B. Chen ¹⁵⁰, B. Chen ¹⁶⁴, C. Chen ^{62a},
H. Chen ^{14c}, H. Chen ²⁹, J. Chen ^{62c}, J. Chen ²⁶, S. Chen ¹⁵², S.J. Chen ^{14c}, X. Chen ^{62c},
X. Chen ^{14b,af}, Y. Chen ^{62a}, C.L. Cheng ¹⁶⁹, H.C. Cheng ^{64a}, A. Cheplakov ³⁸,
E. Cheremushkina ⁴⁸, E. Cherepanova ¹¹³, R. Cherkaoui El Moursli ^{35e}, E. Cheu ⁷, K. Cheung ⁶⁵,
L. Chevalier ¹³⁴, V. Chiarella ⁵³, G. Chiarelli ^{73a}, N. Chiedde ¹⁰¹, G. Chiodini ^{69a},
A.S. Chisholm ²⁰, A. Chitan ^{27b}, M. Chitishvili ¹⁶², Y.H. Chiu ¹⁶⁴, M.V. Chizhov ³⁸, K. Choi ¹¹,
A.R. Chomont ^{74a,74b}, Y. Chou ¹⁰², E.Y.S. Chow ¹¹³, T. Chowdhury ^{33g}, L.D. Christopher ^{33g},

K.L. Chu^{64a}, M.C. Chu^{64a}, X. Chu^{14a,14d}, J. Chudoba¹³⁰, J.J. Chwastowski⁸⁵, D. Cieri¹⁰⁹,
 K.M. Ciesla^{84a}, V. Cindro⁹², A. Ciocio^{17a}, F. Cirotto^{71a,71b}, Z.H. Citron^{168,m}, M. Citterio^{70a},
 D.A. Ciubotaru^{27b}, B.M. Ciungu¹⁵⁴, A. Clark⁵⁶, P.J. Clark⁵², J.M. Clavijo Columbie⁴⁸,
 S.E. Clawson¹⁰⁰, C. Clement^{47a,47b}, J. Clercx⁴⁸, L. Clissa^{23b,23a}, Y. Coadou¹⁰¹,
 M. Cobal^{68a,68c}, A. Coccaro^{57b}, R.F. Coelho Barrue^{129a}, R. Coelho Lopes De Sa¹⁰²,
 S. Coelli^{70a}, H. Cohen¹⁵⁰, A.E.C. Coimbra^{70a,70b}, B. Cole⁴¹, J. Collot⁶⁰,
 P. Conde Muiño^{129a,129g}, M.P. Connell^{33c}, S.H. Connell^{33c}, I.A. Connelly⁵⁹, E.I. Conroy¹²⁵,
 F. Conventi^{71a,ah}, H.G. Cooke²⁰, A.M. Cooper-Sarkar¹²⁵, F. Cormier¹⁶³, L.D. Corpe³⁶,
 M. Corradi^{74a,74b}, E.E. Corrigan⁹⁷, F. Corriveau^{103,y}, A. Cortes-Gonzalez¹⁸, M.J. Costa¹⁶²,
 F. Costanza⁴, D. Costanzo¹³⁸, B.M. Cote¹¹⁸, G. Cowan⁹⁴, J.W. Cowley³², K. Cranmer¹¹⁶,
 S. Crépe-Renaudin⁶⁰, F. Crescioli¹²⁶, M. Cristinziani¹⁴⁰, M. Cristoforetti^{77a,77b,d}, V. Croft¹⁵⁷,
 G. Crosetti^{43b,43a}, A. Cueto³⁶, T. Cuhadar Donszelmann¹⁵⁹, H. Cui^{14a,14d}, Z. Cui⁷,
 A.R. Cukierman¹⁴², W.R. Cunningham⁵⁹, F. Curcio^{43b,43a}, P. Czodrowski³⁶, M.M. Czurylo^{63b},
 M.J. Da Cunha Sargedas De Sousa^{62a}, J.V. Da Fonseca Pinto^{81b}, C. Da Via¹⁰⁰, W. Dabrowski^{84a},
 T. Dado⁴⁹, S. Dahbi^{33g}, T. Dai¹⁰⁵, C. Dallapiccola¹⁰², M. Dam⁴², G. D'amen²⁹,
 V. D'Amico¹⁰⁸, J. Damp⁹⁹, J.R. Dandoy¹²⁷, M.F. Daneri³⁰, M. Danninger¹⁴¹, V. Dao³⁶,
 G. Darbo^{57b}, S. Darmora⁶, S.J. Das^{29,aj}, S. D'Auria^{70a,70b}, C. David^{155b}, T. Davidek¹³²,
 D.R. Davis⁵¹, B. Davis-Purcell³⁴, I. Dawson⁹³, K. De⁸, R. De Asmundis^{71a},
 M. De Beurs¹¹³, N. De Biase⁴⁸, S. De Castro^{23b,23a}, N. De Groot¹¹², P. de Jong¹¹³,
 H. De la Torre¹⁰⁶, A. De Maria^{14c}, A. De Salvo^{74a}, U. De Sanctis^{75a,75b}, A. De Santo¹⁴⁵,
 J.B. De Vivie De Regie⁶⁰, D.V. Dedovich³⁸, J. Degens¹¹³, A.M. Deiana⁴⁴, F. Del Corso^{23b,23a},
 J. Del Peso⁹⁸, F. Del Rio^{63a}, F. Deliot¹³⁴, C.M. Delitzsch⁴⁹, M. Della Pietra^{71a,71b},
 D. Della Volpe⁵⁶, A. Dell'Acqua³⁶, L. Dell'Asta^{70a,70b}, M. Delmastro⁴, P.A. Delsart⁶⁰,
 S. Demers¹⁷¹, M. Demichev³⁸, S.P. Denisov³⁷, L. D'Eramo¹¹⁴, D. Derendarz⁸⁵, F. Derue¹²⁶,
 P. Dervan⁹¹, K. Desch²⁴, K. Dette¹⁵⁴, C. Deutsch²⁴, P.O. Deviveiros³⁶, F.A. Di Bello^{74a,74b},
 A. Di Ciaccio^{75a,75b}, L. Di Ciaccio⁴, A. Di Domenico^{74a,74b}, C. Di Donato^{71a,71b},
 A. Di Girolamo³⁶, G. Di Gregorio^{73a,73b}, A. Di Luca^{77a,77b}, B. Di Micco^{76a,76b},
 R. Di Nardo^{76a,76b}, C. Diaconu¹⁰¹, F.A. Dias¹¹³, T. Dias Do Vale¹⁴¹, M.A. Diaz^{136a,136b},
 F.G. Diaz Capriles²⁴, M. Didenko¹⁶², E.B. Diehl¹⁰⁵, L. Diehl⁵⁴, S. Díez Cornell⁴⁸,
 C. Díez Pardos¹⁴⁰, C. Dimitriadi^{24,160}, A. Dimitrievska^{17a}, W. Ding^{14b}, J. Dingfelder²⁴,
 I-M. Dinu^{27b}, S.J. Dittmeier^{63b}, F. Dittus³⁶, F. Djama¹⁰¹, T. Djobava^{148b}, J.I. Djuvsland¹⁶,
 C. Doglioni^{100,97}, J. Dolejsi¹³², Z. Dolezal¹³², M. Donadelli^{81c}, B. Dong^{62c}, J. Donini⁴⁰,
 A. D'Onofrio^{14c}, M. D'Onofrio⁹¹, J. Dopke¹³³, A. Doria^{71a}, M.T. Dova⁸⁹, A.T. Doyle⁵⁹,
 M.A. Draguet¹²⁵, E. Drechsler¹⁴¹, E. Dreyer¹⁶⁸, I. Drivas-koulouris¹⁰, A.S. Drobac¹⁵⁷,
 M. Drozdova⁵⁶, D. Du^{62a}, T.A. du Pree¹¹³, F. Dubinin³⁷, M. Dubovsky^{28a}, E. Duchovni¹⁶⁸,
 G. Duckeck¹⁰⁸, O.A. Ducu^{27b}, D. Duda¹⁰⁹, A. Dudarev³⁶, M. D'uffizi¹⁰⁰, L. Duflot⁶⁶,
 M. Dührssen³⁶, C. Dülsen¹⁷⁰, A.E. Dumitriu^{27b}, M. Dunford^{63a}, S. Dungs⁴⁹,
 K. Dunne^{47a,47b}, A. Duperrin¹⁰¹, H. Duran Yildiz^{3a}, M. Düren⁵⁸, A. Durglishvili^{148b},
 B.L. Dwyer¹¹⁴, G.I. Dyckes^{17a}, M. Dyndal^{84a}, S. Dysch¹⁰⁰, B.S. Dziedzic⁸⁵,
 Z.O. Earnshaw¹⁴⁵, B. Eckerova^{28a}, M.G. Eggleston⁵¹, E. Egidio Purcino De Souza^{81b},
 L.F. Ehrke⁵⁶, G. Eigen¹⁶, K. Einsweiler^{17a}, T. Ekelof¹⁶⁰, P.A. Ekman⁹⁷, Y. El Ghazali^{35b},
 H. El Jarrari^{35e,147}, A. El Moussaouy^{35a}, V. Ellajosyula¹⁶⁰, M. Ellert¹⁶⁰, F. Ellinghaus¹⁷⁰,
 A.A. Elliot⁹³, N. Ellis³⁶, J. Elmsheuser²⁹, M. Elsing³⁶, D. Emelianov¹³³, A. Emerman⁴¹,
 Y. Enari¹⁵², I. Ene^{17a}, S. Epari¹³, J. Erdmann⁴⁹, A. Ereditato¹⁹, P.A. Erland⁸⁵,
 M. Errenst¹⁷⁰, M. Escalier⁶⁶, C. Escobar¹⁶², E. Etzion¹⁵⁰, G. Evans^{129a}, H. Evans⁶⁷,
 M.O. Evans¹⁴⁵, A. Ezhilov³⁷, S. Ezzarqtouni^{35a}, F. Fabbri⁵⁹, L. Fabbri^{23b,23a}, G. Facini⁹⁵,
 V. Fadeyev¹³⁵, R.M. Fakhrutdinov³⁷, S. Falciano^{74a}, P.J. Falke²⁴, S. Falke³⁶, J. Faltova¹³²,

Y. Fan [ID14a](#), Y. Fang [ID14a,14d](#), G. Fanourakis [ID46](#), M. Fanti [ID70a,70b](#), M. Faraj [ID68a,68b](#), A. Farbin [ID8](#),
 A. Farilla [ID76a](#), T. Farooque [ID106](#), S.M. Farrington [ID52](#), F. Fassi [ID35e](#), D. Fassouliotis [ID9](#),
 M. Faucci Giannelli [ID75a,75b](#), W.J. Fawcett [ID32](#), L. Fayard [ID66](#), P. Federicova [ID130](#), O.L. Fedin [ID37,a](#),
 G. Fedotov [ID37](#), M. Feickert [ID161](#), L. Feligioni [ID101](#), A. Fell [ID138](#), D.E. Fellers [ID122](#), C. Feng [ID62b](#),
 M. Feng [ID14b](#), Z. Feng [ID113](#), M.J. Fenton [ID159](#), A.B. Fenyuk [ID37](#), L. Ferencz [ID48](#), S.W. Ferguson [ID45](#),
 J. Ferrando [ID48](#), A. Ferrari [ID160](#), P. Ferrari [ID113](#), R. Ferrari [ID72a](#), D. Ferrere [ID56](#), C. Ferretti [ID105](#),
 F. Fiedler [ID99](#), A. Filipčič [ID92](#), E.K. Filmer [ID1](#), F. Filthaut [ID112](#), M.C.N. Fiolhais [ID129a,129c,c](#),
 L. Fiorini [ID162](#), F. Fischer [ID140](#), W.C. Fisher [ID106](#), T. Fitschen [ID20](#), I. Fleck [ID140](#), P. Fleischmann [ID105](#),
 T. Flick [ID170](#), L. Flores [ID127](#), M. Flores [ID33d,ad](#), L.R. Flores Castillo [ID64a](#), F.M. Follega [ID77a,77b](#),
 N. Fomin [ID16](#), J.H. Foo [ID154](#), B.C. Forland [ID67](#), A. Formica [ID134](#), A.C. Forti [ID100](#), E. Fortin [ID101](#),
 A.W. Fortman [ID61](#), M.G. Foti [ID17a](#), L. Fountas [ID9j](#), D. Fournier [ID66](#), H. Fox [ID90](#), P. Francavilla [ID73a,73b](#),
 S. Francescato [ID61](#), M. Franchini [ID23b,23a](#), S. Franchino [ID63a](#), D. Francis [ID36](#), L. Franco [ID112](#),
 L. Franconi [ID19](#), M. Franklin [ID61](#), G. Frattari [ID26](#), A.C. Freegard [ID93](#), P.M. Freeman [ID20](#), W.S. Freund [ID81b](#),
 N. Fritzsche [ID50](#), A. Froch [ID54](#), D. Froidevaux [ID36](#), J.A. Frost [ID125](#), Y. Fu [ID62a](#), M. Fujimoto [ID117](#),
 E. Fullana Torregrosa [ID162,*](#), J. Fuster [ID162](#), A. Gabrielli [ID23b,23a](#), A. Gabrielli [ID154](#), P. Gadow [ID48](#),
 G. Gagliardi [ID57b,57a](#), L.G. Gagnon [ID17a](#), G.E. Gallardo [ID125](#), E.J. Gallas [ID125](#), B.J. Gallop [ID133](#),
 R. Gamboa Goni [ID93](#), K.K. Gan [ID118](#), S. Ganguly [ID152](#), J. Gao [ID62a](#), Y. Gao [ID52](#),
 F.M. Garay Walls [ID136a,136b](#), B. Garcia [ID29,aj](#), C. García [ID162](#), J.E. García Navarro [ID162](#),
 J.A. García Pascual [ID14a](#), M. Garcia-Sciveres [ID17a](#), R.W. Gardner [ID39](#), D. Garg [ID79](#), R.B. Garg [ID142,q](#),
 S. Gargiulo [ID54](#), C.A. Garner [ID154](#), V. Garonne [ID29](#), S.J. Gasiorowski [ID137](#), P. Gaspar [ID81b](#), G. Gaudio [ID72a](#),
 V. Gautam [ID13](#), P. Gauzzi [ID74a,74b](#), I.L. Gavrilenko [ID37](#), A. Gavrilyuk [ID37](#), C. Gay [ID163](#), G. Gaycken [ID48](#),
 E.N. Gazis [ID10](#), A.A. Geanta [ID27b,27e](#), C.M. Gee [ID135](#), J. Geisen [ID97](#), M. Geisen [ID99](#), C. Gemme [ID57b](#),
 M.H. Genest [ID60](#), S. Gentile [ID74a,74b](#), S. George [ID94](#), W.F. George [ID20](#), T. Geralis [ID46](#), L.O. Gerlach [ID55](#),
 P. Gessinger-Befurt [ID36](#), M. Ghasemi Bostanabad [ID164](#), M. Ghneimat [ID140](#), A. Ghosal [ID140](#),
 A. Ghosh [ID159](#), A. Ghosh [ID7](#), B. Giacobbe [ID23b](#), S. Giagu [ID74a,74b](#), N. Giangiacomi [ID154](#),
 P. Giannetti [ID73a](#), A. Giannini [ID62a](#), S.M. Gibson [ID94](#), M. Gignac [ID135](#), D.T. Gil [ID84b](#), A.K. Gilbert [ID84a](#),
 B.J. Gilbert [ID41](#), D. Gillberg [ID34](#), G. Gilles [ID113](#), N.E.K. Gillwald [ID48](#), L. Ginabat [ID126](#),
 D.M. Gingrich [ID2,ag](#), M.P. Giordani [ID68a,68c](#), P.F. Giraud [ID134](#), G. Giugliarelli [ID68a,68c](#), D. Giugni [ID70a](#),
 F. Giuli [ID36](#), I. Gkialas [ID9j](#), L.K. Gladilin [ID37](#), C. Glasman [ID98](#), G.R. Gledhill [ID122](#), M. Glisic [ID122](#),
 I. Gnesi [ID43b,f](#), Y. Go [ID29,aj](#), M. Goblirsch-Kolb [ID26](#), D. Godin [ID107](#), S. Goldfarb [ID104](#), T. Golling [ID56](#),
 M.G.D. Gololo [ID33g](#), D. Golubkov [ID37](#), J.P. Gombas [ID106](#), A. Gomes [ID129a,129b](#), G. Gomes Da Silva [ID140](#),
 A.J. Gomez Delegido [ID162](#), R. Goncalves Gama [ID55](#), R. Gonçalo [ID129a,129c](#), G. Gonella [ID122](#),
 L. Gonella [ID20](#), A. Gongadze [ID38](#), F. Gonnella [ID20](#), J.L. Gonski [ID41](#), R.Y. González Andana [ID52](#),
 S. González de la Hoz [ID162](#), S. Gonzalez Fernandez [ID13](#), R. Gonzalez Lopez [ID91](#),
 C. Gonzalez Renteria [ID17a](#), R. Gonzalez Suarez [ID160](#), S. Gonzalez-Sevilla [ID56](#),
 G.R. Gonzalvo Rodriguez [ID162](#), L. Goossens [ID36](#), N.A. Gorasia [ID20](#), P.A. Gorbounov [ID37](#), B. Gorini [ID36](#),
 E. Gorini [ID69a,69b](#), A. Gorišek [ID92](#), A.T. Goshaw [ID51](#), M.I. Gostkin [ID38](#), C.A. Gottardo [ID36](#),
 M. Goughri [ID35b](#), V. Goumarre [ID48](#), A.G. Goussiou [ID137](#), N. Govender [ID33c](#), C. Goy [ID4](#),
 I. Grabowska-Bold [ID84a](#), K. Graham [ID34](#), E. Gramstad [ID124](#), S. Grancagnolo [ID18](#), M. Grandi [ID145](#),
 V. Gratchev [ID37,*](#), P.M. Gravila [ID27f](#), F.G. Gravili [ID69a,69b](#), H.M. Gray [ID17a](#), M. Greco [ID69a,69b](#),
 C. Grefe [ID24](#), I.M. Gregor [ID48](#), P. Grenier [ID142](#), C. Grieco [ID13](#), A.A. Grillo [ID135](#), K. Grimm [ID31,n](#),
 S. Grinstein [ID13,v](#), J.-F. Grivaz [ID66](#), E. Gross [ID168](#), J. Grosse-Knetter [ID55](#), C. Grud [ID105](#), A. Grummer [ID111](#),
 J.C. Grundy [ID125](#), L. Guan [ID105](#), W. Guan [ID169](#), C. Gubbels [ID163](#), J.G.R. Guerrero Rojas [ID162](#),
 G. Guerrieri [ID68a,68b](#), F. Guescini [ID109](#), R. Gugel [ID99](#), J.A.M. Guhit [ID105](#), A. Guida [ID48](#), T. Guillemin [ID4](#),
 E. Guilloton [ID166,133](#), S. Guindon [ID36](#), F. Guo [ID14a,14d](#), J. Guo [ID62c](#), L. Guo [ID66](#), Y. Guo [ID105](#),
 R. Gupta [ID48](#), S. Gurbuz [ID24](#), S.S. Gurdasani [ID54](#), G. Gustavino [ID36](#), M. Guth [ID56](#), P. Gutierrez [ID119](#),
 L.F. Gutierrez Zagazeta [ID127](#), C. Gutschow [ID95](#), C. Guyot [ID134](#), C. Gwenlan [ID125](#), C.B. Gwilliam [ID91](#),

E.S. Haaland ¹²⁴, A. Haas ¹¹⁶, M. Habedank ⁴⁸, C. Haber ^{17a}, H.K. Hadavand ⁸, A. Hadeif ⁹⁹,
 S. Hadzic ¹⁰⁹, M. Haleem ¹⁶⁵, J. Haley ¹²⁰, J.J. Hall ¹³⁸, G.D. Hallewell ¹⁰¹, L. Halser ¹⁹,
 K. Hamano ¹⁶⁴, H. Hamdaoui ^{35e}, M. Hamer ²⁴, G.N. Hamity ⁵², J. Han ^{62b}, K. Han ^{62a},
 L. Han ^{14c}, L. Han ^{62a}, S. Han ^{17a}, Y.F. Han ¹⁵⁴, K. Hanagaki ⁸², M. Hance ¹³⁵,
 D.A. Hangal ^{41,ac}, H. Hanif ¹⁴¹, M.D. Hank ³⁹, R. Hankache ¹⁰⁰, J.B. Hansen ⁴²,
 J.D. Hansen ⁴², P.H. Hansen ⁴², K. Hara ¹⁵⁶, D. Harada ⁵⁶, T. Harenberg ¹⁷⁰, S. Harkusha ³⁷,
 Y.T. Harris ¹²⁵, N.M. Harrison ¹¹⁸, P.F. Harrison ¹⁶⁶, N.M. Hartman ¹⁴², N.M. Hartmann ¹⁰⁸,
 Y. Hasegawa ¹³⁹, A. Hasib ⁵², S. Haug ¹⁹, R. Hauser ¹⁰⁶, M. Havranek ¹³¹, C.M. Hawkes ²⁰,
 R.J. Hawkings ³⁶, S. Hayashida ¹¹⁰, D. Hayden ¹⁰⁶, C. Hayes ¹⁰⁵, R.L. Hayes ¹⁶³, C.P. Hays ¹²⁵,
 J.M. Hays ⁹³, H.S. Hayward ⁹¹, F. He ^{62a}, Y. He ¹⁵³, Y. He ¹²⁶, M.P. Heath ⁵², V. Hedberg ⁹⁷,
 A.L. Heggelund ¹²⁴, N.D. Hehir ⁹³, C. Heidegger ⁵⁴, K.K. Heidegger ⁵⁴, W.D. Heidorn ⁸⁰,
 J. Heilmann ³⁴, S. Heim ⁴⁸, T. Heim ^{17a}, J.G. Heinlein ¹²⁷, J.J. Heinrich ¹²², L. Heinrich ^{109,ae},
 J. Hejbal ¹³⁰, L. Helary ⁴⁸, A. Held ¹⁶⁹, S. Hellesund ¹²⁴, C.M. Helling ¹⁶³, S. Hellman ^{47a,47b},
 C. Helsens ³⁶, R.C.W. Henderson ⁹⁰, L. Henkelmann ³², A.M. Henriques Correia ³⁶, H. Herde ¹⁴²,
 Y. Hernández Jiménez ¹⁴⁴, M.G. Herrmann ¹⁰⁸, T. Herrmann ⁵⁰, G. Herten ⁵⁴,
 R. Hertenberger ¹⁰⁸, L. Hervás ³⁶, N.P. Hesse ^{155a}, H. Hibi ⁸³, E. Higón-Rodríguez ¹⁶²,
 S.J. Hillier ²⁰, I. Hinchliffe ^{17a}, F. Hinterkeuser ²⁴, M. Hirose ¹²³, S. Hirose ¹⁵⁶,
 D. Hirschbuehl ¹⁷⁰, T.G. Hitchings ¹⁰⁰, B. Hiti ⁹², J. Hobbs ¹⁴⁴, R. Hobincu ^{27e}, N. Hod ¹⁶⁸,
 M.C. Hodgkinson ¹³⁸, B.H. Hodgkinson ³², A. Hoecker ³⁶, J. Hofer ⁴⁸, D. Hohn ⁵⁴, T. Holm ²⁴,
 M. Holzbock ¹⁰⁹, L.B.A.H. Hommels ³², B.P. Honan ¹⁰⁰, J. Hong ^{62c}, T.M. Hong ¹²⁸,
 Y. Hong ⁵⁵, J.C. Honig ⁵⁴, A. Hönle ¹⁰⁹, B.H. Hooberman ¹⁶¹, W.H. Hopkins ⁶, Y. Horii ¹¹⁰,
 S. Hou ¹⁴⁷, A.S. Howard ⁹², J. Howarth ⁵⁹, J. Hoya ⁶, M. Hrabovsky ¹²¹, A. Hrynevich ³⁷,
 T. Hryn'ova ⁴, P.J. Hsu ⁶⁵, S.-C. Hsu ¹³⁷, Q. Hu ^{41,ac}, Y.F. Hu ^{14a,14d,ai}, D.P. Huang ⁹⁵,
 S. Huang ^{64b}, X. Huang ^{14c}, Y. Huang ^{62a}, Y. Huang ^{14a}, Z. Huang ¹⁰⁰, Z. Hubacek ¹³¹,
 M. Huebner ²⁴, F. Huegging ²⁴, T.B. Huffman ¹²⁵, M. Huhtinen ³⁶, S.K. Huiberts ¹⁶,
 R. Hulsken ¹⁰³, N. Huseynov ^{12,a}, J. Huston ¹⁰⁶, J. Huth ⁶¹, R. Hyneman ¹⁴², S. Hyrych ^{28a},
 G. Iacobucci ⁵⁶, G. Iakovidis ²⁹, I. Ibragimov ¹⁴⁰, L. Iconomidou-Fayard ⁶⁶, P. Iengo ^{71a,71b},
 R. Iguchi ¹⁵², T. Iizawa ⁵⁶, Y. Ikegami ⁸², A. Ilg ¹⁹, N. Ilic ¹⁵⁴, H. Imam ^{35a},
 T. Ingebretsen Carlson ^{47a,47b}, G. Introzzi ^{72a,72b}, M. Iodice ^{76a}, V. Ippolito ^{74a,74b}, M. Ishino ¹⁵²,
 W. Islam ¹⁶⁹, C. Issever ^{18,48}, S. Istin ^{21a,al}, H. Ito ¹⁶⁷, J.M. Iturbe Ponce ^{64a}, R. Iuppa ^{77a,77b},
 A. Ivina ¹⁶⁸, J.M. Izen ⁴⁵, V. Izzo ^{71a}, P. Jacka ^{130,131}, P. Jackson ¹, R.M. Jacobs ⁴⁸,
 B.P. Jaeger ¹⁴¹, C.S. Jagfeld ¹⁰⁸, G. Jäkel ¹⁷⁰, K. Jakobs ⁵⁴, T. Jakoubek ¹⁶⁸, J. Jamieson ⁵⁹,
 K.W. Janas ^{84a}, G. Jarlskog ⁹⁷, A.E. Jaspan ⁹¹, M. Javurkova ¹⁰², F. Jeanneau ¹³⁴, L. Jeanty ¹²²,
 J. Jejelava ^{148a,aa}, P. Jenni ^{54,g}, C.E. Jessiman ³⁴, S. Jézéquel ⁴, J. Jia ¹⁴⁴, X. Jia ⁶¹,
 X. Jia ^{14a,14d}, Z. Jia ^{14c}, Y. Jiang ^{62a}, S. Jiggins ⁵², J. Jimenez Pena ¹⁰⁹, S. Jin ^{14c}, A. Jinaru ^{27b},
 O. Jinnouchi ¹⁵³, P. Johansson ¹³⁸, K.A. Johns ⁷, D.M. Jones ³², E. Jones ¹⁶⁶, P. Jones ³²,
 R.W.L. Jones ⁹⁰, T.J. Jones ⁹¹, R. Joshi ¹¹⁸, J. Jovicevic ¹⁵, X. Ju ^{17a}, J.J. Junggeburth ³⁶,
 A. Juste Rozas ^{13,v}, S. Kabana ^{136e}, A. Kaczmarzka ⁸⁵, M. Kado ^{74a,74b}, H. Kagan ¹¹⁸,
 M. Kagan ¹⁴², A. Kahn ⁴¹, A. Kahn ¹²⁷, C. Kahra ⁹⁹, T. Kaji ¹⁶⁷, E. Kajomovitz ¹⁴⁹,
 N. Kakati ¹⁶⁸, C.W. Kalderon ²⁹, A. Kamenshchikov ¹⁵⁴, S. Kanayama ¹⁵³, N.J. Kang ¹³⁵,
 Y. Kano ¹¹⁰, D. Kar ^{33g}, K. Karava ¹²⁵, M.J. Kareem ^{155b}, E. Karentzos ⁵⁴, I. Karkanas ¹⁵¹,
 S.N. Karpov ³⁸, Z.M. Karpova ³⁸, V. Kartvelishvili ⁹⁰, A.N. Karyukhin ³⁷, E. Kasimi ¹⁵¹,
 C. Kato ^{62d}, J. Katzy ⁴⁸, S. Kaur ³⁴, K. Kawade ¹³⁹, K. Kawagoe ⁸⁸, T. Kawamoto ¹³⁴,
 G. Kawamura ⁵⁵, E.F. Kay ¹⁶⁴, F.I. Kaya ¹⁵⁷, S. Kazakos ¹³, V.F. Kazanin ³⁷, Y. Ke ¹⁴⁴,
 J.M. Keaveney ^{33a}, R. Keeler ¹⁶⁴, G.V. Kehris ⁶¹, J.S. Keller ³⁴, A.S. Kelly ⁹⁵, D. Kelsey ¹⁴⁵,
 J.J. Kempster ²⁰, K.E. Kennedy ⁴¹, O. Kepka ¹³⁰, B.P. Kerridge ¹⁶⁶, S. Kersten ¹⁷⁰,
 B.P. Kerševan ⁹², S. Keshri ⁶⁶, L. Keszeghova ^{28a}, S. Ketabchi Haghighat ¹⁵⁴, M. Khandoga ¹²⁶,

A. Khanov ¹²⁰, A.G. Kharlamov ³⁷, T. Kharlamova ³⁷, E.E. Khoda ¹³⁷, T.J. Khoo ¹⁸,
 G. Khorauli ¹⁶⁵, J. Khubua ^{148b}, Y.A.R. Khwaira ⁶⁶, M. Kiehn ³⁶, A. Kilgallon ¹²²,
 D.W. Kim ^{47a,47b}, E. Kim ¹⁵³, Y.K. Kim ³⁹, N. Kimura ⁹⁵, A. Kirchhoff ⁵⁵, D. Kirchmeier ⁵⁰,
 C. Kirfel ²⁴, J. Kirk ¹³³, A.E. Kiryunin ¹⁰⁹, T. Kishimoto ¹⁵², D.P. Kisliuk ¹⁵⁴, C. Kitsaki ¹⁰,
 O. Kivernyk ²⁴, M. Klassen ^{63a}, C. Klein ³⁴, L. Klein ¹⁶⁵, M.H. Klein ¹⁰⁵, M. Klein ⁹¹,
 S.B. Klein ⁵⁶, U. Klein ⁹¹, P. Klimek ³⁶, A. Klimentov ²⁹, F. Klimpel ¹⁰⁹, T. Klingl ²⁴,
 T. Klioutchnikova ³⁶, F.F. Klitzner ¹⁰⁸, P. Kluit ¹¹³, S. Kluth ¹⁰⁹, E. Kneringer ⁷⁸,
 T.M. Knight ¹⁵⁴, A. Knue ⁵⁴, D. Kobayashi ⁸⁸, R. Kobayashi ⁸⁶, M. Kocian ¹⁴², P. Kodyš ¹³²,
 D.M. Koeck ¹⁴⁵, P.T. Koenig ²⁴, T. Koffas ³⁴, N.M. Köhler ³⁶, M. Kolb ¹³⁴, I. Koletsou ⁴,
 T. Komarek ¹²¹, K. Köneke ⁵⁴, A.X.Y. Kong ¹, T. Kono ¹¹⁷, N. Konstantinidis ⁹⁵, B. Konya ⁹⁷,
 R. Kopeliansky ⁶⁷, S. Koperny ^{84a}, K. Korcyl ⁸⁵, K. Kordas ¹⁵¹, G. Koren ¹⁵⁰, A. Korn ⁹⁵,
 S. Korn ⁵⁵, I. Korolkov ¹³, N. Korotkova ³⁷, B. Kortman ¹¹³, O. Kortner ¹⁰⁹, S. Kortner ¹⁰⁹,
 W.H. Kostecka ¹¹⁴, V.V. Kostyukhin ¹⁴⁰, A. Kotsokechagia ¹³⁴, A. Kotwal ⁵¹, A. Koulouris ³⁶,
 A. Kourkoumeli-Charalampidi ^{72a,72b}, C. Kourkoumelis ⁹, E. Kourlitis ⁶, O. Kovanda ¹⁴⁵,
 R. Kowalewski ¹⁶⁴, W. Kozanecki ¹³⁴, A.S. Kozhin ³⁷, V.A. Kramarenko ³⁷, G. Kramberger ⁹²,
 P. Kramer ⁹⁹, M.W. Krasny ¹²⁶, A. Krasznahorkay ³⁶, J.A. Kremer ⁹⁹, T. Kresse ⁵⁰,
 J. Kretzschmar ⁹¹, K. Kreul ¹⁸, P. Krieger ¹⁵⁴, F. Krieter ¹⁰⁸, S. Krishnamurthy ¹⁰²,
 A. Krishnan ^{63b}, M. Krivos ¹³², K. Krizka ^{17a}, K. Kroeninger ⁴⁹, H. Kroha ¹⁰⁹, J. Kroll ¹³⁰,
 J. Kroll ¹²⁷, K.S. Krowpman ¹⁰⁶, U. Kruchonak ³⁸, H. Krüger ²⁴, N. Krumnack ⁸⁰, M.C. Kruse ⁵¹,
 J.A. Krzysiak ⁸⁵, A. Kubota ¹⁵³, O. Kuchinskaia ³⁷, S. Kuday ^{3a}, D. Kuechler ⁴⁸,
 J.T. Kuechler ⁴⁸, S. Kuehn ³⁶, T. Kuhl ⁴⁸, V. Kukhtin ³⁸, Y. Kulchitsky ^{37,a},
 S. Kuleshov ^{136d,136b}, M. Kumar ^{33g}, N. Kumari ¹⁰¹, M. Kuna ⁶⁰, A. Kupco ¹³⁰, T. Kupfer ⁴⁹,
 A. Kupich ³⁷, O. Kuprash ⁵⁴, H. Kurashige ⁸³, L.L. Kurchaninov ^{155a}, Y.A. Kurochkin ³⁷,
 A. Kurova ³⁷, E.S. Kuwertz ³⁶, M. Kuze ¹⁵³, A.K. Kvam ¹⁰², J. Kvita ¹²¹, T. Kwan ¹⁰³,
 K.W. Kwok ^{64a}, N.G. Kyriacou ¹⁰⁵, L.A.O. Laatu ¹⁰¹, C. Lacasta ¹⁶², F. Lacava ^{74a,74b},
 H. Lacker ¹⁸, D. Lacour ¹²⁶, N.N. Lad ⁹⁵, E. Ladygin ³⁸, B. Laforge ¹²⁶, T. Lagouri ^{136e},
 S. Lai ⁵⁵, I.K. Lakomic ^{84a}, N. Lalloue ⁶⁰, J.E. Lambert ¹¹⁹, S. Lammers ⁶⁷, W. Lampl ⁷,
 C. Lampoudis ¹⁵¹, A.N. Lancaster ¹¹⁴, E. Lançon ²⁹, U. Landgraf ⁵⁴, M.P.J. Landon ⁹³,
 V.S. Lang ⁵⁴, R.J. Langenberg ¹⁰², A.J. Lankford ¹⁵⁹, F. Lanni ³⁶, K. Lantzsch ²⁴, A. Lanza ^{72a},
 A. Lapertosa ^{57b,57a}, J.F. Laporte ¹³⁴, T. Lari ^{70a}, F. Lasagni Manghi ^{23b}, M. Lassnig ³⁶,
 V. Latonova ¹³⁰, T.S. Lau ^{64a}, A. Laudrain ⁹⁹, A. Laurier ³⁴, S.D. Lawlor ⁹⁴, Z. Lawrence ¹⁰⁰,
 M. Lazzaroni ^{70a,70b}, B. Le ¹⁰⁰, B. Leban ⁹², A. Lebedev ⁸⁰, M. LeBlanc ³⁶, T. LeCompte ⁶,
 F. Ledroit-Guillon ⁶⁰, A.C.A. Lee ⁹⁵, G.R. Lee ¹⁶, L. Lee ⁶¹, S.C. Lee ¹⁴⁷, S. Lee ^{47a,47b},
 T.F. Lee ⁹¹, L.L. Leeuw ^{33c}, H.P. Lefebvre ⁹⁴, M. Lefebvre ¹⁶⁴, C. Leggett ^{17a}, K. Lehmann ¹⁴¹,
 G. Lehmann Miotto ³⁶, M. Leigh ⁵⁶, W.A. Leight ¹⁰², A. Leisos ^{151,u}, M.A.L. Leite ^{81c},
 C.E. Leitgeb ⁴⁸, R. Leitner ¹³², K.J.C. Leney ⁴⁴, T. Lenz ²⁴, S. Leone ^{73a}, C. Leonidopoulos ⁵²,
 A. Leopold ¹⁴³, C. Leroy ¹⁰⁷, R. Les ¹⁰⁶, C.G. Lester ³², M. Levchenko ³⁷, J. Levêque ⁴,
 D. Levin ¹⁰⁵, L.J. Levinson ¹⁶⁸, M.P. Lewicki ⁸⁵, D.J. Lewis ²⁰, B. Li ^{14b}, B. Li ^{62b}, C. Li ^{62a},
 C-Q. Li ^{62c}, H. Li ^{62a}, H. Li ^{62b}, H. Li ^{14c}, H. Li ^{62b}, J. Li ^{62c}, K. Li ¹³⁷, L. Li ^{62c},
 M. Li ^{14a,14d}, Q.Y. Li ^{62a}, S. Li ^{62d,62c,e}, T. Li ^{62b}, X. Li ¹⁰³, Z. Li ^{62b}, Z. Li ¹²⁵, Z. Li ¹⁰³,
 Z. Li ⁹¹, Z. Li ^{14a,14d}, Z. Liang ^{14a}, M. Liberatore ⁴⁸, B. Liberti ^{75a}, K. Lie ^{64c},
 J. Lieber Marin ^{81b}, K. Lin ¹⁰⁶, R.A. Linck ⁶⁷, R.E. Lindley ⁷, J.H. Lindon ², A. Linss ⁴⁸,
 E. Lipeles ¹²⁷, A. Lipniacka ¹⁶, A. Lister ¹⁶³, J.D. Little ⁴, B. Liu ^{14a}, B.X. Liu ¹⁴¹,
 D. Liu ^{62d,62c}, J.B. Liu ^{62a}, J.K.K. Liu ³², K. Liu ^{62d,62c}, M. Liu ^{62a}, M.Y. Liu ^{62a}, P. Liu ^{14a},
 Q. Liu ^{62d,137,62c}, X. Liu ^{62a}, Y. Liu ⁴⁸, Y. Liu ^{14c,14d}, Y.L. Liu ¹⁰⁵, Y.W. Liu ^{62a},
 M. Livan ^{72a,72b}, J. Llorente Merino ¹⁴¹, S.L. Lloyd ⁹³, E.M. Lobodzinska ⁴⁸, P. Loch ⁷,
 S. Loffredo ^{75a,75b}, T. Lohse ¹⁸, K. Lohwasser ¹³⁸, M. Lokajicek ^{130,*}, J.D. Long ¹⁶¹,







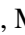








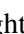
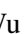




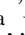

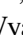





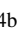
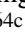
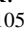
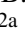
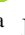
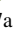
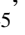






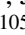
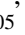



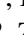

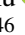


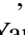
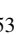


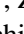

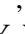

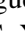
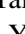


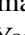
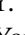







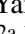
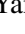
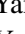

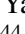


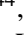
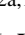
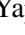





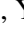








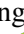
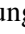
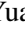
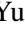

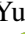



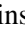
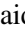
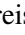


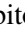


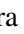

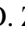






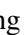










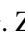




I. Longarini ^{74a,74b}, L. Longo ^{69a,69b}, R. Longo ¹⁶¹, I. Lopez Paz ³⁶, A. Lopez Solis ⁴⁸,
 J. Lorenz ¹⁰⁸, N. Lorenzo Martinez ⁴, A.M. Lory ¹⁰⁸, A. Lösle ⁵⁴, X. Lou ^{47a,47b}, X. Lou ^{14a,14d},
 A. Lounis ⁶⁶, J. Love ⁶, P.A. Love ⁹⁰, J.J. Lozano Bahilo ¹⁶², G. Lu ^{14a,14d}, M. Lu ⁷⁹,
 S. Lu ¹²⁷, Y.J. Lu ⁶⁵, H.J. Lubatti ¹³⁷, C. Luci ^{74a,74b}, F.L. Lucio Alves ^{14c}, A. Lucotte ⁶⁰,
 F. Luehring ⁶⁷, I. Luise ¹⁴⁴, O. Lukianchuk ⁶⁶, O. Lundberg ¹⁴³, B. Lund-Jensen ¹⁴³,
 N.A. Luongo ¹²², M.S. Lutz ¹⁵⁰, D. Lynn ²⁹, H. Lyons ⁹¹, R. Lysak ¹³⁰, E. Lytken ⁹⁷, F. Lyu ^{14a},
 V. Lyubushkin ³⁸, T. Lyubushkina ³⁸, H. Ma ²⁹, L.L. Ma ^{62b}, Y. Ma ⁹⁵, D.M. Mac Donell ¹⁶⁴,
 G. Maccarrone ⁵³, J.C. MacDonald ¹³⁸, R. Madar ⁴⁰, W.F. Mader ⁵⁰, J. Maeda ⁸³, T. Maeno ²⁹,
 M. Maerker ⁵⁰, V. Magerl ⁵⁴, J. Magro ^{68a,68c}, H. Maguire ¹³⁸, D.J. Mahon ⁴¹,
 C. Maidantchik ^{81b}, A. Maio ^{129a,129b,129d}, K. Maj ^{84a}, O. Majersky ^{28a}, S. Majewski ¹²²,
 N. Makovec ⁶⁶, V. Maksimovic ¹⁵, B. Malaescu ¹²⁶, Pa. Malecki ⁸⁵, V.P. Maleev ³⁷,
 F. Malek ⁶⁰, D. Malito ^{43b,43a}, U. Mallik ⁷⁹, C. Malone ³², S. Maltezos ¹⁰, S. Malyukov ³⁸,
 J. Mamuzic ¹³, G. Mancini ⁵³, G. Manco ^{72a,72b}, J.P. Mandalia ⁹³, I. Mandić ⁹²,
 L. Manhaes de Andrade Filho ^{81a}, I.M. Maniatis ¹⁵¹, M. Manisha ¹³⁴, J. Manjarres Ramos ⁵⁰,
 D.C. Mankad ¹⁶⁸, A. Mann ¹⁰⁸, B. Mansoulie ¹³⁴, S. Manzoni ³⁶, A. Marantis ^{151,u},
 G. Marchiori ⁵, M. Marcisovsky ¹³⁰, L. Marcoccia ^{75a,75b}, C. Marcon ^{70a,70b}, M. Marinescu ²⁰,
 M. Marjanovic ¹¹⁹, Z. Marshall ^{17a}, S. Marti-Garcia ¹⁶², T.A. Martin ¹⁶⁶, V.J. Martin ⁵²,
 B. Martin dit Latour ¹⁶, L. Martinelli ^{74a,74b}, M. Martinez ^{13,v}, P. Martinez Agullo ¹⁶²,
 V.I. Martinez Outschoorn ¹⁰², P. Martinez Suarez ¹³, S. Martin-Haugh ¹³³, V.S. Martoiu ^{27b},
 A.C. Martyniuk ⁹⁵, A. Marzin ³⁶, S.R. Maschek ¹⁰⁹, L. Masetti ⁹⁹, T. Mashimo ¹⁵²,
 J. Masik ¹⁰⁰, A.L. Maslennikov ³⁷, L. Massa ^{23b}, P. Massarotti ^{71a,71b}, P. Mastrandrea ^{73a,73b},
 A. Mastroberardino ^{43b,43a}, T. Masubuchi ¹⁵², T. Mathisen ¹⁶⁰, N. Matsuzawa ¹⁵², J. Maurer ^{27b},
 B. Mačec ⁹², D.A. Maximov ³⁷, R. Mazini ¹⁴⁷, I. Maznas ¹⁵¹, M. Mazza ¹⁰⁶, S.M. Mazza ¹³⁵,
 C. Mc Ginn ²⁹, J.P. Mc Gowan ¹⁰³, S.P. Mc Kee ¹⁰⁵, T.G. McCarthy ¹⁰⁹, W.P. McCormack ^{17a},
 E.F. McDonald ¹⁰⁴, A.E. McDougall ¹¹³, J.A. Mcfayden ¹⁴⁵, G. Mchedlidze ^{148b},
 R.P. Mckenzie ^{33g}, T.C. Mclachlan ⁴⁸, D.J. Mclaughlin ⁹⁵, K.D. McLean ¹⁶⁴, S.J. McMahon ¹³³,
 P.C. McNamara ¹⁰⁴, C.M. Mcpartland ⁹¹, R.A. McPherson ^{164,y}, T. Megy ⁴⁰, S. Mehlhase ¹⁰⁸,
 A. Mehta ⁹¹, B. Meirose ⁴⁵, D. Melini ¹⁴⁹, B.R. Mellado Garcia ^{33g}, A.H. Melo ⁵⁵,
 F. Meloni ⁴⁸, E.D. Mendes Gouveia ^{129a}, A.M. Mendes Jacques Da Costa ²⁰, H.Y. Meng ¹⁵⁴,
 L. Meng ⁹⁰, S. Menke ¹⁰⁹, M. Mentink ³⁶, E. Meoni ^{43b,43a}, C. Merlassino ¹²⁵,
 L. Merola ^{71a,71b}, C. Meroni ^{70a,70b}, G. Merz ¹⁰⁵, O. Meshkov ³⁷, J.K.R. Meshreki ¹⁴⁰,
 J. Metcalfe ⁶, A.S. Mete ⁶, C. Meyer ⁶⁷, J-P. Meyer ¹³⁴, M. Michetti ¹⁸, R.P. Middleton ¹³³,
 L. Mijović ⁵², G. Mikenberg ¹⁶⁸, M. Mikestikova ¹³⁰, M. Mikuž ⁹², H. Mildner ¹³⁸,
 A. Milic ¹⁵⁴, C.D. Milke ⁴⁴, D.W. Miller ³⁹, L.S. Miller ³⁴, A. Milov ¹⁶⁸, D.A. Milstead ^{47a,47b},
 T. Min ^{14c}, A.A. Minaenko ³⁷, I.A. Minashvili ^{148b}, L. Mince ⁵⁹, A.I. Mincer ¹¹⁶, B. Mindur ^{84a},
 M. Mineev ³⁸, Y. Mino ⁸⁶, L.M. Mir ¹³, M. Miralles Lopez ¹⁶², M. Mironova ¹²⁵, T. Mitani ¹⁶⁷,
 A. Mitra ¹⁶⁶, V.A. Mitsou ¹⁶², O. Miu ¹⁵⁴, P.S. Miyagawa ⁹³, Y. Miyazaki ⁸⁸, A. Mizukami ⁸²,
 J.U. Mjörnmark ⁹⁷, T. Mkrtchyan ^{63a}, T. Mlinarevic ⁹⁵, M. Mlynarikova ³⁶, T. Moa ^{47a,47b},
 S. Mobius ⁵⁵, K. Mochizuki ¹⁰⁷, P. Moder ⁴⁸, P. Mogg ¹⁰⁸, A.F. Mohammed ^{14a,14d},
 S. Mohapatra ⁴¹, G. Mokgatitswane ^{33g}, B. Mondal ¹⁴⁰, S. Mondal ¹³¹, K. Mönig ⁴⁸,
 E. Monnier ¹⁰¹, L. Monsonis Romero ¹⁶², J. Montejo Berlingen ³⁶, M. Montella ¹¹⁸,
 F. Monticelli ⁸⁹, N. Morange ⁶⁶, A.L. Moreira De Carvalho ^{129a}, M. Moreno Llácer ¹⁶²,
 C. Moreno Martinez ¹³, P. Morettini ^{57b}, S. Morgenstern ¹⁶⁶, M. Morii ⁶¹, M. Morinaga ¹⁵²,
 V. Morisbak ¹²⁴, A.K. Morley ³⁶, F. Morodei ^{74a,74b}, L. Morvaj ³⁶, P. Moschovakos ³⁶,
 B. Moser ³⁶, M. Mosidze ^{148b}, T. Moskalets ⁵⁴, P. Moskvitina ¹¹², J. Moss ^{31,o}, E.J.W. Moyses ¹⁰²,
 S. Muanza ¹⁰¹, J. Mueller ¹²⁸, D. Muenstermann ⁹⁰, R. Müller ¹⁹, G.A. Mullier ⁹⁷, J.J. Mullin ¹²⁷,
 D.P. Mungo ^{70a,70b}, J.L. Munoz Martinez ¹³, D. Munoz Perez ¹⁶², F.J. Munoz Sanchez ¹⁰⁰,

M. Murin [ID100](#), W.J. Murray [ID166,133](#), A. Murrone [ID70a,70b](#), J.M. Muse [ID119](#), M. Muškinja [ID17a](#),
C. Mwewa [ID29](#), A.G. Myagkov [ID37,a](#), A.J. Myers [ID8](#), A.A. Myers [ID128](#), G. Myers [ID67](#), M. Myska [ID131](#),
B.P. Nachman [ID17a](#), O. Nackenhorst [ID49](#), A. Nag [ID50](#), K. Nagai [ID125](#), K. Nagano [ID82](#), J.L. Nagle [ID29,aj](#),
E. Nagy [ID101](#), A.M. Nairz [ID36](#), Y. Nakahama [ID82](#), K. Nakamura [ID82](#), H. Nanjo [ID123](#), R. Narayan [ID44](#),
E.A. Narayanan [ID111](#), I. Naryshkin [ID37](#), M. Naseri [ID34](#), C. Nass [ID24](#), G. Navarro [ID22a](#),
J. Navarro-Gonzalez [ID162](#), R. Nayak [ID150](#), A. Nayaz [ID18](#), P.Y. Nechaeva [ID37](#), F. Nechansky [ID48](#),
L. Nedic [ID125](#), T.J. Neep [ID20](#), A. Negri [ID72a,72b](#), M. Negrini [ID23b](#), C. Nellist [ID112](#), C. Nelson [ID103](#),
K. Nelson [ID105](#), S. Nemecek [ID130](#), M. Nessi [ID36,h](#), M.S. Neubauer [ID161](#), F. Neuhaus [ID99](#),
J. Neundorff [ID48](#), R. Newhouse [ID163](#), P.R. Newman [ID20](#), C.W. Ng [ID128](#), Y.S. Ng [ID18](#), Y.W.Y. Ng [ID159](#),
B. Ngair [ID35e](#), H.D.N. Nguyen [ID107](#), R.B. Nickerson [ID125](#), R. Nicolaidou [ID134](#), J. Nielsen [ID135](#),
M. Niemeyer [ID55](#), N. Nikipforou [ID36](#), V. Nikolaenko [ID37,a](#), I. Nikolic-Audit [ID126](#), K. Nikolopoulos [ID20](#),
P. Nilsson [ID29](#), H.R. Nindhito [ID56](#), A. Nisati [ID74a](#), N. Nishu [ID2](#), R. Nisius [ID109](#), J.-E. Nitschke [ID50](#),
E.K. Nkadimeng [ID33g](#), S.J. Noacco Rosende [ID89](#), T. Nobe [ID152](#), D.L. Noel [ID32](#), Y. Noguchi [ID86](#),
T. Nommensen [ID146](#), M.A. Nomura [ID29](#), M.B. Norfolk [ID138](#), R.R.B. Norisam [ID95](#), B.J. Norman [ID34](#),
J. Novak [ID92](#), T. Novak [ID48](#), O. Novgorodova [ID50](#), L. Novotny [ID131](#), R. Novotny [ID111](#), L. Nozka [ID121](#),
K. Ntekas [ID159](#), E. Nurse [ID95](#), F.G. Oakham [ID34,ag](#), J. Ocariz [ID126](#), A. Ochi [ID83](#), I. Ochoa [ID129a](#),
S. Oerdek [ID160](#), A. Ogrodnik [ID84a](#), A. Oh [ID100](#), C.C. Ohm [ID143](#), H. Oide [ID153](#), R. Oishi [ID152](#),
M.L. Ojeda [ID48](#), Y. Okazaki [ID86](#), M.W. O'Keefe [ID91](#), Y. Okumura [ID152](#), A. Olariu [ID27b](#),
L.F. Oleiro Seabra [ID129a](#), S.A. Olivares Pino [ID136e](#), D. Oliveira Damazio [ID29](#), D. Oliveira Goncalves [ID81a](#),
J.L. Oliver [ID159](#), M.J.R. Olsson [ID159](#), A. Olszewski [ID85](#), J. Olszowska [ID85,*](#), Ö.O. Öncel [ID54](#),
D.C. O'Neil [ID141](#), A.P. O'Neill [ID19](#), A. Onofre [ID129a,129e](#), P.U.E. Onyisi [ID11](#), M.J. Oreglia [ID39](#),
G.E. Orellana [ID89](#), D. Orestano [ID76a,76b](#), N. Orlando [ID13](#), R.S. Orr [ID154](#), V. O'Shea [ID59](#),
R. Ospanov [ID62a](#), G. Otero y Garzon [ID30](#), H. Otono [ID88](#), P.S. Ott [ID63a](#), G.J. Ottino [ID17a](#), M. Ouchrif [ID35d](#),
J. Ouellette [ID29,aj](#), F. Ould-Saada [ID124](#), M. Owen [ID59](#), R.E. Owen [ID133](#), K.Y. Oyulmaz [ID21a](#),
V.E. Ozcan [ID21a](#), N. Ozturk [ID8](#), S. Ozturk [ID21d](#), J. Pacalt [ID121](#), H.A. Pacey [ID32](#), K. Pachal [ID51](#),
A. Pacheco Pages [ID13](#), C. Padilla Aranda [ID13](#), G. Padovano [ID74a,74b](#), S. Pagan Griso [ID17a](#),
G. Palacino [ID67](#), A. Palazzo [ID69a,69b](#), S. Palazzo [ID52](#), S. Palestini [ID36](#), M. Palka [ID84b](#), J. Pan [ID171](#),
T. Pan [ID64a](#), D.K. Panchal [ID11](#), C.E. Pandini [ID113](#), J.G. Panduro Vazquez [ID94](#), H. Pang [ID14b](#), P. Pani [ID48](#),
G. Panizzo [ID68a,68c](#), L. Paolozzi [ID56](#), C. Papadatos [ID107](#), S. Parajuli [ID44](#), A. Paramonov [ID6](#),
C. Paraskevopoulos [ID10](#), D. Paredes Hernandez [ID64b](#), T.H. Park [ID154](#), M.A. Parker [ID32](#), F. Parodi [ID57b,57a](#),
E.W. Parrish [ID114](#), V.A. Parrish [ID52](#), J.A. Parsons [ID41](#), U. Parzefall [ID54](#), B. Pascual Dias [ID107](#),
L. Pascual Dominguez [ID150](#), V.R. Pascuzzi [ID17a](#), F. Pasquali [ID113](#), E. Pasqualucci [ID74a](#), S. Passaggio [ID57b](#),
F. Pastore [ID94](#), P. Pasuwan [ID47a,47b](#), P. Patel [ID85](#), J.R. Pater [ID100](#), J. Patton [ID91](#), T. Pauly [ID36](#),
J. Pearkes [ID142](#), M. Pedersen [ID124](#), R. Pedro [ID129a](#), S.V. Peleganchuk [ID37](#), O. Penc [ID36](#), E.A. Pender [ID52](#),
C. Peng [ID64b](#), H. Peng [ID62a](#), K.E. Penski [ID108](#), M. Penzin [ID37](#), B.S. Peralva [ID81d](#),
A.P. Pereira Peixoto [ID60](#), L. Pereira Sanchez [ID47a,47b](#), D.V. Perepelitsa [ID29,aj](#), E. Perez Codina [ID155a](#),
M. Perganti [ID10](#), L. Perini [ID70a,70b,*](#), H. Pernegger [ID36](#), S. Perrella [ID36](#), A. Perrevoort [ID112](#), O. Perrin [ID40](#),
K. Peters [ID48](#), R.F.Y. Peters [ID100](#), B.A. Petersen [ID36](#), T.C. Petersen [ID42](#), E. Petit [ID101](#), V. Petousis [ID131](#),
C. Petridou [ID151](#), A. Petrukhin [ID140](#), M. Pettee [ID17a](#), N.E. Pettersson [ID36](#), A. Petukhov [ID37](#),
K. Petukhova [ID132](#), A. Peyaud [ID134](#), R. Pezoa [ID136f](#), L. Pezzotti [ID36](#), G. Pezzullo [ID171](#), T.M. Pham [ID169](#),
T. Pham [ID104](#), P.W. Phillips [ID133](#), M.W. Phipps [ID161](#), G. Piacquadio [ID144](#), E. Pianori [ID17a](#),
F. Piazza [ID70a,70b](#), R. Piegaia [ID30](#), D. Pietreanu [ID27b](#), A.D. Pilkington [ID100](#), M. Pinamonti [ID68a,68c](#),
J.L. Pinfeld [ID2](#), B.C. Pinheiro Pereira [ID129a](#), C. Pitman Donaldson [ID95](#), D.A. Pizzi [ID34](#),
L. Pizzimento [ID75a,75b](#), A. Pizzini [ID113](#), M.-A. Pleier [ID29](#), V. Plesanovs [ID54](#), V. Pleskot [ID132](#),
E. Plotnikova [ID38](#), G. Poddar [ID4](#), R. Poettgen [ID97](#), L. Poggioli [ID126](#), I. Pogrebnyak [ID106](#), D. Pohl [ID24](#),
I. Pokharel [ID55](#), S. Polacek [ID132](#), G. Polesello [ID72a](#), A. Poley [ID141,155a](#), R. Polifka [ID131](#), A. Polini [ID23b](#),
C.S. Pollard [ID125](#), Z.B. Pollock [ID118](#), V. Polychronakos [ID29](#), E. Pompa Pacchi [ID74a,74b](#),

D. Ponomarenko [ID37](#), L. Pontecorvo [ID36](#), S. Popa [ID27a](#), G.A. Popeneciu [ID27d](#),
 D.M. Portillo Quintero [ID155a](#), S. Pospisil [ID131](#), P. Postolache [ID27c](#), K. Potamianos [ID125](#), I.N. Potrap [ID38](#),
 C.J. Potter [ID32](#), H. Potti [ID1](#), T. Poulsen [ID48](#), J. Poveda [ID162](#), M.E. Pozo Astigarraga [ID36](#),
 A. Prades Ibanez [ID162](#), M.M. Prapa [ID46](#), S. Prell [ID80](#), J. Pretel [ID54](#), D. Price [ID100](#), M. Primavera [ID69a](#),
 M.A. Principe Martin [ID98](#), M.L. Proffitt [ID137](#), N. Proklova [ID127](#), K. Prokofiev [ID64c](#), G. Proto [ID75a,75b](#),
 S. Protopopescu [ID29](#), J. Proudfoot [ID6](#), M. Przybycien [ID84a](#), J.E. Puddefoot [ID138](#), D. Pudzha [ID37](#),
 P. Puzo [ID66](#), D. Pyatiizbyantseva [ID37](#), J. Qian [ID105](#), D. Qichen [ID100](#), Y. Qin [ID100](#), T. Qiu [ID93](#), A. Quadt [ID55](#),
 M. Queitsch-Maitland [ID100](#), G. Quetant [ID56](#), G. Rabanal Bolanos [ID61](#), D. Rafanoharana [ID54](#),
 F. Ragusa [ID70a,70b](#), J.L. Rainbolt [ID39](#), J.A. Raine [ID56](#), S. Rajagopalan [ID29](#), E. Ramakoti [ID37](#),
 K. Ran [ID48,14d](#), N.P. Rapheeha [ID33g](#), V. Raskina [ID126](#), D.F. Rassloff [ID63a](#), S. Rave [ID99](#), B. Ravina [ID55](#),
 I. Ravinovich [ID168](#), M. Raymond [ID36](#), A.L. Read [ID124](#), N.P. Readioff [ID138](#), D.M. Rebutzi [ID72a,72b](#),
 G. Redlinger [ID29](#), K. Reeves [ID45](#), J.A. Reidelsturz [ID170](#), D. Reikher [ID150](#), A. Reiss [ID99](#), A. Rej [ID140](#),
 C. Rembser [ID36](#), A. Renardi [ID48](#), M. Renda [ID27b](#), M.B. Rendel [ID109](#), A.G. Rennie [ID59](#), S. Resconi [ID70a](#),
 M. Ressegotti [ID57b,57a](#), E.D. Resseguie [ID17a](#), S. Rettie [ID95](#), B. Reynolds [ID118](#), E. Reynolds [ID17a](#),
 M. Rezaei Estabragh [ID170](#), O.L. Rezanova [ID37](#), P. Reznicek [ID132](#), E. Ricci [ID77a,77b](#), R. Richter [ID109](#),
 S. Richter [ID47a,47b](#), E. Richter-Was [ID84b](#), M. Ridel [ID126](#), P. Rieck [ID116](#), P. Riedler [ID36](#),
 M. Rijssenbeek [ID144](#), A. Rimoldi [ID72a,72b](#), M. Rimoldi [ID48](#), L. Rinaldi [ID23b,23a](#), T.T. Rinn [ID29](#),
 M.P. Rinnagel [ID108](#), G. Ripellino [ID143](#), I. Riu [ID13](#), P. Rivadeneira [ID48](#), J.C. Rivera Vergara [ID164](#),
 F. Rizatdinova [ID120](#), E. Rizvi [ID93](#), C. Rizzi [ID56](#), B.A. Roberts [ID166](#), B.R. Roberts [ID17a](#),
 S.H. Robertson [ID103,y](#), M. Robin [ID48](#), D. Robinson [ID32](#), C.M. Robles Gajardo [ID136f](#),
 M. Robles Manzano [ID99](#), A. Robson [ID59](#), A. Rocchi [ID75a,75b](#), C. Roda [ID73a,73b](#), S. Rodriguez Bosca [ID63a](#),
 Y. Rodriguez Garcia [ID22a](#), A. Rodriguez Rodriguez [ID54](#), A.M. Rodríguez Vera [ID155b](#), S. Roe [ID36](#),
 J.T. Roemer [ID159](#), A.R. Roepe-Gier [ID119](#), J. Roggel [ID170](#), O. Röhne [ID124](#), R.A. Rojas [ID164](#), B. Roland [ID54](#),
 C.P.A. Roland [ID67](#), J. Roloff [ID29](#), A. Romaniouk [ID37](#), E. Romano [ID72a,72b](#), M. Romano [ID23b](#),
 A.C. Romero Hernandez [ID161](#), N. Rompotis [ID91](#), L. Roos [ID126](#), S. Rosati [ID74a](#), B.J. Rosser [ID39](#),
 E. Rossi [ID4](#), E. Rossi [ID71a,71b](#), L.P. Rossi [ID57b](#), L. Rossini [ID48](#), R. Rosten [ID118](#), M. Rotaru [ID27b](#),
 B. Rottler [ID54](#), D. Rousseau [ID66](#), D. Rousso [ID32](#), G. Rovelli [ID72a,72b](#), A. Roy [ID161](#), A. Rozanov [ID101](#),
 Y. Rozen [ID149](#), X. Ruan [ID33g](#), A. Rubio Jimenez [ID162](#), A.J. Ruby [ID91](#), V.H. Ruelas Rivera [ID18](#),
 T.A. Ruggeri [ID1](#), F. Rühr [ID54](#), A. Ruiz-Martinez [ID162](#), A. Rummler [ID36](#), Z. Rurikova [ID54](#),
 N.A. Rusakovich [ID38](#), H.L. Russell [ID164](#), J.P. Rutherford [ID7](#), K. Rybacki [ID90](#), M. Rybar [ID132](#),
 E.B. Rye [ID124](#), A. Ryzhov [ID37](#), J.A. Sabater Iglesias [ID56](#), P. Sabatini [ID162](#), L. Sabetta [ID74a,74b](#),
 H.F.W. Sadrozinski [ID135](#), F. Safai Tehrani [ID74a](#), B. Safarzadeh Samani [ID145](#), M. Safdari [ID142](#),
 S. Saha [ID103](#), M. Sahinsky [ID109](#), M. Saimpert [ID134](#), M. Saito [ID152](#), T. Saito [ID152](#), D. Salamani [ID36](#),
 G. Salamanna [ID76a,76b](#), A. Salnikov [ID142](#), J. Salt [ID162](#), A. Salvador Salas [ID13](#), D. Salvatore [ID43b,43a](#),
 F. Salvatore [ID145](#), A. Salzburger [ID36](#), D. Sammel [ID54](#), D. Sampsonidis [ID151](#), D. Sampsonidou [ID62d,62c](#),
 J. Sánchez [ID162](#), A. Sanchez Pineda [ID4](#), V. Sanchez Sebastian [ID162](#), H. Sandaker [ID124](#), C.O. Sander [ID48](#),
 J.A. Sandesara [ID102](#), M. Sandhoff [ID170](#), C. Sandoval [ID22b](#), D.P.C. Sankey [ID133](#), A. Sansoni [ID53](#),
 L. Santi [ID74a,74b](#), C. Santoni [ID40](#), H. Santos [ID129a,129b](#), S.N. Santpur [ID17a](#), A. Santra [ID168](#),
 K.A. Saoucha [ID138](#), J.G. Saraiva [ID129a,129d](#), J. Sardain [ID7](#), O. Sasaki [ID82](#), K. Sato [ID156](#), C. Sauer [ID63b](#),
 F. Sauerburger [ID54](#), E. Sauvan [ID4](#), P. Savard [ID154,ag](#), R. Sawada [ID152](#), C. Sawyer [ID133](#), L. Sawyer [ID96](#),
 I. Sayago Galvan [ID162](#), C. Sbarra [ID23b](#), A. Sbrizzi [ID23b,23a](#), T. Scanlon [ID95](#), J. Schaarschmidt [ID137](#),
 P. Schacht [ID109](#), D. Schaefer [ID39](#), U. Schäfer [ID99](#), A.C. Schaffer [ID66](#), D. Schaile [ID108](#),
 R.D. Schamberger [ID144](#), E. Schanet [ID108](#), C. Scharf [ID18](#), M.M. Schefer [ID19](#), V.A. Schegelsky [ID37](#),
 D. Scheirich [ID132](#), F. Schenck [ID18](#), M. Schernau [ID159](#), C. Scheulen [ID55](#), C. Schiavi [ID57b,57a](#),
 Z.M. Schillaci [ID26](#), E.J. Schioppa [ID69a,69b](#), M. Schioppa [ID43b,43a](#), B. Schlag [ID99](#), K.E. Schleicher [ID54](#),
 S. Schlenker [ID36](#), K. Schmieden [ID99](#), C. Schmitt [ID99](#), S. Schmitt [ID48](#), L. Schoeffel [ID134](#),
 A. Schoening [ID63b](#), P.G. Scholer [ID54](#), E. Schopf [ID125](#), M. Schott [ID99](#), J. Schovancova [ID36](#),

S. Schramm [ID⁵⁶](#), F. Schroeder [ID¹⁷⁰](#), H-C. Schultz-Coulon [ID^{63a}](#), M. Schumacher [ID⁵⁴](#), B.A. Schumm [ID¹³⁵](#),
 Ph. Schune [ID¹³⁴](#), A. Schwartzman [ID¹⁴²](#), T.A. Schwarz [ID¹⁰⁵](#), Ph. Schwemling [ID¹³⁴](#), R. Schwienhorst [ID¹⁰⁶](#),
 A. Sciandra [ID¹³⁵](#), G. Sciolla [ID²⁶](#), F. Scuri [ID^{73a}](#), F. Scutti [ID¹⁰⁴](#), C.D. Sebastiani [ID⁹¹](#), K. Sedlaczek [ID⁴⁹](#),
 P. Seema [ID¹⁸](#), S.C. Seidel [ID¹¹¹](#), A. Seiden [ID¹³⁵](#), B.D. Seidlitz [ID⁴¹](#), T. Seiss [ID³⁹](#), C. Seitz [ID⁴⁸](#),
 J.M. Seixas [ID^{81b}](#), G. Sekhniaidze [ID^{71a}](#), S.J. Sekula [ID⁴⁴](#), L. Selem [ID⁴](#), N. Semprini-Cesari [ID^{23b,23a}](#),
 S. Sen [ID⁵¹](#), D. Sengupta [ID⁵⁶](#), V. Senthilkumar [ID¹⁶²](#), L. Serin [ID⁶⁶](#), L. Serkin [ID^{68a,68b}](#), M. Sessa [ID^{76a,76b}](#),
 H. Severini [ID¹¹⁹](#), S. Sevova [ID¹⁴²](#), F. Sforza [ID^{57b,57a}](#), A. Sfyrta [ID⁵⁶](#), E. Shabalina [ID⁵⁵](#), R. Shaheen [ID¹⁴³](#),
 J.D. Shahinian [ID¹²⁷](#), N.W. Shaikh [ID^{47a,47b}](#), D. Shaked Renous [ID¹⁶⁸](#), L.Y. Shan [ID^{14a}](#), M. Shapiro [ID^{17a}](#),
 A. Sharma [ID³⁶](#), A.S. Sharma [ID¹⁶³](#), P. Sharma [ID⁷⁹](#), S. Sharma [ID⁴⁸](#), P.B. Shatalov [ID³⁷](#), K. Shaw [ID¹⁴⁵](#),
 S.M. Shaw [ID¹⁰⁰](#), Q. Shen [ID^{62c,5}](#), P. Sherwood [ID⁹⁵](#), L. Shi [ID⁹⁵](#), C.O. Shimmin [ID¹⁷¹](#), Y. Shimogama [ID¹⁶⁷](#),
 J.D. Shinner [ID⁹⁴](#), I.P.J. Shipsey [ID¹²⁵](#), S. Shirabe [ID⁶⁰](#), M. Shiyakova [ID^{38,x}](#), J. Shlomi [ID¹⁶⁸](#),
 M.J. Shochet [ID³⁹](#), J. Shojaii [ID¹⁰⁴](#), D.R. Shope [ID¹²⁴](#), S. Shrestha [ID^{118,ak}](#), E.M. Shrif [ID^{33g}](#),
 M.J. Shroff [ID¹⁶⁴](#), P. Sicho [ID¹³⁰](#), A.M. Sickles [ID¹⁶¹](#), E. Sideras Haddad [ID^{33g}](#), A. Sidoti [ID^{23b}](#),
 F. Siegert [ID⁵⁰](#), Dj. Sijacki [ID¹⁵](#), R. Sikora [ID^{84a}](#), F. Sili [ID⁸⁹](#), J.M. Silva [ID²⁰](#), M.V. Silva Oliveira [ID³⁶](#),
 S.B. Silverstein [ID^{47a}](#), S. Simion [ID⁶⁶](#), R. Simoniello [ID³⁶](#), E.L. Simpson [ID⁵⁹](#), N.D. Simpson [ID⁹⁷](#),
 S. Simsek [ID^{21d}](#), S. Sindhu [ID⁵⁵](#), P. Sinervo [ID¹⁵⁴](#), V. Sinetckii [ID³⁷](#), S. Singh [ID¹⁴¹](#), S. Singh [ID¹⁵⁴](#),
 S. Sinha [ID⁴⁸](#), S. Sinha [ID^{33g}](#), M. Sioli [ID^{23b,23a}](#), I. Siral [ID¹²²](#), S.Yu. Sivoklov [ID^{37,*}](#), J. Sjölin [ID^{47a,47b}](#),
 A. Skaf [ID⁵⁵](#), E. Skorda [ID⁹⁷](#), P. Skubic [ID¹¹⁹](#), M. Slawinska [ID⁸⁵](#), V. Smakhtin [ID¹⁶⁸](#), B.H. Smart [ID¹³³](#),
 J. Smiesko [ID³⁶](#), S.Yu. Smirnov [ID³⁷](#), Y. Smirnov [ID³⁷](#), L.N. Smirnova [ID^{37,a}](#), O. Smirnova [ID⁹⁷](#),
 A.C. Smith [ID⁴¹](#), E.A. Smith [ID³⁹](#), H.A. Smith [ID¹²⁵](#), J.L. Smith [ID⁹¹](#), R. Smith [ID¹⁴²](#), M. Smizanska [ID⁹⁰](#),
 K. Smolek [ID¹³¹](#), A. Smykiewicz [ID⁸⁵](#), A.A. Snesev [ID³⁷](#), H.L. Snoek [ID¹¹³](#), S. Snyder [ID²⁹](#),
 R. Sobie [ID^{164,y}](#), A. Soffer [ID¹⁵⁰](#), C.A. Solans Sanchez [ID³⁶](#), E.Yu. Soldatov [ID³⁷](#), U. Soldevila [ID¹⁶²](#),
 A.A. Solodkov [ID³⁷](#), S. Solomon [ID⁵⁴](#), A. Soloshenko [ID³⁸](#), K. Solovieva [ID⁵⁴](#), O.V. Solovyanov [ID³⁷](#),
 V. Solovyev [ID³⁷](#), P. Sommer [ID³⁶](#), A. Sonay [ID¹³](#), W.Y. Song [ID^{155b}](#), A. Sopczak [ID¹³¹](#), A.L. Sopio [ID⁹⁵](#),
 F. Sopkova [ID^{28b}](#), V. Sothilingam [ID^{63a}](#), S. Sottocornola [ID^{72a,72b}](#), R. Soualah [ID^{115b}](#), Z. Soumami [ID^{35e}](#),
 D. South [ID⁴⁸](#), S. Spagnolo [ID^{69a,69b}](#), M. Spalla [ID¹⁰⁹](#), F. Spanò [ID⁹⁴](#), D. Sperlich [ID⁵⁴](#), G. Spigo [ID³⁶](#),
 M. Spina [ID¹⁴⁵](#), S. Spinalli [ID⁹⁰](#), D.P. Spiteri [ID⁵⁹](#), M. Spousta [ID¹³²](#), E.J. Staats [ID³⁴](#), A. Stabile [ID^{70a,70b}](#),
 R. Stamen [ID^{63a}](#), M. Stamenkovic [ID¹¹³](#), A. Stampekis [ID²⁰](#), M. Standke [ID²⁴](#), E. Stanecka [ID⁸⁵](#),
 M.V. Stange [ID⁵⁰](#), B. Stanislaus [ID^{17a}](#), M.M. Stanitzki [ID⁴⁸](#), M. Stankaityte [ID¹²⁵](#), B. Stapf [ID⁴⁸](#),
 E.A. Starchenko [ID³⁷](#), G.H. Stark [ID¹³⁵](#), J. Stark [ID^{101,ab}](#), D.M. Starko [ID^{155b}](#), P. Staroba [ID¹³⁰](#),
 P. Starovoitov [ID^{63a}](#), S. Stärz [ID¹⁰³](#), R. Staszewski [ID⁸⁵](#), G. Stavropoulos [ID⁴⁶](#), J. Steentoft [ID¹⁶⁰](#),
 P. Steinberg [ID²⁹](#), A.L. Steinhebel [ID¹²²](#), B. Stelzer [ID^{141,155a}](#), H.J. Stelzer [ID¹²⁸](#), O. Stelzer-Chilton [ID^{155a}](#),
 H. Stenzel [ID⁵⁸](#), T.J. Stevenson [ID¹⁴⁵](#), G.A. Stewart [ID³⁶](#), M.C. Stockton [ID³⁶](#), G. Stoicea [ID^{27b}](#),
 M. Stolarski [ID^{129a}](#), S. Stonjek [ID¹⁰⁹](#), A. Straessner [ID⁵⁰](#), J. Strandberg [ID¹⁴³](#), S. Strandberg [ID^{47a,47b}](#),
 M. Strauss [ID¹¹⁹](#), T. Strebler [ID¹⁰¹](#), P. Strizenec [ID^{28b}](#), R. Ströhmer [ID¹⁶⁵](#), D.M. Strom [ID¹²²](#), L.R. Strom [ID⁴⁸](#),
 R. Stroynowski [ID⁴⁴](#), A. Strubig [ID^{47a,47b}](#), S.A. Stucci [ID²⁹](#), B. Stugu [ID¹⁶](#), J. Stupak [ID¹¹⁹](#), N.A. Styles [ID⁴⁸](#),
 D. Su [ID¹⁴²](#), S. Su [ID^{62a}](#), W. Su [ID^{62d,137,62c}](#), X. Su [ID^{62a,66}](#), K. Sugizaki [ID¹⁵²](#), V.V. Sulín [ID³⁷](#),
 M.J. Sullivan [ID⁹¹](#), D.M.S. Sultan [ID^{77a,77b}](#), L. Sultanaliyeva [ID³⁷](#), S. Sultansoy [ID^{3b}](#), T. Sumida [ID⁸⁶](#),
 S. Sun [ID¹⁰⁵](#), S. Sun [ID¹⁶⁹](#), O. Sunneborn Gudnadottir [ID¹⁶⁰](#), M.R. Sutton [ID¹⁴⁵](#), M. Svatos [ID¹³⁰](#),
 M. Swiatlowski [ID^{155a}](#), T. Swirski [ID¹⁶⁵](#), I. Sykora [ID^{28a}](#), M. Sykora [ID¹³²](#), T. Sykora [ID¹³²](#), D. Ta [ID⁹⁹](#),
 K. Tackmann [ID^{48,w}](#), A. Taffard [ID¹⁵⁹](#), R. Tafirout [ID^{155a}](#), J.S. Tafuya Vargas [ID⁶⁶](#), R.H.M. Taibah [ID¹²⁶](#),
 R. Takashima [ID⁸⁷](#), K. Takeda [ID⁸³](#), E.P. Takeva [ID⁵²](#), Y. Takubo [ID⁸²](#), M. Talby [ID¹⁰¹](#), A.A. Talyshev [ID³⁷](#),
 K.C. Tam [ID^{64b}](#), N.M. Tamir [ID¹⁵⁰](#), A. Tanaka [ID¹⁵²](#), J. Tanaka [ID¹⁵²](#), R. Tanaka [ID⁶⁶](#), M. Tanasini [ID^{57b,57a}](#),
 J. Tang [ID^{62c}](#), Z. Tao [ID¹⁶³](#), S. Tapia Araya [ID⁸⁰](#), S. Tapprogge [ID⁹⁹](#), A. Tarek Abouelfadl Mohamed [ID¹⁰⁶](#),
 S. Tarem [ID¹⁴⁹](#), K. Tariq [ID^{62b}](#), G. Tarna [ID^{27b}](#), G.F. Tartarelli [ID^{70a}](#), P. Tas [ID¹³²](#), M. Tasevsky [ID¹³⁰](#),
 E. Tassi [ID^{43b,43a}](#), A.C. Tate [ID¹⁶¹](#), G. Tateno [ID¹⁵²](#), Y. Tayalati [ID^{35e}](#), G.N. Taylor [ID¹⁰⁴](#), W. Taylor [ID^{155b}](#),
 H. Teagle [ID⁹¹](#), A.S. Tee [ID¹⁶⁹](#), R. Teixeira De Lima [ID¹⁴²](#), P. Teixeira-Dias [ID⁹⁴](#), J.J. Teoh [ID¹⁵⁴](#),

K. Terashi ¹⁵², J. Terron ⁹⁸, S. Terzo ¹³, M. Testa ⁵³, R.J. Teuscher ^{154,y}, A. Thaler ⁷⁸,
 O. Theiner ⁵⁶, N. Themistokleous ⁵², T. Thevenaux-Pelzer ¹⁸, O. Thielmann ¹⁷⁰, D.W. Thomas⁹⁴,
 J.P. Thomas ²⁰, E.A. Thompson ⁴⁸, P.D. Thompson ²⁰, E. Thomson ¹²⁷, E.J. Thorpe ⁹³,
 Y. Tian ⁵⁵, V. Tikhomirov ^{37,a}, Yu.A. Tikhonov ³⁷, S. Timoshenko³⁷, E.X.L. Ting ¹, P. Tipton ¹⁷¹,
 S. Tisserant ¹⁰¹, S.H. Tlou ^{33g}, A. Tnourji ⁴⁰, K. Todome ^{23b,23a}, S. Todorova-Nova ¹³², S. Todt⁵⁰,
 M. Togawa ⁸², J. Tojo ⁸⁸, S. Tokár ^{28a}, K. Tokushuku ⁸², R. Tombs ³², M. Tomoto ^{82,110},
 L. Tompkins ^{142,q}, K.W. Topolnicki ^{84b}, P. Tornambe ¹⁰², E. Torrence ¹²², H. Torres ⁵⁰,
 E. Torró Pastor ¹⁶², M. Toscani ³⁰, C. Tosciri ³⁹, D.R. Tovey ¹³⁸, A. Traeet¹⁶, I.S. Trandafir ^{27b},
 T. Trefzger ¹⁶⁵, A. Tricoli ²⁹, I.M. Trigger ^{155a}, S. Trincaz-Duvoid ¹²⁶, D.A. Trischuk ²⁶,
 B. Trocmé ⁶⁰, A. Trofymov ⁶⁶, C. Troncon ^{70a}, L. Truong ^{33c}, M. Trzebinski ⁸⁵, A. Trzupiek ⁸⁵,
 F. Tsai ¹⁴⁴, M. Tsai ¹⁰⁵, A. Tsiamis ¹⁵¹, P.V. Tsiarehshka³⁷, S. Tsigaridas ^{155a}, A. Tsigotis ^{151,u},
 V. Tsiskaridze ¹⁴⁴, E.G. Tskhadadze ^{148a}, M. Tsopoulou ¹⁵¹, Y. Tsujikawa ⁸⁶, I.I. Tsukerman ³⁷,
 V. Tsulaia ^{17a}, S. Tsuno ⁸², O. Tsur¹⁴⁹, D. Tsybychev ¹⁴⁴, Y. Tu ^{64b}, A. Tudorache ^{27b},
 V. Tudorache ^{27b}, A.N. Tuna ³⁶, S. Turchikhin ³⁸, I. Turk Cakir ^{3a}, R. Turra ^{70a}, T. Turtuvshin ³⁸,
 P.M. Tuts ⁴¹, S. Tzamarias ¹⁵¹, P. Tzanis ¹⁰, E. Tzovara ⁹⁹, K. Uchida¹⁵², F. Ukegawa ¹⁵⁶,
 P.A. Ulloa Poblete ^{136c}, G. Unal ³⁶, M. Unal ¹¹, A. Undrus ²⁹, G. Unel ¹⁵⁹, J. Urban ^{28b},
 P. Urquijo ¹⁰⁴, G. Usai ⁸, R. Ushioda ¹⁵³, M. Usman ¹⁰⁷, Z. Uysal ^{21b}, V. Vacek ¹³¹,
 B. Vachon ¹⁰³, K.O.H. Vadla ¹²⁴, T. Vafeiadis ³⁶, C. Valderanis ¹⁰⁸, E. Valdes Santurio ^{47a,47b},
 M. Valente ^{155a}, S. Valentinetti ^{23b,23a}, A. Valero ¹⁶², A. Vallier ^{101,ab}, J.A. Valls Ferrer ¹⁶²,
 T.R. Van Daalen ¹³⁷, P. Van Gemmeren ⁶, M. Van Rijnbach ^{124,36}, S. Van Stroud ⁹⁵,
 I. Van Vulpen ¹¹³, M. Vanadia ^{75a,75b}, W. Vandelli ³⁶, M. Vandenbroucke ¹³⁴, E.R. Vandewall ¹²⁰,
 D. Vannicola ¹⁵⁰, L. Vannoli ^{57b,57a}, R. Vari ^{74a}, E.W. Varnes ⁷, C. Varni ^{17a}, T. Varol ¹⁴⁷,
 D. Varouchas ⁶⁶, L. Varriale ¹⁶², K.E. Varvell ¹⁴⁶, M.E. Vasile ^{27b}, L. Vaslin⁴⁰, G.A. Vasquez ¹⁶⁴,
 F. Vazeille ⁴⁰, T. Vazquez Schroeder ³⁶, J. Veatch ³¹, V. Vecchio ¹⁰⁰, M.J. Veen ¹⁰²,
 I. Veliscek ¹²⁵, L.M. Veloce ¹⁵⁴, F. Veloso ^{129a,129c}, S. Veneziano ^{74a}, A. Ventura ^{69a,69b},
 A. Verbytskyi ¹⁰⁹, M. Verducci ^{73a,73b}, C. Vergis ²⁴, M. Verissimo De Araujo ^{81b},
 W. Verkerke ¹¹³, J.C. Vermeulen ¹¹³, C. Vernieri ¹⁴², P.J. Verschuuren ⁹⁴, M. Vessella ¹⁰²,
 M.C. Vetterli ^{141,ag}, A. Vgenopoulos ¹⁵¹, N. Viaux Maira ^{136f}, T. Vickey ¹³⁸,
 O.E. Vickey Boeriu ¹³⁸, G.H.A. Viehhauser ¹²⁵, L. Viganì ^{63b}, M. Villa ^{23b,23a},
 M. Villaplana Perez ¹⁶², E.M. Villhauer⁵², E. Vilucchi ⁵³, M.G. Vincter ³⁴, G.S. Virdee ²⁰,
 A. Vishwakarma ⁵², C. Vittori ^{23b,23a}, I. Vivarelli ¹⁴⁵, V. Vladimirov¹⁶⁶, E. Voevodina ¹⁰⁹,
 F. Vogel ¹⁰⁸, P. Vokac ¹³¹, J. Von Ahnen ⁴⁸, E. Von Toerne ²⁴, B. Vormwald ³⁶, V. Vorobel ¹³²,
 K. Vorobev ³⁷, M. Vos ¹⁶², J.H. Vosseveld ⁹¹, M. Vozak ¹¹³, L. Vozdecky ⁹³, N. Vranjes ¹⁵,
 M. Vranjes Milosavljevic ¹⁵, M. Vreeswijk ¹¹³, R. Vuillermet ³⁶, O. Vujanovic ⁹⁹, I. Vukotic ³⁹,
 S. Wada ¹⁵⁶, C. Wagner¹⁰², W. Wagner ¹⁷⁰, S. Wahdan ¹⁷⁰, H. Wahlberg ⁸⁹, R. Wakasa ¹⁵⁶,
 M. Wakida ¹¹⁰, V.M. Walbrecht ¹⁰⁹, J. Walder ¹³³, R. Walker ¹⁰⁸, W. Walkowiak ¹⁴⁰,
 A.M. Wang ⁶¹, A.Z. Wang ¹⁶⁹, C. Wang ^{62a}, C. Wang ^{62c}, H. Wang ^{17a}, J. Wang ^{64a},
 P. Wang ⁴⁴, R.-J. Wang ⁹⁹, R. Wang ⁶¹, R. Wang ⁶, S.M. Wang ¹⁴⁷, S. Wang ^{62b}, T. Wang ^{62a},
 W.T. Wang ⁷⁹, W.X. Wang ^{62a}, X. Wang ^{14c}, X. Wang ¹⁶¹, X. Wang ^{62c}, Y. Wang ^{62d},
 Y. Wang ^{14c}, Z. Wang ¹⁰⁵, Z. Wang ^{62d,51,62c}, Z. Wang ¹⁰⁵, A. Warburton ¹⁰³, R.J. Ward ²⁰,
 N. Warrack ⁵⁹, A.T. Watson ²⁰, M.F. Watson ²⁰, G. Watts ¹³⁷, B.M. Waugh ⁹⁵, A.F. Webb ¹¹,
 C. Weber ²⁹, M.S. Weber ¹⁹, S.M. Weber ^{63a}, C. Wei^{62a}, Y. Wei ¹²⁵, A.R. Weidberg ¹²⁵,
 J. Weingarten ⁴⁹, M. Weirich ⁹⁹, C. Weiser ⁵⁴, C.J. Wells ⁴⁸, T. Wenaus ²⁹, B. Wendland ⁴⁹,
 T. Wengler ³⁶, N.S. Wenke¹⁰⁹, N. Wermes ²⁴, M. Wessels ^{63a}, K. Whalen ¹²², A.M. Wharton ⁹⁰,
 A.S. White ⁶¹, A. White ⁸, M.J. White ¹, D. Whiteson ¹⁵⁹, L. Wickremasinghe ¹²³,
 W. Wiedenmann ¹⁶⁹, C. Wiel ⁵⁰, M. Wielers ¹³³, N. Wieseotte⁹⁹, C. Wiglesworth ⁴²,
 L.A.M. Wiik-Fuchs ⁵⁴, D.J. Wilbern¹¹⁹, H.G. Wilkens ³⁶, D.M. Williams ⁴¹, H.H. Williams¹²⁷,

S. Williams , S. Willocq , P.J. Windischhofer , F. Winklmeier , B.T. Winter , M. Wittgen , M. Wobisch , R. Wölker , J. Wollrath , M.W. Wolter , H. Wolters , V.W.S. Wong , A.F. Wongel , S.D. Worm , B.K. Wosiek , K.W. Woźniak , K. Wraight , J. Wu , M. Wu , M. Wu , S.L. Wu , X. Wu , Y. Wu , Z. Wu , J. Wuerzinger , T.R. Wyatt , B.M. Wynne , S. Xella , L. Xia , M. Xia , J. Xiang , X. Xiao , M. Xie , X. Xie , J. Xiong , I. Xiotidis , D. Xu , H. Xu , H. Xu , L. Xu , R. Xu , T. Xu , W. Xu , Y. Xu , Z. Xu , Z. Xu , B. Yabsley , S. Yacoub , N. Yamaguchi , Y. Yamaguchi , H. Yamauchi , T. Yamazaki , Y. Yamazaki , J. Yan , S. Yan , Z. Yan , H.J. Yang , H.T. Yang , S. Yang , T. Yang , X. Yang , X. Yang , Y. Yang , Z. Yang , W.-M. Yao , Y.C. Yap , H. Ye , J. Ye , S. Ye , X. Ye , Y. Yeh , I. Yeletsikh , M.R. Yexley , P. Yin , K. Yorita , C.J.S. Young , C. Young , M. Yuan , R. Yuan , L. Yue , X. Yue , M. Zaazoua , B. Zabinski , E. Zaid , T. Zakareishvili , N. Zakharchuk , S. Zambito , J.A. Zamora Saa , J. Zang , D. Zanzi , O. Zaplatilek , S.V. Zeibner , C. Zeitnitz , J.C. Zeng , D.T. Zenger Jr , O. Zenin , T. Ženiš , S. Zenz , S. Zerradi , D. Zerwas , B. Zhang , D.F. Zhang , G. Zhang , J. Zhang , J. Zhang , K. Zhang , L. Zhang , P. Zhang , R. Zhang , S. Zhang , T. Zhang , X. Zhang , X. Zhang , Z. Zhang , Z. Zhang , H. Zhao , P. Zhao , T. Zhao , Y. Zhao , Z. Zhao , A. Zhemchugov , X. Zheng , Z. Zheng , D. Zhong , B. Zhou , C. Zhou , H. Zhou , N. Zhou , Y. Zhou , C.G. Zhu , C. Zhu , H.L. Zhu , H. Zhu , J. Zhu , Y. Zhu , Y. Zhu , X. Zhuang , K. Zhukov , V. Zhulanov , N.I. Zimine , J. Zinsser , M. Ziolkowski , L. Živković , A. Zoccoli , K. Zoch , T.G. Zorbas , O. Zormpa , W. Zou , L. Zwalinski .

¹Department of Physics, University of Adelaide, Adelaide; Australia.

²Department of Physics, University of Alberta, Edmonton AB; Canada.

³(^a)Department of Physics, Ankara University, Ankara; (^b)Division of Physics, TOBB University of Economics and Technology, Ankara; Türkiye.

⁴LAPP, Université Savoie Mont Blanc, CNRS/IN2P3, Annecy; France.

⁵APC, Université Paris Cité, CNRS/IN2P3, Paris; France.

⁶High Energy Physics Division, Argonne National Laboratory, Argonne IL; United States of America.

⁷Department of Physics, University of Arizona, Tucson AZ; United States of America.

⁸Department of Physics, University of Texas at Arlington, Arlington TX; United States of America.

⁹Physics Department, National and Kapodistrian University of Athens, Athens; Greece.

¹⁰Physics Department, National Technical University of Athens, Zografou; Greece.

¹¹Department of Physics, University of Texas at Austin, Austin TX; United States of America.

¹²Institute of Physics, Azerbaijan Academy of Sciences, Baku; Azerbaijan.

¹³Institut de Física d'Altes Energies (IFAE), Barcelona Institute of Science and Technology, Barcelona; Spain.

¹⁴(^a)Institute of High Energy Physics, Chinese Academy of Sciences, Beijing; (^b)Physics Department, Tsinghua University, Beijing; (^c)Department of Physics, Nanjing University, Nanjing; (^d)University of Chinese Academy of Science (UCAS), Beijing; China.

¹⁵Institute of Physics, University of Belgrade, Belgrade; Serbia.

¹⁶Department for Physics and Technology, University of Bergen, Bergen; Norway.

¹⁷(^a)Physics Division, Lawrence Berkeley National Laboratory, Berkeley CA; (^b)University of California, Berkeley CA; United States of America.

- ¹⁸Institut für Physik, Humboldt Universität zu Berlin, Berlin; Germany.
- ¹⁹Albert Einstein Center for Fundamental Physics and Laboratory for High Energy Physics, University of Bern, Bern; Switzerland.
- ²⁰School of Physics and Astronomy, University of Birmingham, Birmingham; United Kingdom.
- ²¹(^a) Department of Physics, Bogazici University, Istanbul; (^b) Department of Physics Engineering, Gaziantep University, Gaziantep; (^c) Department of Physics, Istanbul University, Istanbul; (^d) Istinye University, Sariyer, Istanbul; Türkiye.
- ²²(^a) Facultad de Ciencias y Centro de Investigaciones, Universidad Antonio Nariño, Bogotá; (^b) Departamento de Física, Universidad Nacional de Colombia, Bogotá; Colombia.
- ²³(^a) Dipartimento di Fisica e Astronomia A. Righi, Università di Bologna, Bologna; (^b) INFN Sezione di Bologna; Italy.
- ²⁴Physikalisches Institut, Universität Bonn, Bonn; Germany.
- ²⁵Department of Physics, Boston University, Boston MA; United States of America.
- ²⁶Department of Physics, Brandeis University, Waltham MA; United States of America.
- ²⁷(^a) Transilvania University of Brasov, Brasov; (^b) Horia Hulubei National Institute of Physics and Nuclear Engineering, Bucharest; (^c) Department of Physics, Alexandru Ioan Cuza University of Iasi, Iasi; (^d) National Institute for Research and Development of Isotopic and Molecular Technologies, Physics Department, Cluj-Napoca; (^e) University Politehnica Bucharest, Bucharest; (^f) West University in Timisoara, Timisoara; (^g) Faculty of Physics, University of Bucharest, Bucharest; Romania.
- ²⁸(^a) Faculty of Mathematics, Physics and Informatics, Comenius University, Bratislava; (^b) Department of Subnuclear Physics, Institute of Experimental Physics of the Slovak Academy of Sciences, Kosice; Slovak Republic.
- ²⁹Physics Department, Brookhaven National Laboratory, Upton NY; United States of America.
- ³⁰Universidad de Buenos Aires, Facultad de Ciencias Exactas y Naturales, Departamento de Física, y CONICET, Instituto de Física de Buenos Aires (IFIBA), Buenos Aires; Argentina.
- ³¹California State University, CA; United States of America.
- ³²Cavendish Laboratory, University of Cambridge, Cambridge; United Kingdom.
- ³³(^a) Department of Physics, University of Cape Town, Cape Town; (^b) iThemba Labs, Western Cape; (^c) Department of Mechanical Engineering Science, University of Johannesburg, Johannesburg; (^d) National Institute of Physics, University of the Philippines Diliman (Philippines); (^e) University of South Africa, Department of Physics, Pretoria; (^f) University of Zululand, KwaDlangezwa; (^g) School of Physics, University of the Witwatersrand, Johannesburg; South Africa.
- ³⁴Department of Physics, Carleton University, Ottawa ON; Canada.
- ³⁵(^a) Faculté des Sciences Ain Chock, Réseau Universitaire de Physique des Hautes Energies - Université Hassan II, Casablanca; (^b) Faculté des Sciences, Université Ibn-Tofail, Kénitra; (^c) Faculté des Sciences Semlalia, Université Cadi Ayyad, LPHEA-Marrakech; (^d) LPMR, Faculté des Sciences, Université Mohamed Premier, Oujda; (^e) Faculté des sciences, Université Mohammed V, Rabat; (^f) Institute of Applied Physics, Mohammed VI Polytechnic University, Ben Guerir; Morocco.
- ³⁶CERN, Geneva; Switzerland.
- ³⁷Affiliated with an institute covered by a cooperation agreement with CERN.
- ³⁸Affiliated with an international laboratory covered by a cooperation agreement with CERN.
- ³⁹Enrico Fermi Institute, University of Chicago, Chicago IL; United States of America.
- ⁴⁰LPC, Université Clermont Auvergne, CNRS/IN2P3, Clermont-Ferrand; France.
- ⁴¹Nevis Laboratory, Columbia University, Irvington NY; United States of America.
- ⁴²Niels Bohr Institute, University of Copenhagen, Copenhagen; Denmark.
- ⁴³(^a) Dipartimento di Fisica, Università della Calabria, Rende; (^b) INFN Gruppo Collegato di Cosenza, Laboratori Nazionali di Frascati; Italy.

- ⁴⁴Physics Department, Southern Methodist University, Dallas TX; United States of America.
- ⁴⁵Physics Department, University of Texas at Dallas, Richardson TX; United States of America.
- ⁴⁶National Centre for Scientific Research "Demokritos", Agia Paraskevi; Greece.
- ⁴⁷(^a) Department of Physics, Stockholm University; (^b) Oskar Klein Centre, Stockholm; Sweden.
- ⁴⁸Deutsches Elektronen-Synchrotron DESY, Hamburg and Zeuthen; Germany.
- ⁴⁹Fakultät Physik, Technische Universität Dortmund, Dortmund; Germany.
- ⁵⁰Institut für Kern- und Teilchenphysik, Technische Universität Dresden, Dresden; Germany.
- ⁵¹Department of Physics, Duke University, Durham NC; United States of America.
- ⁵²SUPA - School of Physics and Astronomy, University of Edinburgh, Edinburgh; United Kingdom.
- ⁵³INFN e Laboratori Nazionali di Frascati, Frascati; Italy.
- ⁵⁴Physikalisches Institut, Albert-Ludwigs-Universität Freiburg, Freiburg; Germany.
- ⁵⁵II. Physikalisches Institut, Georg-August-Universität Göttingen, Göttingen; Germany.
- ⁵⁶Département de Physique Nucléaire et Corpusculaire, Université de Genève, Genève; Switzerland.
- ⁵⁷(^a) Dipartimento di Fisica, Università di Genova, Genova; (^b) INFN Sezione di Genova; Italy.
- ⁵⁸II. Physikalisches Institut, Justus-Liebig-Universität Giessen, Giessen; Germany.
- ⁵⁹SUPA - School of Physics and Astronomy, University of Glasgow, Glasgow; United Kingdom.
- ⁶⁰LPSC, Université Grenoble Alpes, CNRS/IN2P3, Grenoble INP, Grenoble; France.
- ⁶¹Laboratory for Particle Physics and Cosmology, Harvard University, Cambridge MA; United States of America.
- ⁶²(^a) Department of Modern Physics and State Key Laboratory of Particle Detection and Electronics, University of Science and Technology of China, Hefei; (^b) Institute of Frontier and Interdisciplinary Science and Key Laboratory of Particle Physics and Particle Irradiation (MOE), Shandong University, Qingdao; (^c) School of Physics and Astronomy, Shanghai Jiao Tong University, Key Laboratory for Particle Astrophysics and Cosmology (MOE), SKLPPC, Shanghai; (^d) Tsung-Dao Lee Institute, Shanghai; China.
- ⁶³(^a) Kirchhoff-Institut für Physik, Ruprecht-Karls-Universität Heidelberg, Heidelberg; (^b) Physikalisches Institut, Ruprecht-Karls-Universität Heidelberg, Heidelberg; Germany.
- ⁶⁴(^a) Department of Physics, Chinese University of Hong Kong, Shatin, N.T., Hong Kong; (^b) Department of Physics, University of Hong Kong, Hong Kong; (^c) Department of Physics and Institute for Advanced Study, Hong Kong University of Science and Technology, Clear Water Bay, Kowloon, Hong Kong; China.
- ⁶⁵Department of Physics, National Tsing Hua University, Hsinchu; Taiwan.
- ⁶⁶IJCLab, Université Paris-Saclay, CNRS/IN2P3, 91405, Orsay; France.
- ⁶⁷Department of Physics, Indiana University, Bloomington IN; United States of America.
- ⁶⁸(^a) INFN Gruppo Collegato di Udine, Sezione di Trieste, Udine; (^b) ICTP, Trieste; (^c) Dipartimento Politecnico di Ingegneria e Architettura, Università di Udine, Udine; Italy.
- ⁶⁹(^a) INFN Sezione di Lecce; (^b) Dipartimento di Matematica e Fisica, Università del Salento, Lecce; Italy.
- ⁷⁰(^a) INFN Sezione di Milano; (^b) Dipartimento di Fisica, Università di Milano, Milano; Italy.
- ⁷¹(^a) INFN Sezione di Napoli; (^b) Dipartimento di Fisica, Università di Napoli, Napoli; Italy.
- ⁷²(^a) INFN Sezione di Pavia; (^b) Dipartimento di Fisica, Università di Pavia, Pavia; Italy.
- ⁷³(^a) INFN Sezione di Pisa; (^b) Dipartimento di Fisica E. Fermi, Università di Pisa, Pisa; Italy.
- ⁷⁴(^a) INFN Sezione di Roma; (^b) Dipartimento di Fisica, Sapienza Università di Roma, Roma; Italy.
- ⁷⁵(^a) INFN Sezione di Roma Tor Vergata; (^b) Dipartimento di Fisica, Università di Roma Tor Vergata, Roma; Italy.
- ⁷⁶(^a) INFN Sezione di Roma Tre; (^b) Dipartimento di Matematica e Fisica, Università Roma Tre, Roma; Italy.
- ⁷⁷(^a) INFN-TIFPA; (^b) Università degli Studi di Trento, Trento; Italy.
- ⁷⁸Universität Innsbruck, Department of Astro and Particle Physics, Innsbruck; Austria.
- ⁷⁹University of Iowa, Iowa City IA; United States of America.

- ⁸⁰Department of Physics and Astronomy, Iowa State University, Ames IA; United States of America.
- ⁸¹(^a) Departamento de Engenharia Elétrica, Universidade Federal de Juiz de Fora (UFJF), Juiz de Fora; (^b) Universidade Federal do Rio De Janeiro COPPE/EE/IF, Rio de Janeiro; (^c) Instituto de Física, Universidade de São Paulo, São Paulo; (^d) Rio de Janeiro State University, Rio de Janeiro; Brazil.
- ⁸²KEK, High Energy Accelerator Research Organization, Tsukuba; Japan.
- ⁸³Graduate School of Science, Kobe University, Kobe; Japan.
- ⁸⁴(^a) AGH University of Krakow, Faculty of Physics and Applied Computer Science, Krakow; (^b) Marian Smoluchowski Institute of Physics, Jagiellonian University, Krakow; Poland.
- ⁸⁵Institute of Nuclear Physics Polish Academy of Sciences, Krakow; Poland.
- ⁸⁶Faculty of Science, Kyoto University, Kyoto; Japan.
- ⁸⁷Kyoto University of Education, Kyoto; Japan.
- ⁸⁸Research Center for Advanced Particle Physics and Department of Physics, Kyushu University, Fukuoka ; Japan.
- ⁸⁹Instituto de Física La Plata, Universidad Nacional de La Plata and CONICET, La Plata; Argentina.
- ⁹⁰Physics Department, Lancaster University, Lancaster; United Kingdom.
- ⁹¹Oliver Lodge Laboratory, University of Liverpool, Liverpool; United Kingdom.
- ⁹²Department of Experimental Particle Physics, Jožef Stefan Institute and Department of Physics, University of Ljubljana, Ljubljana; Slovenia.
- ⁹³School of Physics and Astronomy, Queen Mary University of London, London; United Kingdom.
- ⁹⁴Department of Physics, Royal Holloway University of London, Egham; United Kingdom.
- ⁹⁵Department of Physics and Astronomy, University College London, London; United Kingdom.
- ⁹⁶Louisiana Tech University, Ruston LA; United States of America.
- ⁹⁷Fysiska institutionen, Lunds universitet, Lund; Sweden.
- ⁹⁸Departamento de Física Teórica C-15 and CIAFF, Universidad Autónoma de Madrid, Madrid; Spain.
- ⁹⁹Institut für Physik, Universität Mainz, Mainz; Germany.
- ¹⁰⁰School of Physics and Astronomy, University of Manchester, Manchester; United Kingdom.
- ¹⁰¹CPPM, Aix-Marseille Université, CNRS/IN2P3, Marseille; France.
- ¹⁰²Department of Physics, University of Massachusetts, Amherst MA; United States of America.
- ¹⁰³Department of Physics, McGill University, Montreal QC; Canada.
- ¹⁰⁴School of Physics, University of Melbourne, Victoria; Australia.
- ¹⁰⁵Department of Physics, University of Michigan, Ann Arbor MI; United States of America.
- ¹⁰⁶Department of Physics and Astronomy, Michigan State University, East Lansing MI; United States of America.
- ¹⁰⁷Group of Particle Physics, University of Montreal, Montreal QC; Canada.
- ¹⁰⁸Fakultät für Physik, Ludwig-Maximilians-Universität München, München; Germany.
- ¹⁰⁹Max-Planck-Institut für Physik (Werner-Heisenberg-Institut), München; Germany.
- ¹¹⁰Graduate School of Science and Kobayashi-Maskawa Institute, Nagoya University, Nagoya; Japan.
- ¹¹¹Department of Physics and Astronomy, University of New Mexico, Albuquerque NM; United States of America.
- ¹¹²Institute for Mathematics, Astrophysics and Particle Physics, Radboud University/Nikhef, Nijmegen; Netherlands.
- ¹¹³Nikhef National Institute for Subatomic Physics and University of Amsterdam, Amsterdam; Netherlands.
- ¹¹⁴Department of Physics, Northern Illinois University, DeKalb IL; United States of America.
- ¹¹⁵(^a) New York University Abu Dhabi, Abu Dhabi; (^b) University of Sharjah, Sharjah; United Arab Emirates.
- ¹¹⁶Department of Physics, New York University, New York NY; United States of America.

- ¹¹⁷Ochanomizu University, Otsuka, Bunkyo-ku, Tokyo; Japan.
- ¹¹⁸Ohio State University, Columbus OH; United States of America.
- ¹¹⁹Homer L. Dodge Department of Physics and Astronomy, University of Oklahoma, Norman OK; United States of America.
- ¹²⁰Department of Physics, Oklahoma State University, Stillwater OK; United States of America.
- ¹²¹Palacký University, Joint Laboratory of Optics, Olomouc; Czech Republic.
- ¹²²Institute for Fundamental Science, University of Oregon, Eugene, OR; United States of America.
- ¹²³Graduate School of Science, Osaka University, Osaka; Japan.
- ¹²⁴Department of Physics, University of Oslo, Oslo; Norway.
- ¹²⁵Department of Physics, Oxford University, Oxford; United Kingdom.
- ¹²⁶LPNHE, Sorbonne Université, Université Paris Cité, CNRS/IN2P3, Paris; France.
- ¹²⁷Department of Physics, University of Pennsylvania, Philadelphia PA; United States of America.
- ¹²⁸Department of Physics and Astronomy, University of Pittsburgh, Pittsburgh PA; United States of America.
- ¹²⁹^(a)Laboratório de Instrumentação e Física Experimental de Partículas - LIP, Lisboa;^(b)Departamento de Física, Faculdade de Ciências, Universidade de Lisboa, Lisboa;^(c)Departamento de Física, Universidade de Coimbra, Coimbra;^(d)Centro de Física Nuclear da Universidade de Lisboa, Lisboa;^(e)Departamento de Física, Universidade do Minho, Braga;^(f)Departamento de Física Teórica y del Cosmos, Universidad de Granada, Granada (Spain);^(g)Departamento de Física, Instituto Superior Técnico, Universidade de Lisboa, Lisboa; Portugal.
- ¹³⁰Institute of Physics of the Czech Academy of Sciences, Prague; Czech Republic.
- ¹³¹Czech Technical University in Prague, Prague; Czech Republic.
- ¹³²Charles University, Faculty of Mathematics and Physics, Prague; Czech Republic.
- ¹³³Particle Physics Department, Rutherford Appleton Laboratory, Didcot; United Kingdom.
- ¹³⁴IRFU, CEA, Université Paris-Saclay, Gif-sur-Yvette; France.
- ¹³⁵Santa Cruz Institute for Particle Physics, University of California Santa Cruz, Santa Cruz CA; United States of America.
- ¹³⁶^(a)Departamento de Física, Pontificia Universidad Católica de Chile, Santiago;^(b)Millennium Institute for Subatomic physics at high energy frontier (SAPHIR), Santiago;^(c)Instituto de Investigación Multidisciplinario en Ciencia y Tecnología, y Departamento de Física, Universidad de La Serena;^(d)Universidad Andres Bello, Department of Physics, Santiago;^(e)Instituto de Alta Investigación, Universidad de Tarapacá, Arica;^(f)Departamento de Física, Universidad Técnica Federico Santa María, Valparaíso; Chile.
- ¹³⁷Department of Physics, University of Washington, Seattle WA; United States of America.
- ¹³⁸Department of Physics and Astronomy, University of Sheffield, Sheffield; United Kingdom.
- ¹³⁹Department of Physics, Shinshu University, Nagano; Japan.
- ¹⁴⁰Department Physik, Universität Siegen, Siegen; Germany.
- ¹⁴¹Department of Physics, Simon Fraser University, Burnaby BC; Canada.
- ¹⁴²SLAC National Accelerator Laboratory, Stanford CA; United States of America.
- ¹⁴³Department of Physics, Royal Institute of Technology, Stockholm; Sweden.
- ¹⁴⁴Departments of Physics and Astronomy, Stony Brook University, Stony Brook NY; United States of America.
- ¹⁴⁵Department of Physics and Astronomy, University of Sussex, Brighton; United Kingdom.
- ¹⁴⁶School of Physics, University of Sydney, Sydney; Australia.
- ¹⁴⁷Institute of Physics, Academia Sinica, Taipei; Taiwan.
- ¹⁴⁸^(a)E. Andronikashvili Institute of Physics, Iv. Javakhishvili Tbilisi State University, Tbilisi;^(b)High Energy Physics Institute, Tbilisi State University, Tbilisi;^(c)University of Georgia, Tbilisi; Georgia.

- ¹⁴⁹Department of Physics, Technion, Israel Institute of Technology, Haifa; Israel.
- ¹⁵⁰Raymond and Beverly Sackler School of Physics and Astronomy, Tel Aviv University, Tel Aviv; Israel.
- ¹⁵¹Department of Physics, Aristotle University of Thessaloniki, Thessaloniki; Greece.
- ¹⁵²International Center for Elementary Particle Physics and Department of Physics, University of Tokyo, Tokyo; Japan.
- ¹⁵³Department of Physics, Tokyo Institute of Technology, Tokyo; Japan.
- ¹⁵⁴Department of Physics, University of Toronto, Toronto ON; Canada.
- ¹⁵⁵(^a) TRIUMF, Vancouver BC; (^b) Department of Physics and Astronomy, York University, Toronto ON; Canada.
- ¹⁵⁶Division of Physics and Tomonaga Center for the History of the Universe, Faculty of Pure and Applied Sciences, University of Tsukuba, Tsukuba; Japan.
- ¹⁵⁷Department of Physics and Astronomy, Tufts University, Medford MA; United States of America.
- ¹⁵⁸United Arab Emirates University, Al Ain; United Arab Emirates.
- ¹⁵⁹Department of Physics and Astronomy, University of California Irvine, Irvine CA; United States of America.
- ¹⁶⁰Department of Physics and Astronomy, University of Uppsala, Uppsala; Sweden.
- ¹⁶¹Department of Physics, University of Illinois, Urbana IL; United States of America.
- ¹⁶²Instituto de Física Corpuscular (IFIC), Centro Mixto Universidad de Valencia - CSIC, Valencia; Spain.
- ¹⁶³Department of Physics, University of British Columbia, Vancouver BC; Canada.
- ¹⁶⁴Department of Physics and Astronomy, University of Victoria, Victoria BC; Canada.
- ¹⁶⁵Fakultät für Physik und Astronomie, Julius-Maximilians-Universität Würzburg, Würzburg; Germany.
- ¹⁶⁶Department of Physics, University of Warwick, Coventry; United Kingdom.
- ¹⁶⁷Waseda University, Tokyo; Japan.
- ¹⁶⁸Department of Particle Physics and Astrophysics, Weizmann Institute of Science, Rehovot; Israel.
- ¹⁶⁹Department of Physics, University of Wisconsin, Madison WI; United States of America.
- ¹⁷⁰Fakultät für Mathematik und Naturwissenschaften, Fachgruppe Physik, Bergische Universität Wuppertal, Wuppertal; Germany.
- ¹⁷¹Department of Physics, Yale University, New Haven CT; United States of America.
- ^a Also Affiliated with an institute covered by a cooperation agreement with CERN.
- ^b Also at An-Najah National University, Nablus; Palestine.
- ^c Also at Borough of Manhattan Community College, City University of New York, New York NY; United States of America.
- ^d Also at Bruno Kessler Foundation, Trento; Italy.
- ^e Also at Center for High Energy Physics, Peking University; China.
- ^f Also at Centro Studi e Ricerche Enrico Fermi; Italy.
- ^g Also at CERN, Geneva; Switzerland.
- ^h Also at Département de Physique Nucléaire et Corpusculaire, Université de Genève, Genève; Switzerland.
- ⁱ Also at Departament de Física de la Universitat Autònoma de Barcelona, Barcelona; Spain.
- ^j Also at Department of Financial and Management Engineering, University of the Aegean, Chios; Greece.
- ^k Also at Department of Physics and Astronomy, Michigan State University, East Lansing MI; United States of America.
- ^l Also at Department of Physics and Astronomy, University of Louisville, Louisville, KY; United States of America.
- ^m Also at Department of Physics, Ben Gurion University of the Negev, Beer Sheva; Israel.
- ⁿ Also at Department of Physics, California State University, East Bay; United States of America.
- ^o Also at Department of Physics, California State University, Sacramento; United States of America.

- p* Also at Department of Physics, King's College London, London; United Kingdom.
- q* Also at Department of Physics, Stanford University, Stanford CA; United States of America.
- r* Also at Department of Physics, University of Fribourg, Fribourg; Switzerland.
- s* Also at Department of Physics, University of Thessaly; Greece.
- t* Also at Department of Physics, Westmont College, Santa Barbara; United States of America.
- u* Also at Hellenic Open University, Patras; Greece.
- v* Also at Institutio Catalana de Recerca i Estudis Avancats, ICREA, Barcelona; Spain.
- w* Also at Institut für Experimentalphysik, Universität Hamburg, Hamburg; Germany.
- x* Also at Institute for Nuclear Research and Nuclear Energy (INRNE) of the Bulgarian Academy of Sciences, Sofia; Bulgaria.
- y* Also at Institute of Particle Physics (IPP); Canada.
- z* Also at Institute of Physics, Azerbaijan Academy of Sciences, Baku; Azerbaijan.
- aa* Also at Institute of Theoretical Physics, Ilia State University, Tbilisi; Georgia.
- ab* Also at L2IT, Université de Toulouse, CNRS/IN2P3, UPS, Toulouse; France.
- ac* Also at Lawrence Livermore National Laboratory, Livermore; United States of America.
- ad* Also at National Institute of Physics, University of the Philippines Diliman (Philippines); Philippines.
- ae* Also at Technical University of Munich, Munich; Germany.
- af* Also at The Collaborative Innovation Center of Quantum Matter (CICQM), Beijing; China.
- ag* Also at TRIUMF, Vancouver BC; Canada.
- ah* Also at Università di Napoli Parthenope, Napoli; Italy.
- ai* Also at University of Chinese Academy of Sciences (UCAS), Beijing; China.
- aj* Also at University of Colorado Boulder, Department of Physics, Colorado; United States of America.
- ak* Also at Washington College, Maryland; United States of America.
- al* Also at Yeditepe University, Physics Department, Istanbul; Türkiye.
- * Deceased